博士論文

Development of Asymmetric C–C Bond Forming Reactions Utilizing 7-Azaindoline Amides and Photocatalytic Functionalization of α-Oxy C(sp^3)–H Bond

（7-アザインドリンアミドを用いた触媒的不斉炭素－炭素結合形成反応と光触媒・Ni 触媒によるエーテルのα-C(sp^3)–H 官能基化反応の開発）

孫　仲冬　(SUN ZHONGDONG)

Acknowledgements

First and foremost, I would like to express my deep and sincere appreciation to my supervisor Prof. Masakatsu Shibasaki for giving me the opportunity to do research with him during the past few years and supporting me to apply for the PhD degree. His guidance, support and patience throughout the course of this research is very much appreciated and will not be forgotten. Special thanks to Dr. Naoya Kumagai for his helpful discussions and suggestions in my research. I am thankful to Prof. Motomu Kanai for allowing me as a PhD candidate.

Many thanks to all the staff that helped me over the last years in BIKAKEN. I want to thank Dr. Ryuichi Sawa, Ms. Yumiko Kubota and Dr. Kiyoko Iijima for their assistance in NMR and HRMS work. Many thanks to Dr. Tomoyuki Kimura for his assistance in X-ray crystallography analysis. I am thankful to Ms. Yuko Suya and Ms. Mariko Okui for the kind helps they have offered. Also, I want to thank all the lab members in Shibasaki's group for their kind help to me. Without the support from all of you this dissertation would not have been possible.

Last, but not least, I would like to thank my family and friends for their support throughout this journey.

Zhongdong Sun

October 2018

Abbreviations

Ac	acetyl
Ar	aryl
aq.	aqueous
Bn	benzyl
Boc	*tert*-butoxycarbonyl
bpy	2,2'-bipyridine
Cbz	benzyloxycarbonyl
CFL	compact fluorescent lamp
cod	1,5-cyclooctadiene
Cs	cesium
Cu	copper
Cy	cyclohexyl
DABCO	1,4-diazabicyclo[2.2.2]octane
DBU	1,8-diazabicyclo[5.4.0]undec-7-ene
DCM	dichloromethane
DME	1,2-dimethoxyethane
DMF	*N*,*N*-dimethylformamide
DMSO	dimethyl sulfoxide
Dpp	diphenylphosphinoyl
dr	diastereomeric ratio
dtbbpy	4,4′-di-*tert*-butyl-2,2′-dipyridyl
ee	enantiomeric excess
eq	equivalent
ESI	electrospray ionization
Et	ethyl
Et_3N	triethylamine
Et_2O	ethyl ether
EtOH	ethanol
h	hour
HRMS	high resolution mass spectrometry
HPLC	high performance liquid chromatography
Hz	hertz
^{i}Pr	isopropyl
IR	infrared spectroscopy
Ir	iridium
J	coupling constant
K	potassium
LC-MS	liquid chromatography-mass spectrometry
LED	Light-emitting diode
Li	lithium
M	molar concentration
Me	methyl
MeOH	methanol
min	minute
mM	micromolar concentration
m.p.	melting point
Ms	methanesulfonyl
MS	mass spectrometry

μwave	microwave
Na	sodium
^{n}Bu	normal butyl
Ni	nickel
NMR	nuclear magnetic resonance
NOE	Nuclear Overhauser effect
Nu	nucleophile
Pd	palladium
PG	protecting group
Ph	phenyl
ppm	parts per million
PTLC	preparative thin-layer chromatography
quant.	quantitative
rac	racemic
Ru	ruthenium
rt	room temperature
t	time
T	temperature
^{t}Bu	*tert*-butyl
THF	tetrahydrofuran
thioDpp	diphenylthiophosphinoyl
TLC	thin layer chromatography
TMS	tetramethylsilane
Tol	tolyl
Ts	*p*-toluenesulfonyl
UV	ultraviolet
Xyl	3,5-dimethylphenyl

Table of Contents

1. Chapter 1. Development of Asymmetric C–C Bond Forming Reactions Utilizing 7-Azaindoline Amides

1.1 Direct Catalytic Asymmetric Mannich-Type Reaction of α-Azido 7-Azaindoline Amide

1.1.1 Introduction

Chiral α,β-diamino acid derivatives have been regarded as synthetically versatile building blocks for their widespread presence in a number of therapeutically valuable molecules such as antibiotic Streptothricin F, Type III secretion system inhibitor Guadinomine B, Capreomycin used for tuberculosis treatment, and also in antihypertensive drug Imidapril.[1] Because of this reason, considerable attention has been focused on devising stereoselective access to α,β-diamino acid derivatives (Figure 1).

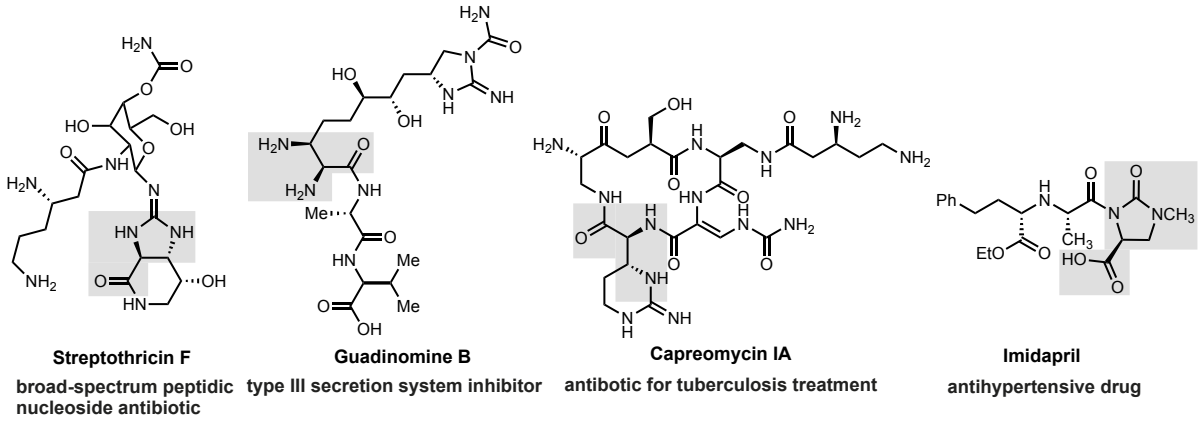

Figure 1. α,β-Diamino acid derivatives in natural products

Synthesis of optically active α,β-diamino acid derivatives with two vicinal nitrogen-bearing stereogenic centers leaves a challenge for synthetic chemists. The straightforward strategy to confront this challenge is that forging a C-C bond with two chiral centers via a catalytic asymmetric reaction in one step. Prior endeavor to the synthesis of enantioenriched α,β-diamino acid derivatives mainly focused on catalytic asymmetric Mannich-type reactions of glycine Schiff bases with imines.[2,3] For good examples, in 2003, Jørgensen demonstrated the first catalytic asymmetric Mannich-type reaction of glycine Schiff base.[3a] A chiral phosphino-oxazaoline/Cu(I) complex stabilized imino glycine ester anion was generated in the presence of base and acted as nucleophile toward *N*-protected imines. This method provided an easy entry to synthesize chiral α,β-diamino acid in a diastereoselective and enantioselective fashion (Scheme 1).

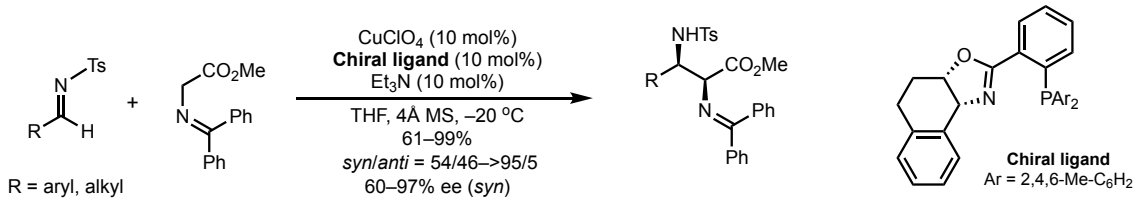

Bernardi, L. Gothelf, A. S. Hazell, R.G. Jørgensen, K. A. *J. Org. Chem.* **2003**, 68, 2583.

Scheme 1.

In 2005, Ohshima and Shibasaki reported a chiral phase-transfer catalyst (*S*,*S*)-TaDiAS catalyzed asymmetric Mannich-type reaction of glycine Schiff base.[3b] The tartrate-derived diammonium salt (*S*,*S*)-TaDiAS showed high efficiency and provided *syn*-selective products in excellent yield and diastereoselective with moderate to good enantioselectivity. Easily removable Boc-protected imines were compatible with the catalytic system (Scheme 2).

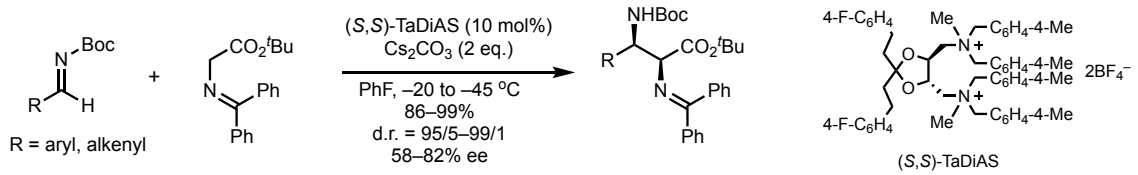

Okada, A.; Shibuguchi, T.; Ohshima, T.; Masu, H.; Yamaguchi, K.; Shibasaki, M. *Angew. Chem., Int. Ed.* **2005**, *44*, 4564.

Scheme 2.

In 2008, Wu and co-workers developed a diastereoselective switchable enantioselective Mannich-type reaction.[3c] Both *syn* and *anti* diastereoisomers were accessible in excellent yield and enantioselectivity (Scheme 3).

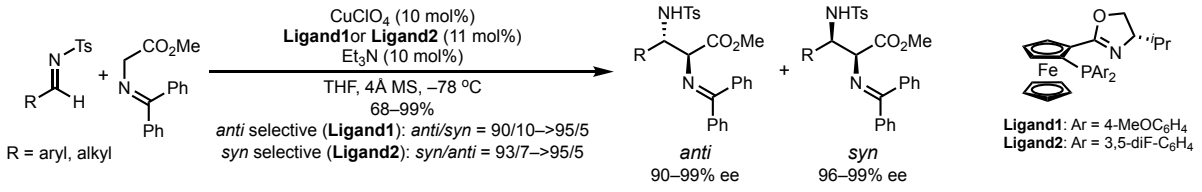

Yan, X. X.; Peng, Q.; Li, Q.; Zhang, K.; Yao, J.; Hou, X. L.; Wu, Y. D. *J. Am. Chem. Soc.* **2008**, *130*, 14362.

Scheme 3.

Meanwhile, Arrayás and Carretero showcased an *anti*-selective enantioselective catalytic Mannich-type reaction of glycine Schiff base with unique 8-quinolylsulfonly-protected aldimines.[3d] The selection of the protecting group was the key to attaining good reactivity and high diastereo- and enantioselectivity (Scheme 4).

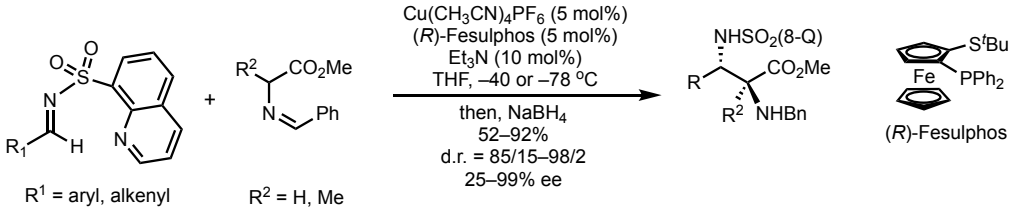

Hernández-Toribio, J.; Arrayás, R. G.; Carretero, J. C. *J. Am. Chem. Soc.* **2008**, *130*, 16150.

Scheme 4.

In 2013, a cyclopropenimine-catalyzed enantioselective Mannich-type reaction of glycine Schiff base has been reported by Lambert.[3e] The reaction has a good substrate generality. Boc-protected aromatic and aliphatic aldimines were both amenable (Scheme 5).

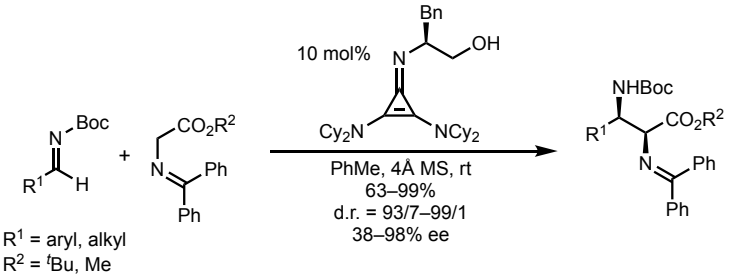

Bandar, J. S.; Lambert, T. H. *J. Am. Chem. Soc.* **2013**, *135*, 11799.

Scheme 5.

It is noticeable that the *syn*-α,β-diamino acid derivatives are predominant products in the Mannich-type reactions employing glycinate Schiff bases and *N*-Boc imines, on the other hand, the *anti*-α,β-diamino acid counterparts are accessible only when *N*-sulfonyl imines are incorporated into Mannich-type reactions. Given that removing

the sulfonyl group of the Mannich adduct can be chanllenging, development of a synthetic procedure toward *anti*-α,β-diamino acid derivatives with tractable *N*-protecting group is anticipated.

Recently, our group introduced a newly designed α-azido 7-azaindoline amide **1-N$_3$**,[4] which served as a latent enolate in a direct catalytic asymmetric aldol reaction affording enantioenriched β-hydroxy-α-amino acid analogues in diastereodivergent manner (Figure 2a).[5] ^{15}N NMR experiment showed no coordination between Cu(I) cation and negatively charged ^{15}N atom of the azido group. A nuclear Overhauser effect was observed between the amide α-proton and protons of 7-azaindoline moiety. These combined NMR studies indicated a bidentate coordination of the substrate to Cu(I) and a Z-enolate was probably generated during the reaction (Figure 2b). Similar strategy has been applied ingeniously in a direct catalytic asymmetric Mannich-type reaction of α-CF3 amide **1-CF$_3$** (Figure 2c).[6] The catalytic generation of α-CF3 enolate benefitted from the coordination of 7-azaindoline moiety with Cu(I), which prevented the β-elimination of fluoride upon metal enolate formation. X-ray analysis further confirmed the bidentate coordination of the substrate to Cu(I) (Figure 2d). These results prompted me to focus on a direct catalytic asymmetric Mannich-type reaction via soft Lewis acid/hard Brønsted base cooperative catalysis employing the α-azido amide **1-N$_3$** as a pronucleophile, allowing for a concise, efficient access to chiral α,β-diamino acid derivatives (Figure 2e).[7] The azide functionality could be regarded as a masked amine or an origin for further azide-specific transformations.[8]

(a)

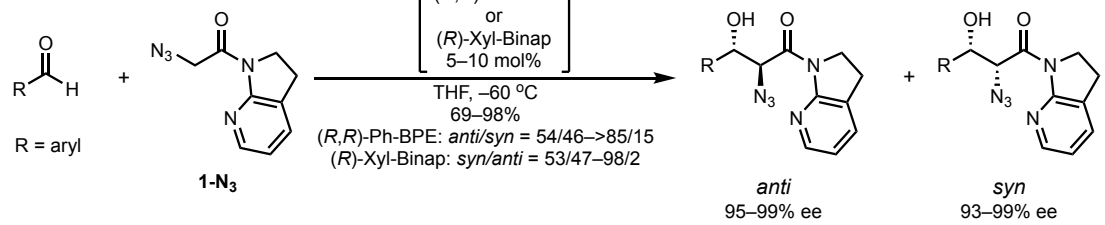

Weidner, K.; Sun, Z.; Kumagai, N.; Shibasaki, M. *Angew. Chem., Int. Ed.* **2015**, *54*, 6236.

(b)

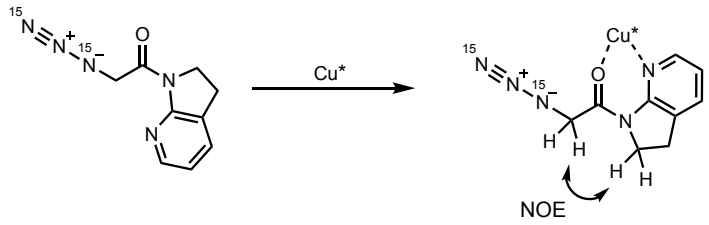

Cu* :Cu(I)/(*R*,*R*)-Ph-BPE complex

(c)

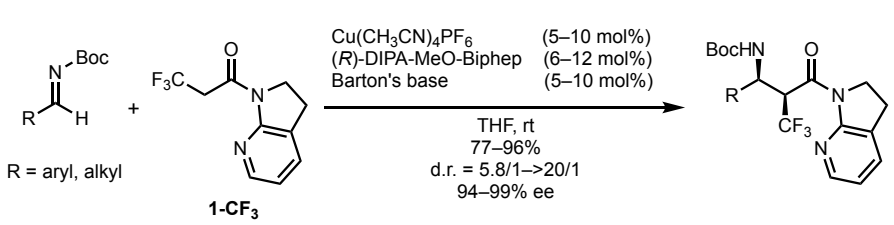

Yin, L.; Brewitz, L.; Kumagai, N.; Shibasaki, M. *J. Am. Chem. Soc.* **2014**, *136*, 17958.

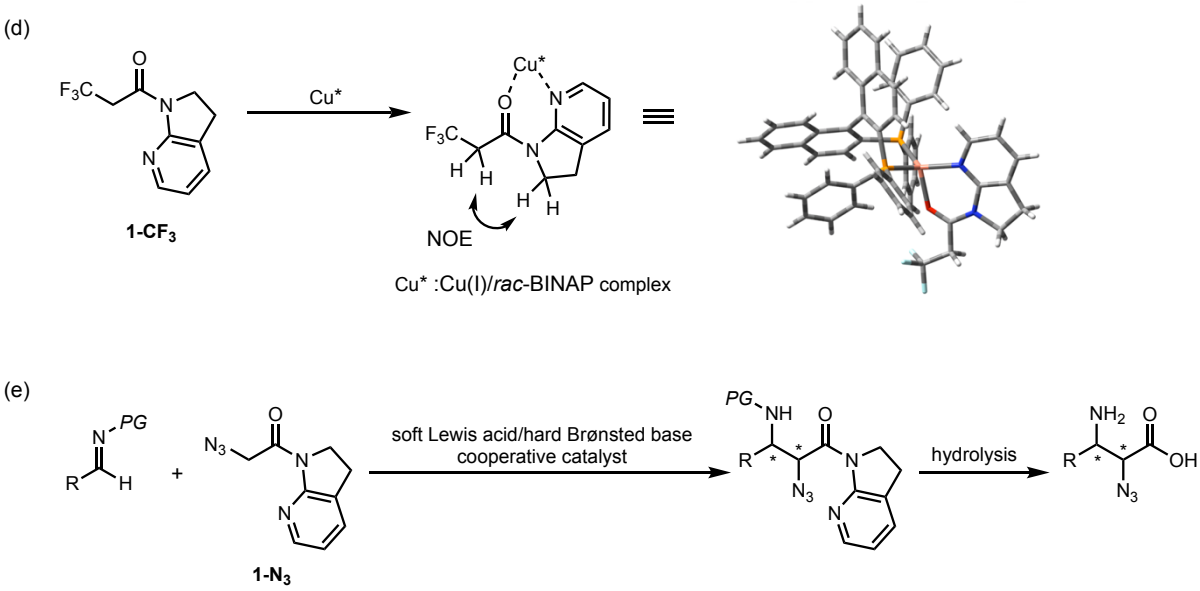

Figure 2. Usage of 7-azaindoline amides in asymmetric C–C bond forming reactions

1.1.2 Screening of reaction conditions

To start with, aldimine electrophiles with different protecting groups were investigated for this catalytic Mannich-type reaction. Catalyst consisting of Cu(I)/(*R*)-Xyl-Binap complex and Barton's base was used in the preliminary study. It was found that diphenylthiophosphinyl(ThioDPP)-protected aldimine **4a** provided better diastereoselectivity and enantioselectivity over Boc- and diphenylphosphinyl(DPP)-protected aldimines (Table 1).[9]

Table 1. Investigation of protecting groups for imine[a]

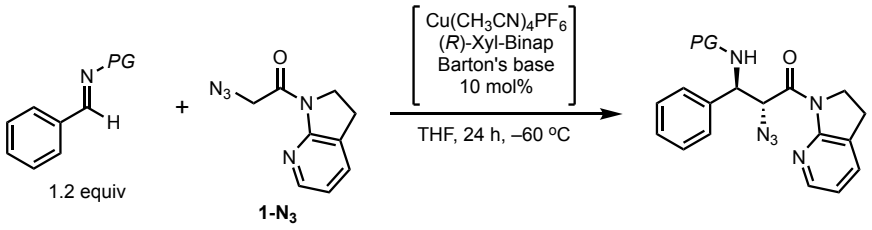

entry	imine *PG* =		yield[a] (%)	*anti*/*syn*[b]	ee[c] (%)
1	Boc	**2**	>99	80/20	87
2	Dpp	**3**	>99	72/28	86
3	ThioDpp	**4a**	88	84/16	99

[a] **1-N$_3$**: 0.1 mmol, imines: 0.12 mmol.
[a] Determined by ^{1}H NMR using 3,4,5-trichloropyridine as an internal standard.
[b] Determined by ^{1}H NMR analysis of the crude mixture.
[c] Determined by chiral stationary phase HPLC analysis. Absolute configuration was not determined.

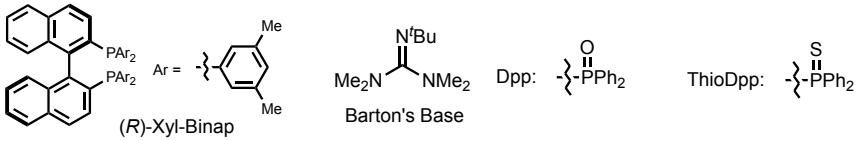

Encouraged by this result, next, ligand screening was performed in order to improve yield, diastereoselectivity and enantioselectivity (Table 2). Various biaryl-type bisphosphine chiral ligands were screened. Ligands with bulky pendants, such as (*R*)-DTBM-Garphos (entry 6), (*R*)-3,4,5-Trimethoxyl-MeO-Biphep (entry 9) and (*R*)-

DIPA-MeO-Biphep (entry 10), gave poor conversion. Among the chiral ligands tested, (*R*)-Xyl-Segphos (entry 11) afforded highest yield, diastereoslectivity and excellent enantio excess. The reaction proceeded smoothly using 5 mol% catalyst loading but longer reaction time was needed (entry 12).

Table 2. Ligand screening[a]

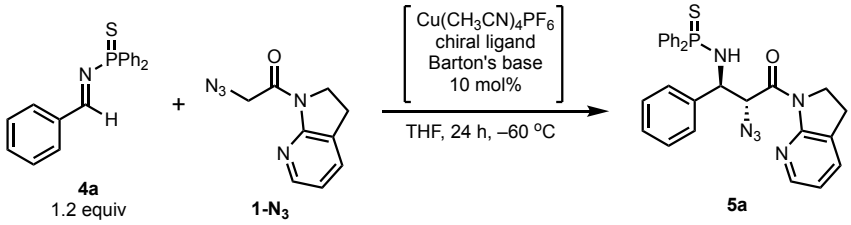

entry	chiral ligand	yield[b] (%)	*anti*/*syn*[c]	ee[d] (%)
1	(*R*)-Tol-Binap	57	84/16	98
2	(*R*)-Xyl-Binap	88	84/16	99
3	(*R*)-Tol-Garphos	35	83/17	90
4	(*R*)-Xyl-Garphos	65	91/9	96
5	(*R*)-DMM-Garphos	80	90/10	98
6	(*R*)-DTBM-Garphos	no reaction	–	–
7	(*R*)-Tol-MeO-Biphep	38	86/14	96
8	(*R*)-Xyl-MeO-Biphep	94	91/9	97
9	(*R*)-3,4,5-Trimethoxyl-MeO-Biphep	8	–	–
10	(*R*)-DIPA-MeO-Biphep	no reaction	–	–
11	(*R*)-Xyl-Segphos	95	91/9	97
12[e]	(*R*)-Xyl-Segphos	90	91/9	97

[a] **1-N$_3$**: 0.1 mmol, **4a**: 0.12 mmol.
[b] Determined by ^{1}H NMR using 3,4,5-trichloropyridine as an internal standard.
[c] Determined by ^{1}H NMR analysis of the crude mixture.
[d] Determined by chiral stationary phase HPLC analysis.
[e] 5 mol% catalyst loading, 48 h, –60 °C.

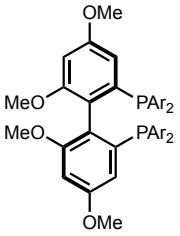

Ar = 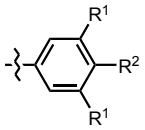

(*R*)-Tol-Garphos: R^1=H, R^2=Me
(*R*)-Xyl-Garphos: R^1=Me, R^2=H
(*R*)-DMM-Garphos: R^1=Me, R^2=H: R^1=R^2=OMe
(*R*)-DTBM-Garphos: R^1=^{t}Bu, R^2=OMe

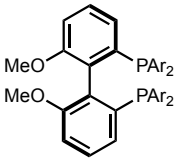

Ar = 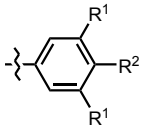

(*R*)-Tol-MeO-Biphep: R^1=H, R^2=Me
(*R*)-Xyl-MeO-Biphep: R^1=Me, R^2=H
(*R*)-3,4,5-Trimethoxyl-MeO-Biphep: R^1=R^2=OMe
(*R*)-DIPA-MeO-Biphep: R^1=^{i}Pr, R^2=NMe_2

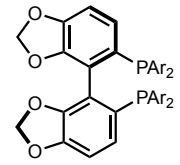

Ar = 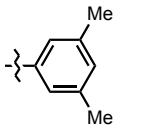

(*R*)-Xyl-Segphos

Next, a protocol for synthesis of enantioenriched α-azido-β-amino acid **6a** was devised. The Mannich reaction achieved full conversion with 91/9 dr and 97% ee, subsequently, the Mannich adduct **5a** underwent a facile hydrolysis under acidic conditions to give the *anti*-α-azido-β-amino acid **6a** in 86% yield over 2 steps (Scheme 6).

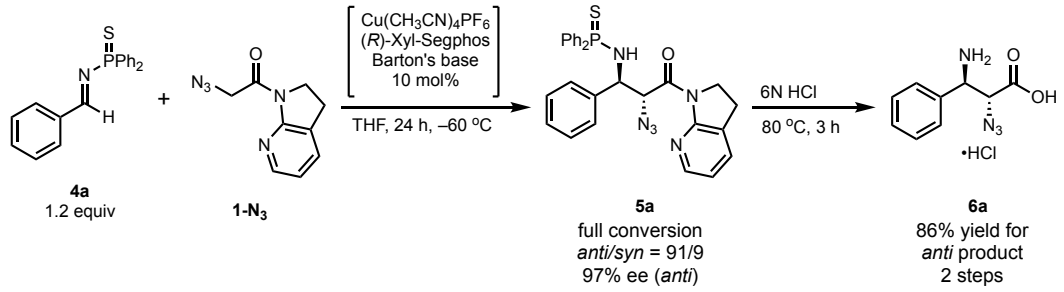

Scheme 6. Protocol for synthesis of α-azido-β-amino acid

1.1.3 Substrate scope

Table 3. Substrate scope[a]

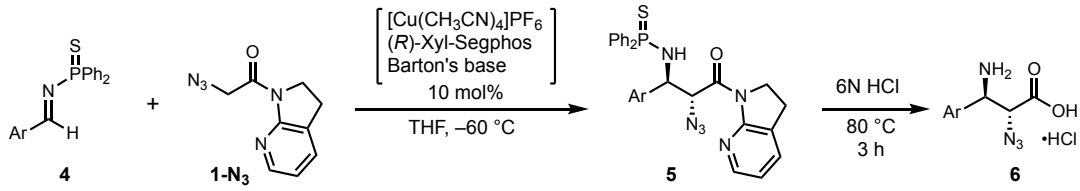

entry	imine **3** Ar =	*t* (h)	**6**	yield[b] (%)	*anti*/*syn*[c]	ee[d] (%)	entry	imine **3** Ar =	*t* (h)	**6**	yield[b] (%)	*anti*/*syn*[c]	ee[d] (%)
1	**4a**	24	**6a**	86	91/9	98	8	**4h**	24	**6h**	84	93/7	98
2	**4b**	48	**6b**	70	91/9	94	9	**4i**	24	**6i**	74	95/5	96
3	**4c**	48	**6c**	71	91/9	98	10	**4j**	24	**6j**	84	92/8	97
4	**4d**	48	**6d**	73	91/9	92	11	**4k**	24	**6k**	70	96/4	84
5	**4e**	24	**6e**	86	92/8	97	12	**4l**	24	**6l**	80	90/10	95
6	**4f**	24	**6f**	82	90/10	95	13	**4m**	24	**6m**	75	90/10	95
7	**4g**	24	**6g**	75	96/4	89	14	**4n**	48	**6n**	71	92/8	98

[a] **1-N$_3$**: 0.3 mmol, **4**: 0.36 mmol.
[b] Isolated yield of *anti*-β-amino-α-azido acid **6**.
[c] Determined by ^{1}H NMR analysis of the crude product **5**.
[d] Determined by chiral stationary phase HPLC analysis of a small aliquot of **5**.

Next, I explored the substrate scope using this protocol. Aldimines with various substitutions on the aromatic ring were applicable for this protocol. Isolated yields of *anti*-α-azido-β-amino acids were shown in Table 3. Electron-

efficient imines showed lower reactivity in the Mannich-type reactions and needed longer time to complete the reactions (entry 3, 4). Halogen-substituted imines generally exhibited good compatibility (entry 5–11). Only *o*-Cl and *o*-Br substitutions imines resulted in slightly lower enantio excess due to steric factors (entry 7, 11). *p*-CF_3 substituted and heteroaromatic imines were also suitable substrates (entry 12–14).

The catalytic system was robust enough to scale up (Scheme 7). The gram-scale Mannich-type reaction was promoted by 5 mol% catalyst into full conversion efficiently without damaging diastereoselectivity and enantioselectivity. It's worth noting that the *anti*-product **5e** could be directly recrystallized from reaction crude in 86% yield in a diastereomerically and enantiomerically pure form.

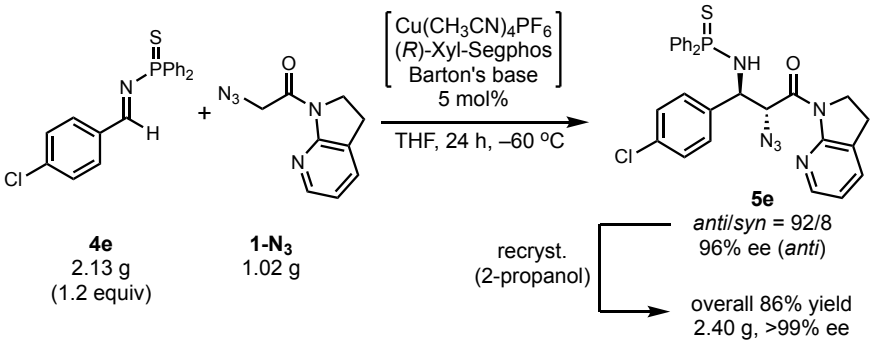

Scheme 7. Gram-scale Mannich-type reaction

Although aliphatic imine behaved almost unreactive in this Mannich-type reaction, α,β-unsaturated imines could provide products in moderate yield and diastereoselectivity with high enantioselectivity (Scheme 8).

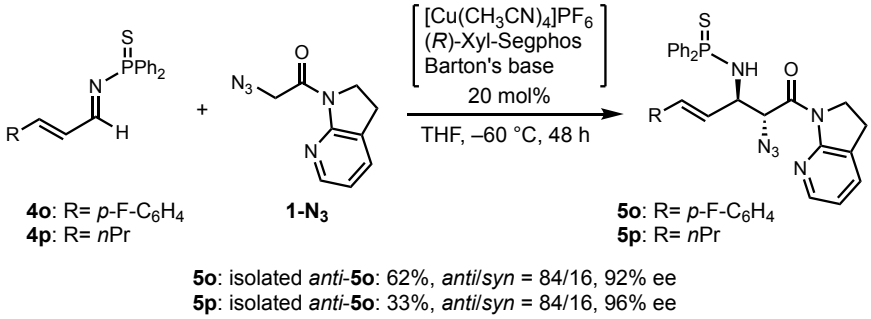

Scheme 8. Mannich-type reactions of α,β-unsaturated imines

1.1.4 Determination of absolute configuration

Single crystals of **5e** were obtained from 2-propanol at room temperature. The relative and absolute configurations of other products were deduced by analogy (Figure 3).

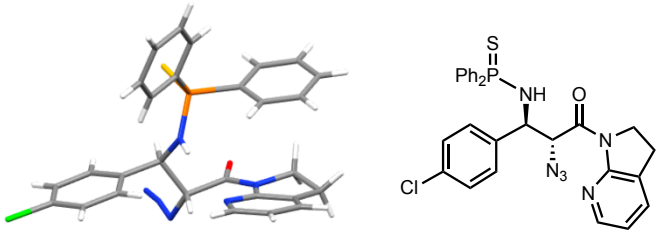

Figure 3. The structure of **5e**. White: hydrogen, gray: carbon,

blue: nitrogen, red: oxygen, light green: chlorine.

1.1.5 Preparation of 1-N_3/Cu^I/*rac*-Binap complex

In the previous report of direct catalytic asymmetric aldol reaction of α-azido 7-azaindoline amide, upon addition of soft Lewis acidic Cu^I, isomerizable *E* conformation of 7-azaindoline amide changes into *Z* conformation readily, which has been confirmed by NMR spectroscopy in solution phase. To further prove this observation, a single crystal of **1-N_3**/Cu^I/*rac*-Binap complex was prepared for X-ray crystallography analysis (Figure 4). Single crystals of **1-N_3**/Cu^I/*rac*-Binap complex were obtained from 0.02 M solution of the mixture comprising of *rac*-Binap : $[Cu(CH_3CN)_4]PF_6$: **1-N_3** = 1:1:1 in acetone at 5 °C.

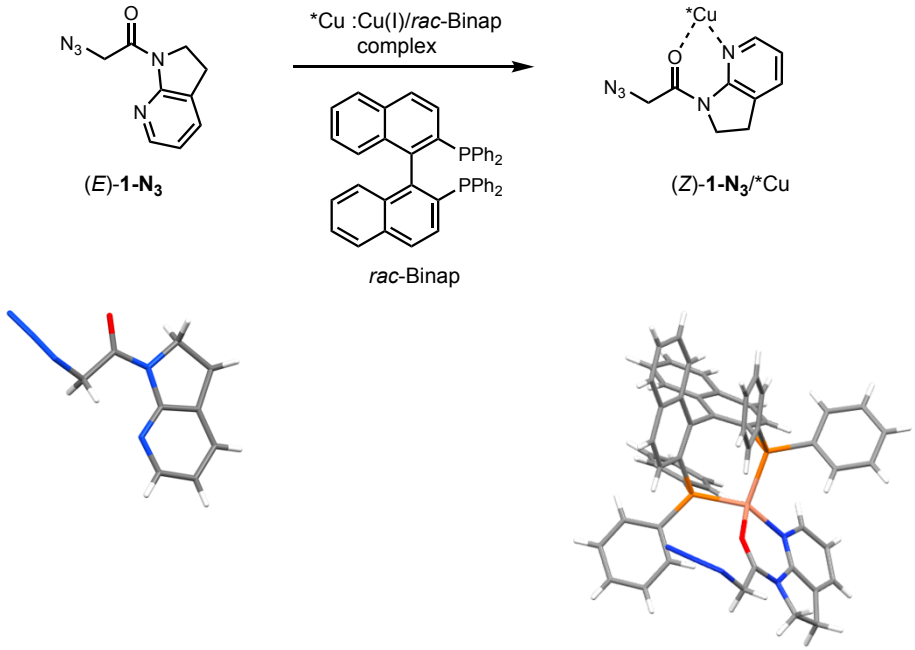

Figure 4. Bidentate coordination mode of **1-N_3** to Cu^I/*rac*-Binap complex. Color code for X-ray structure; White: hydrogen, gray: carbon, blue: nitrogen, red: oxygen, orange: phosphorus, pink: copper.

1.1.6 Control experiments

The essential of bidentate coordination of 7-azaindoline amide with Cu^I for enolization of amide was proved by the failed reactions using structurally similar α-azido amides **1a-N_3**–**1d-N_3** (Figure 5).

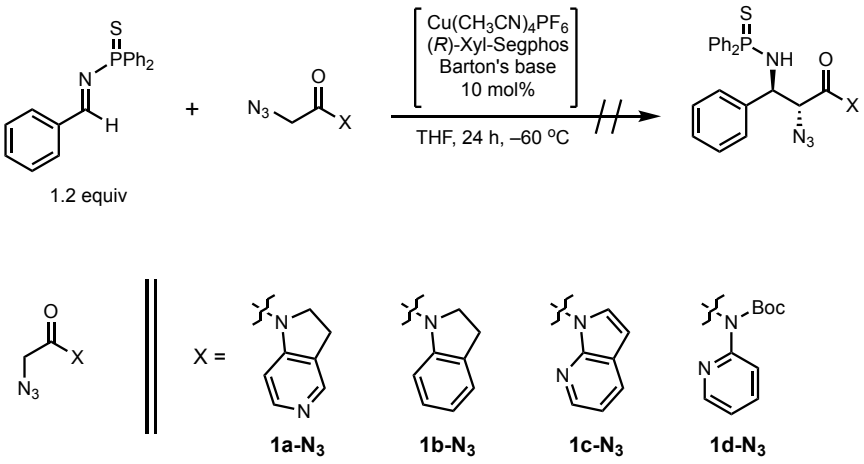

Figure 5. Failed reactions of structurally similar α-azido amides **1a-N_3**–**1d-N_3**

1.1.7 Product transformations

The recrystallized optically pure **5e** underwent a facile hydrolysis into **6e**. The *anti*-α,β-diamino acid **7** was obtained through a Pd/C-mediated reduction of azido group (Figure 6). **6e** could be cyclized into the α-azido-β-lactam **8** by treated with MsCl/$NaHCO_3$. The structure of lactam **8** was confirmed by X-ray crystallography analysis. Methanolysis of **5e** in 2M HCl/MeOH gave the methyl ester **9** in 88% yield after recrystallization. The methyl ester **9** could also be transformed into α-azido-β-amino acid **6e** after hydrolysis. The azido group could be chemoselectively reduced in the peptide **10** with Cbz carbamate intact.

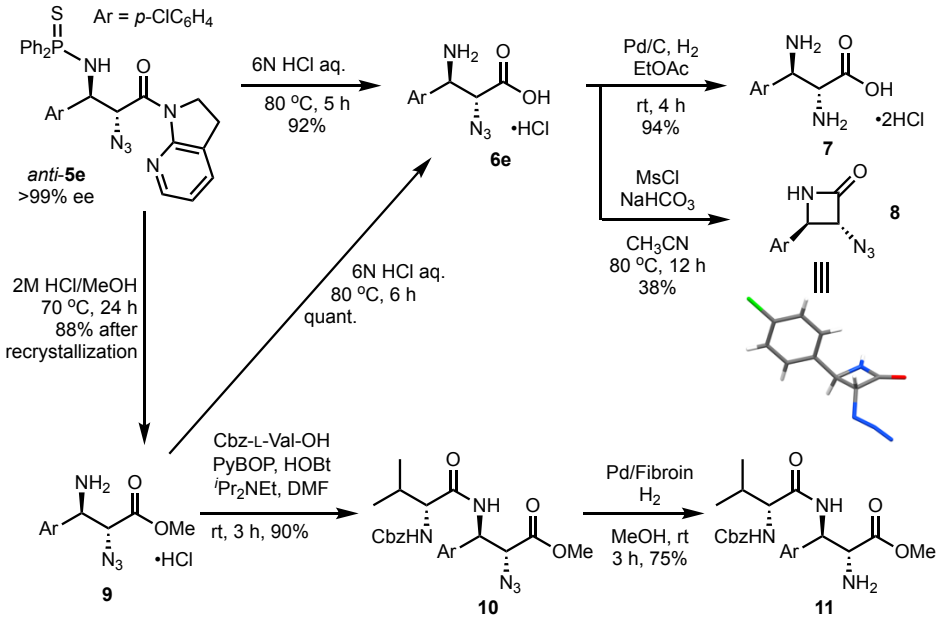

Figure 6. Transformations of product **5e**

The azide-specific transformation was also investigated. The attempt of applying the peptide **10** with the coupling reagent phosphinoester **12** in traceless Staudinger ligation was unsatisfactory (Figure 7).[10] Although the iminophosphorane **14** was quickly generated after the reaction started, the nucleophilic attack of nitrogen atom to the phenol ester moiety seemed very sluggish due to the bulkiness of substituents on α-amino carbon atom. Thus, the more facile hydrolysis of iminophosphorane **14** proceeded to yield Staudinger reduction product **11** instead of ligation route to amide product **13**. Under the best conditions, amide coupling product **13** was obtained in 19% yield.

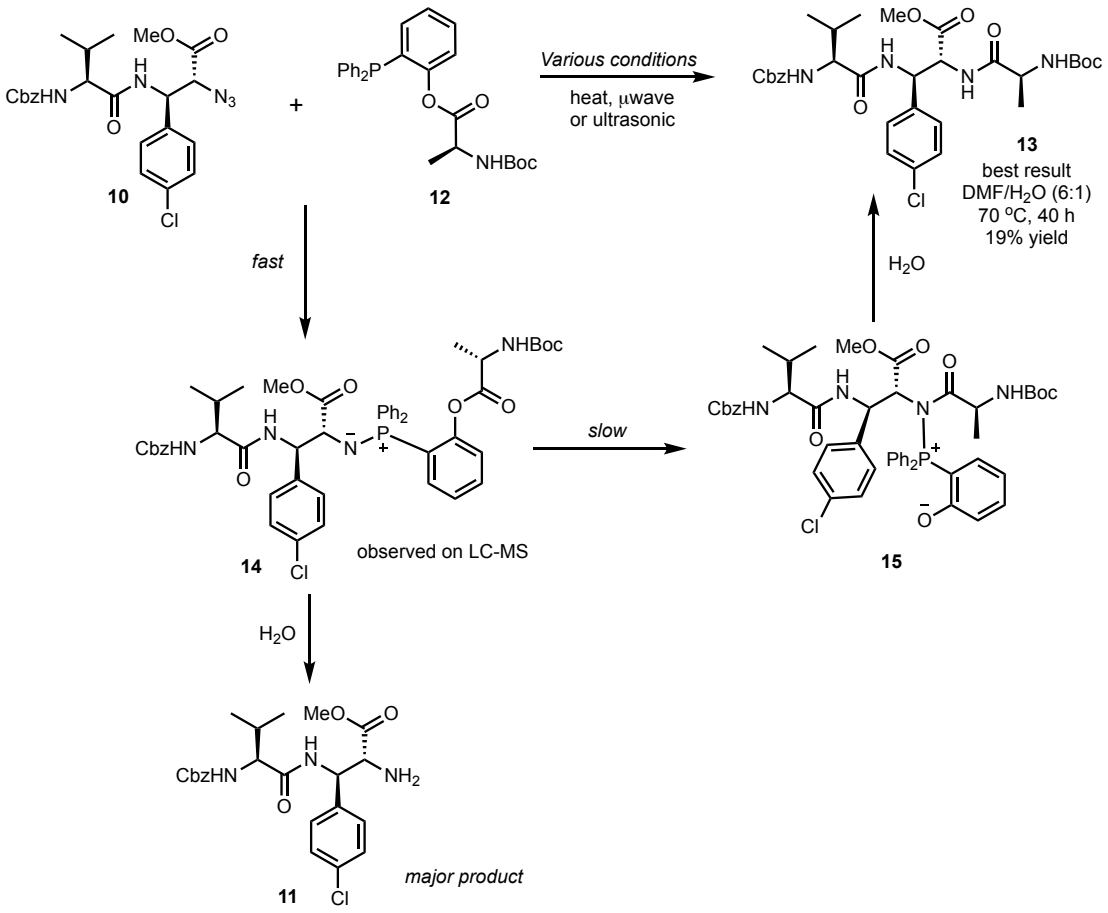

Figure 7. Staudinger ligation of **10** with **12**

Replacing the coupling reagent **12** with phosphinothioester **16** didn't yield target peptide **13**. Using a less bulky peptide **17** didn't improve the result (Figure 8).[10d]

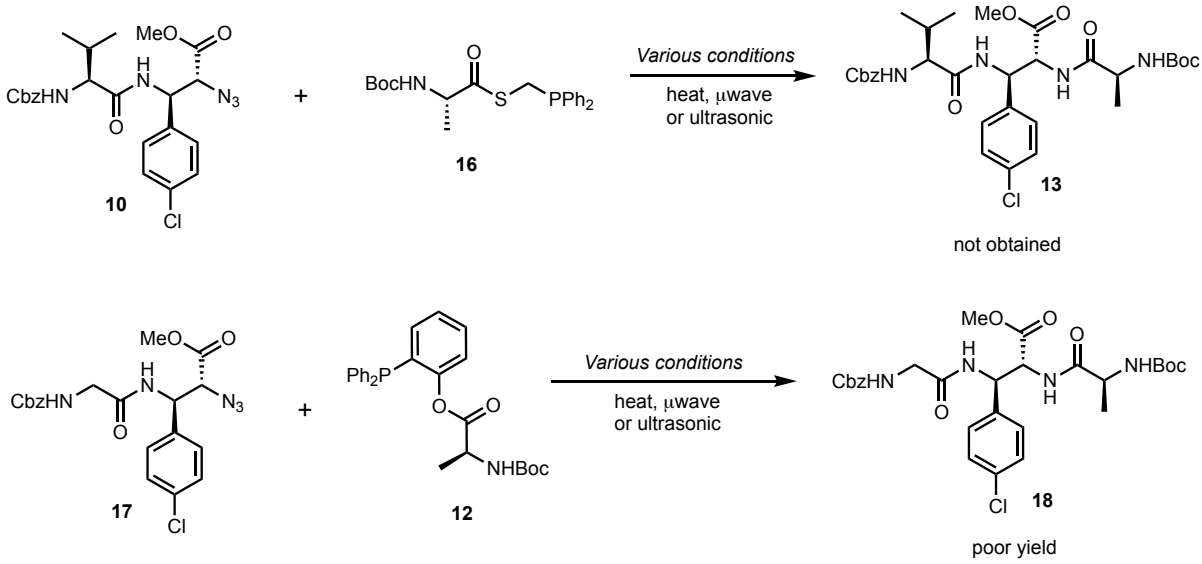

Figure 8. Staudinger ligation of **10** and **17**

1.2 Direct Catalytic Asymmetric 1,6-Conjugate Addition of 7-Azaindoline Amides to *para*-Quinone Methides

1.2.1 Introduction

para-Quinone methides (*p*-QMs),[11] which can be found in a variety of natural products,[12] are constructed by carbonyl and olefinic moieties, and chemically defined as neutral and zwitterionic resonance entities.

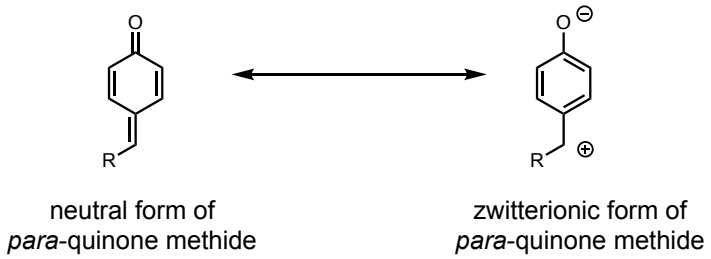

Figure 9. Resonance structures of *p*-QMs

In nature, because of the intrinsic electrophilic reactivity, *p*-QMs can be found as highly reactive intermediates in many biological processes. In synthetic chemistry, *p*-QMs can be exploited as versatile conjugate acceptors,[13] especially in asymmetric 1,6-conjugate additions,[14] providing possible accesses to synthetically valuable diarylmethine stereogenic centers,[15] which are found in natural products and pharmaceuticals, such as (+)-sertraline, (*R*)-tolterodine and podophyllotoxin (Figure 10).[16]

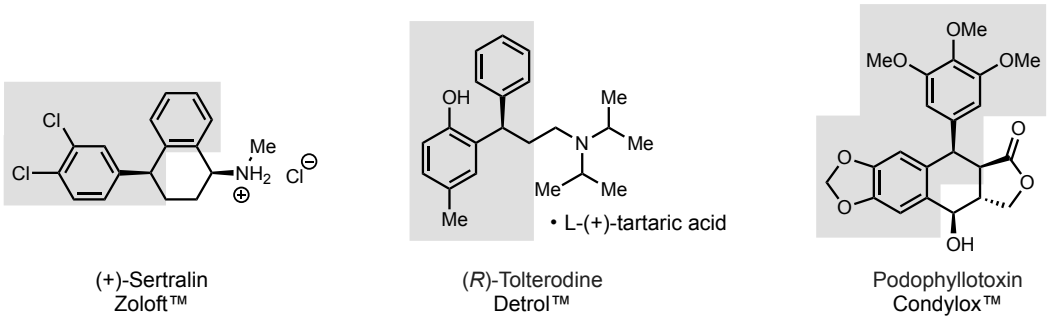

Figure 10. Diarylmethine stereocenters in bioactive molecules

In 2013, Fan's group documented an enantioselective catalytic 1,6-conjugate addition of *p*-QMs with malonate esters under phase-transfer catalysis.[14a] Soon after, Jørgensen's group developed a chiral amine catalyzed asymmetric 1,6-conjugate addition of *p*-QMs with aldehydes.[14b] In 2016, Deng and co-workers realized an asymmetric 1,6-conjugate addition of *p*-QMs with glycine Schiff bases by employing a Cu(I)/Ph-Foxap complex. The reaction afforded chiral β-bis-aryl-α-amino acids in excellent stereoselectivity (Scheme 9).[14c]

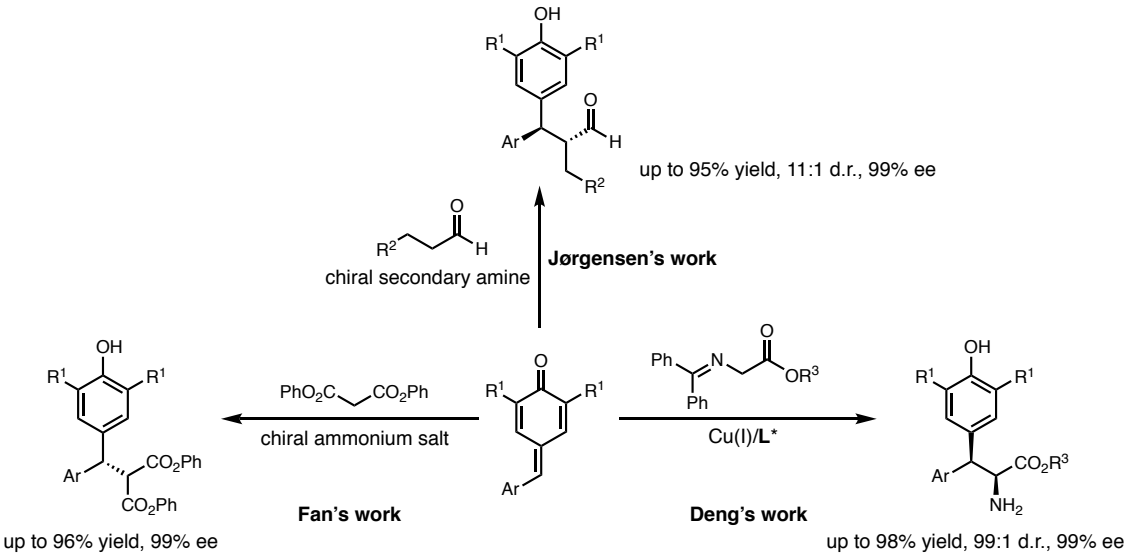

Scheme 9. Selected examples of asymmetric 1,6-conjugate addition of *p*-QMs

In the continuing exploration of direct catalytic enolization chemistry in our group, 7-azaindoline amides were discovered as prominent enolate precursors using soft Lewis acid/hard Brønsted base cooperative catalysis, albeit amide was known resistant to enolization (Scheme 10).[4-6,17-21] The strategy to tackle this problem is by introducing a bidentate coordination between 7-azaindoline amide and soft Lewis acid metal center. Upon addition of soft Lewis acid metal, isomerizable *E* conformation of 7-azaindoline amide changes into *Z* conformation readily, which has been confirmed by NMR spectroscopy in solution phase and X-ray crystallography. The generated amide-metal complex undergoes enolization smoothly in the presence of hard Brønsted base, then capturing the catalytically generated enolate by electrophile forges C–C bond. To date, this strategy has been successfully implemented to asymmetric C–C bond forming reactions using 7-azaindoline amides bearing different functional groups (-R_F,[6,17] -N_3,[5,18] -alkyl,[19] -halogen,[20] -OBn[21]) at α-position with aldehydes, ketones and imines electrophiles. As a continuous research on 7-azaindoline amides in asymmetric C–C bond forming reactions, a direct catalytic asymmetric 1,6-conjugated addition of 7-azaindoline amides to *p*-QMs was envisioned.

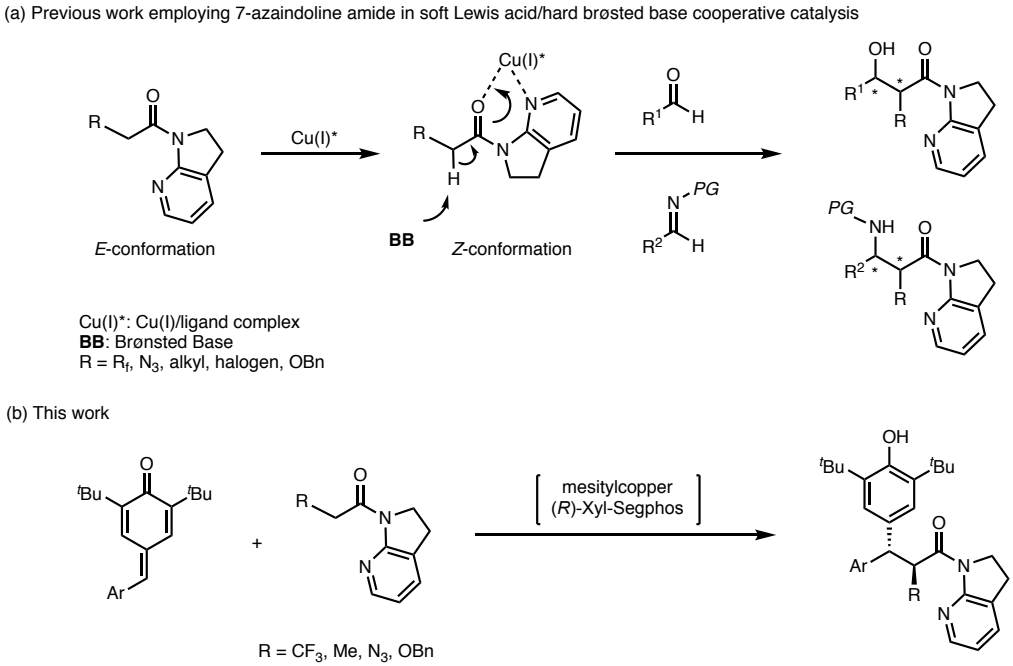

Scheme 10. (a) Previous work of 7-azaindoline amides in asymmetric C–C bond forming reactions and (b) This work on asymmetric 1,6-conjugate addition of *p*-QMs

1.2.2 Screening of reaction conditions

I began the study with probing the reaction of *p*-QMs **19a** and α-CF_3 7-azaindoline amide **1-CF$_3$**, which could be easily enolized under soft Lewis acid/hard Brønsted base cooperative catalysis and applied in our previous reports of aldol and Mannich reactions. The catalyst comprising 10 mol % mesitylcopper and (*S*,*S*)-Ph-BPE (**L1**) could promote the 1,6-addition reaction at room temperature (Table 4). Although only moderate stereoselectivity (8.6/1 d.r., 76% ee) was achieved, 1,6-adduct **20a** was formed in high yield (93%) in preference for the *anti* isomer (Table 4, entry 1). This result encouraged me to investigate other chiral ligands to further improve the stereoselectivity. After a brief screening of biaryl-type bisphosphine ligands, ligand with tighter dihedral angle and bulkier substituents, (*R*)-Xyl-Segphos (**L5**), provided satisfactory result both in stereoselectivity (>20/1 d.r., 97% ee) and yield (97%). On the other hand, reactions using planar chiral ferrocene-based ligands (**L6**, **L7**) provided 1,6-addition product **20a** with lower stereoselectity albeit in high yield (entry 6, 7). In entry 8, the reaction could be ran using 5 mol % instead of 10 mol % catalyst loading without erosion of stereoselectivity and yield. Thus, the conditions of entry 8 were set as standard conditions for exploring the scope of *p*-QMs.

Table 4. Ligand screening[a]

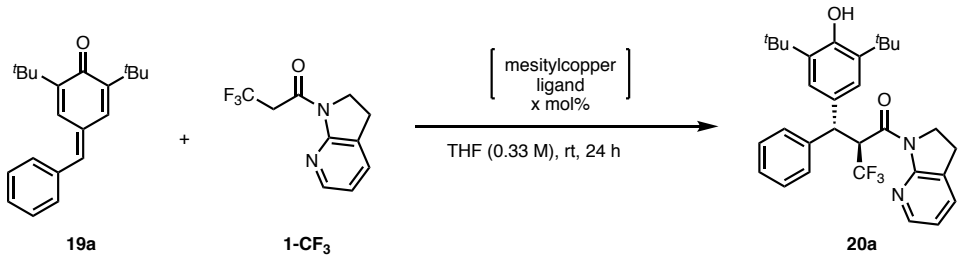

19a **1-CF$_3$** **20a**

entry	ligand	x (mol%)	yield[b] (%)	*anti/syn*[c]	ee[d] (%)
1	**L1**	10	93	8.6/1	76
2	**L2**	10	90	7.3/1	76
3	**L3**	10	98	>20/1	91
4	**L4**	10	95	6.9/1	89
5	**L5**	10	98	>20/1	97
6	**L6**	10	94	8.3/1	31
7	**L7**	10	90	6.6/1	70
8	**L5**	5	97[e]	>20/1	97

[a] **1-CF$_3$**: 0.1 mmol, **19a**: 0.12 mmol.
[b] Determined by ^{1}H NMR using 1,3,5-trimethoxybenzene as an internal standard.
[c] Determined by 1H NMR analysis of the crude product.
[d] Determined by chiral stationary phase HPLC analysis.
[e] Isolated yield.

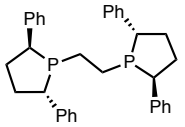

L1: (*S*,*S*)-Ph-BPE

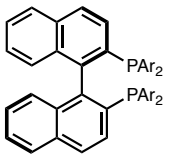

L2: (*R*)-Tol-Binap
Ar = p-tolyl
L3: (*R*)-Xyl-Binap
Ar = 3,5-xylyl

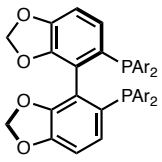

L4: (*R*)-Segphos
Ar = Ph
L5: (*R*)-Xyl-Segphos
Ar = 3,5-xylyl

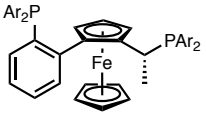

L6: (R,R_p)-Walphos
Ar = 3,5-xylyl
SL-W009-1

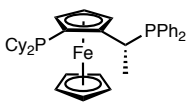

L7: (R,S_p)-Josiphos
SL-J004-1

1.2.3 Substrate scope

Table 5. Substrate scope[a]

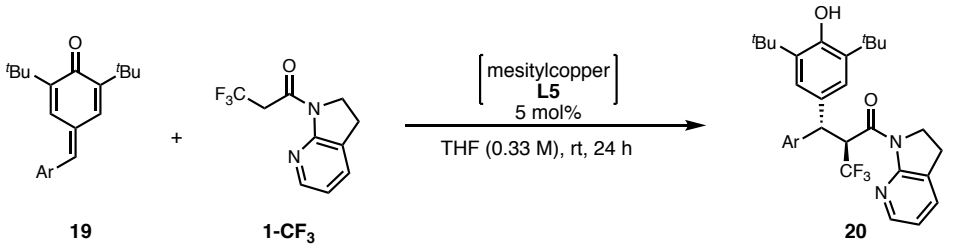

entry	product **20** Ar =	yield[b] (%)	*anti*/*syn*[c]	ee[d] (%)	entry	product **20** Ar =	yield[b] (%)	*anti*/*syn*[c]	ee[d] (%)
1[e]	**20a** ***>3g product***	97	>20/1	97	12	**20l**	95	>20/1	96
2	**20b**	95	>20/1	96	13	**20m**	93	>20/1	96
3	**20c**	92	>20/1	92	14	**20n**	95	>20/1	96
4	**20d**	96	>20/1	95	15	**20o**	94	>20/1	96
5	**20e**	93	>20/1	93	16	**20p**	94	>20/1	96
6	**20f**	93	>20/1	98	17	**20q**	97	>20/1	97
7	**20g**	98	>20/1	97	18	**20r**	95	>20/1	96
8	**20h**	96	>20/1	96	19	**20s**	91	>20/1	96
9	**20i**	94	>20/1	97	20	**20t**	96	>20/1	94
10	**20j**	96	>20/1	96	21[f]	**20u**	80	8.6/1	96
11	**20k**	94	>20/1	97					

[a] **1-CF$_3$**: 0.2 mmol, **19**: 0.24 mmol.
[b] Isolated yield.
[c] Determined by ^{1}H NMR analysis of the crude product.
[d] Determined by chiral stationary phase HPLC analysis.
[e] **1-CF$_3$**: 6.0 mmol, **19**: 7.2 mmol.
[f] 10 mol% of catalyst was used.

Substrate scope is delineated in Table 5. Substrates having electron withdrawing groups, such as ester, cyano group, trifluoromethyl and nitro group, at *para*-position could be applied to this catalysis (**20b**-**e**). High yield and stereoselectivity were achieved for these electron-deficient substrates. Cyano- and nitro-substituted 1,6-addition products were obtained with marginal erosion of enantioselectivity. Reactions using 1,3-benzodioxolyl and

naphthalenyl-contained substrates proceeded smoothly to give the corresponding products in high yield and stereoselectivity (**20f**, **20g**). Halogen substituents on substrates didn't impair the catalytic efficiency of Cu/**L5** complex. In general, halogen substituted *p*-QMs were well-tolerated and afforded excellent yield and stereoselectivity in regardless of substitution position (**20h**-**p**). Methoxy substituted electron-efficient substrates also showed good reactivity toward 7-azaindoline amide **1-CF$_3$** pronucleophile under standard conditions (**20q**-**s**), which indicated that the current catalyst system had a good compatibility in terms of electronic property of substrates. Next, *o*-Me substituted *para*-quinone methide was tested (**20t**). Slightly diminished enantioselectivity was observed probably due to steric factor. Last, for furan-based *p*-QM, 10 mol % catalyst loading was necessary to reach high conversion (**20u**).

It's notable that the present mesitylcopper/**L5** catalytic system accommodates other 7-azaindoline amides with different α-substituents, e.g., α-Me, α-N$_3$, and α-OBn in 1,6-additon reactions (Table 6). Alkylamide was known to be resistant to enolization, however, in this case alkylamide **1-Me** behaved as a latent enolate that could readily undergo enolization and react with electrophilic *p*-QM **19a** to afford product **21** in 72% yield with good stereoselectivity (14/1 d.r., 87% ee). Reaction using α-N$_3$ amide **1-N$_3$** delivered β-bis-aryl-α-amino acid analogue product **22** in high yield (83%). Low reaction temperature (–40 ºC) was key to achieving satisfactory stereoselectivity (10/1 d.r., 90% ee). An α-oxygen functionalized amide **1-OBn** was also applicable in this 1,6-addition reaction. Using same combination of mesitylcopper and **L5** as the catalyst, β-bis-aryl-α-hydroxy amide product **23** was formed in high yield (81%) and stereoselectivity (8.5/1 d.r., 90% ee).

Table 6. 1,6-Conjugate addition of amides **1-Me**, **1-N$_3$** and **1-OBn**[a]

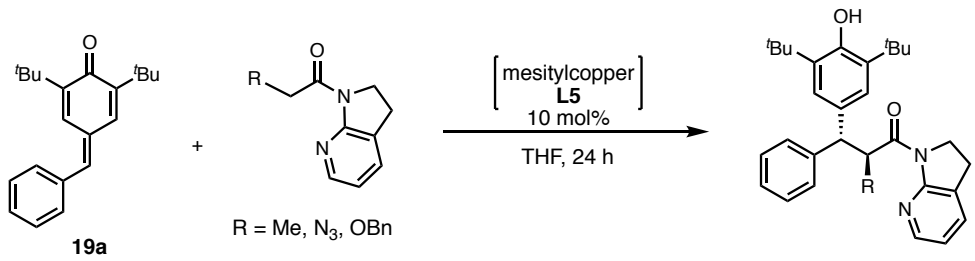

entry	amide	R =	temp (°C)	conc. (M)	product	yield[b] (%)	*anti/syn*[c]	ee[d] (%)
1	**1-Me**	Me	0	0.33	**21**	72	14/1	87
2	**1-N$_3$**	N$_3$	–40	0.1	**22**	83	10/1	90
3	**1-OBn**	OBn	rt	0.33	**23**	81	8.5/1	90

[a] amides: 0.2 mmol, **19a**: 0.24 mmol.
[b] Isolated yield.
[c] Determined by ^{1}H NMR analysis of the crude product.
[d] Determined by chiral stationary phase HPLC analysis.

The reaction profiles of amides **1-CF$_3$**, **1-Me**, **1-N$_3$** and **1-OBn** using *p*-QM **19a** as 1,6-acceptor were plotted in Figure 11. Under unified conditions using 10 mol % of mesitylcopper/**L5** at 0 ºC in 0.1 M concentration, amide **1-N$_3$** showed the highest reaction rate and reached full conversion first in 2 h. Reaction of amide **1-CF$_3$** achieved completion within 24 h, while amide **1-Me** underperformed in low concentration conditions (0.1 M). The conversion curve of amide **1-OBn** was sluggish during the recorded period. These results reflected the electron-withdrawing property of α-substituents on the amides.

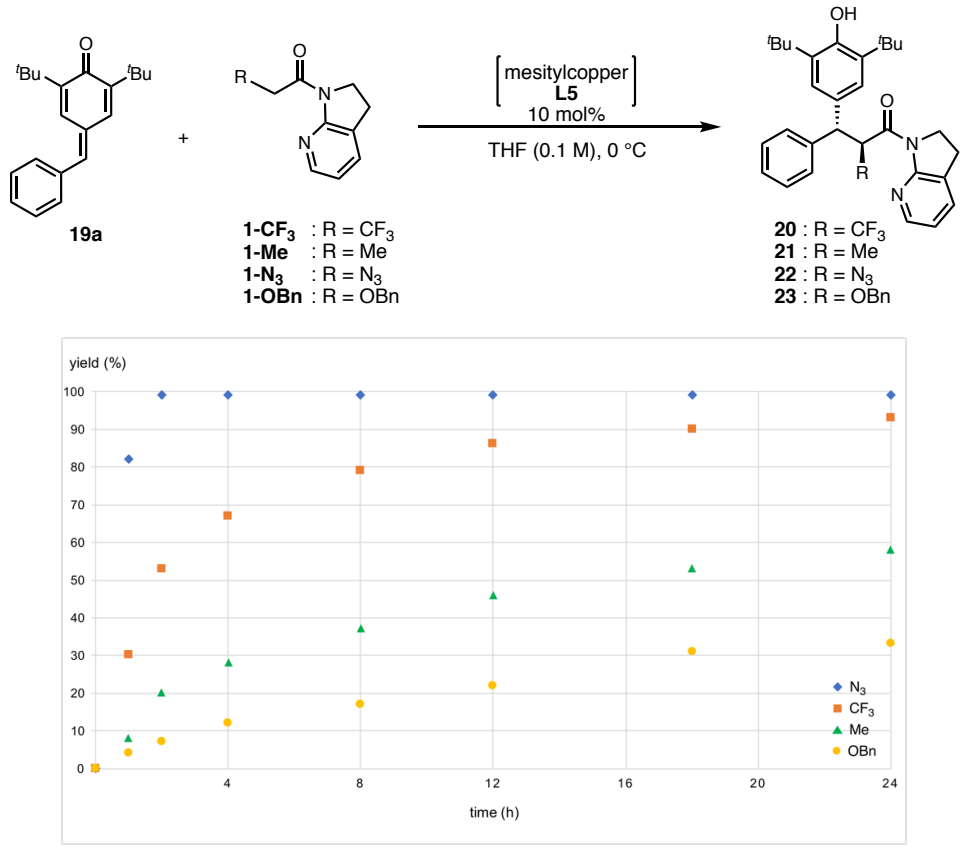

Figure 11. Reaction profile of 7-azaindoline amides with different α-substituents

1.2.4 Product transformations

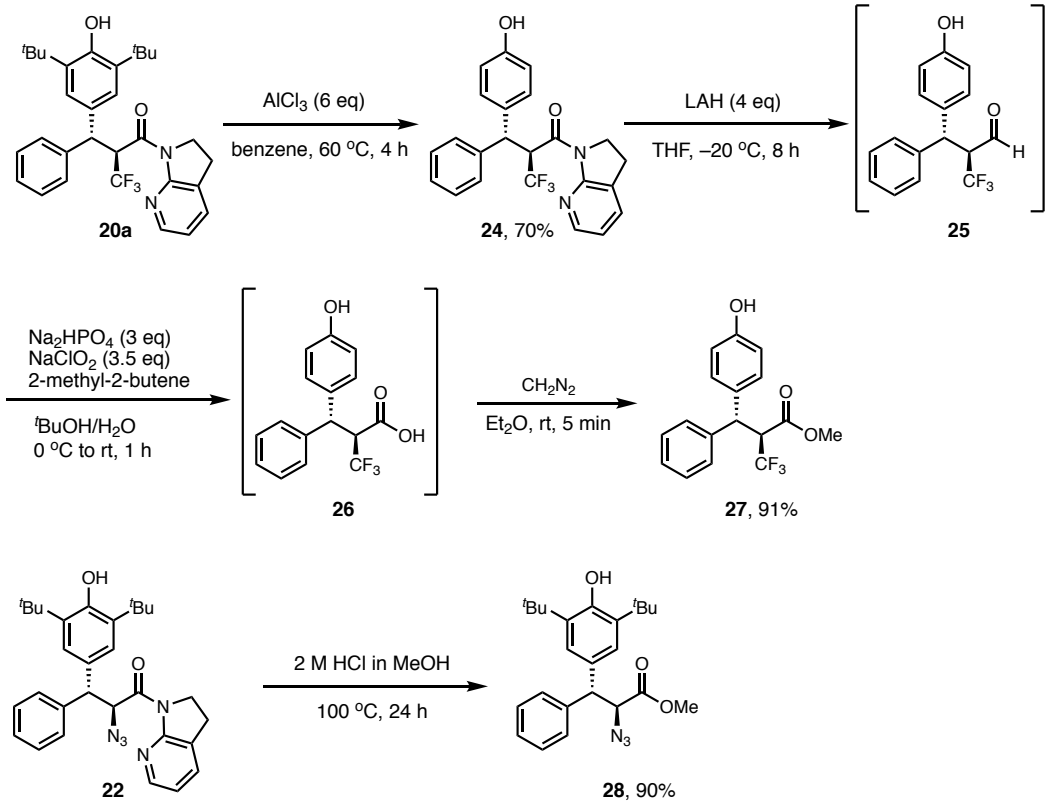

Scheme 11. Transformations of reaction products

1.2.5 Determination of absolute configuration

Single crystals of **20k** were obtained from dichloromethane/hexane at –20 °C (Figure 12).

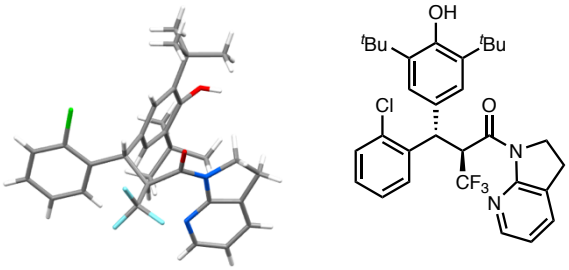

Figure 12. The structure of **20k**. White: hydrogen, gray: carbon, blue: nitrogen, red: oxygen, light green: chlorine, water blue: fluorine.

Single crystals of **24** were obtained from dichloromethane/hexane at room temperature (Figure 13).

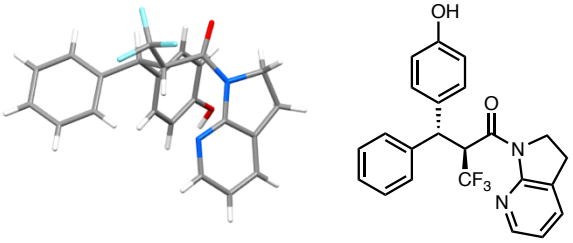

Figure 13. The structure of **24**. White: hydrogen, gray: carbon, blue: nitrogen, red: oxygen, water blue: fluorine.

The absolute configuration of the product derived from **1-Me** was determined by X-ray crystallography of **21**. Single crystals of **21** were obtained from dichloromethane/hexane at room temperature (Figure 14).

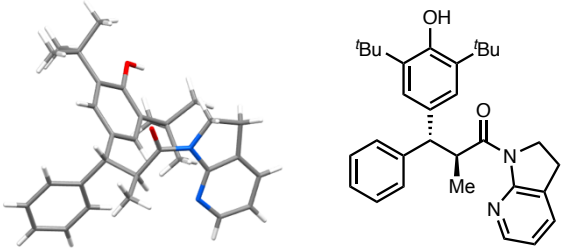

Figure 14. The structure of **21**. White: hydrogen, gray: carbon, blue: nitrogen, red: oxygen.

The absolute configuration of the product derived from **1-N$_3$** was determined by X-ray crystallography of **28**. Single crystals of **28** were obtained from dichloromethane/hexane at room temperature (Figure 15).

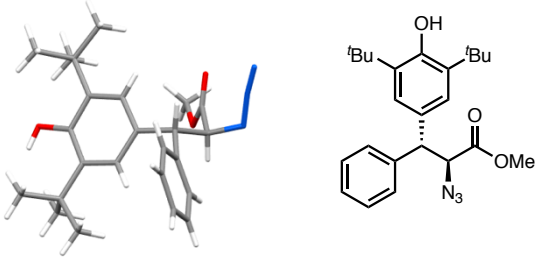

Figure 15. The structure of **28**. White: hydrogen, gray: carbon, blue: nitrogen, red: oxygen.

The absolute configuration of the product derived from **1-OBn** was determined by X-ray crystallography of **23**. Single crystals of **23** were obtained from dichloromethane/hexane at room temperature (Figure 16).

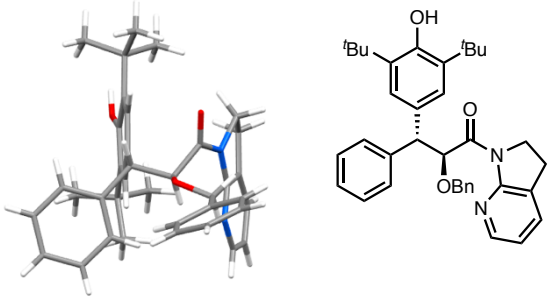

Figure 16. The structure of **23**. White: hydrogen, gray: carbon, blue: nitrogen, red: oxygen.

1.3 Summary

In summary, 7-azaindoline amides have been proved to be potent nucleophiles in soft Lewis acid/hard Brønsted base cooperative catalysis. Particularly in this context, α-azido 7-azaindoline amide was successfully employed in a synthetic protocol of enantioenriched α-azido-β-amino acids (Scheme 12). The *anti*-α,β-diamino acid was obtained after hydrogenation of azido group.

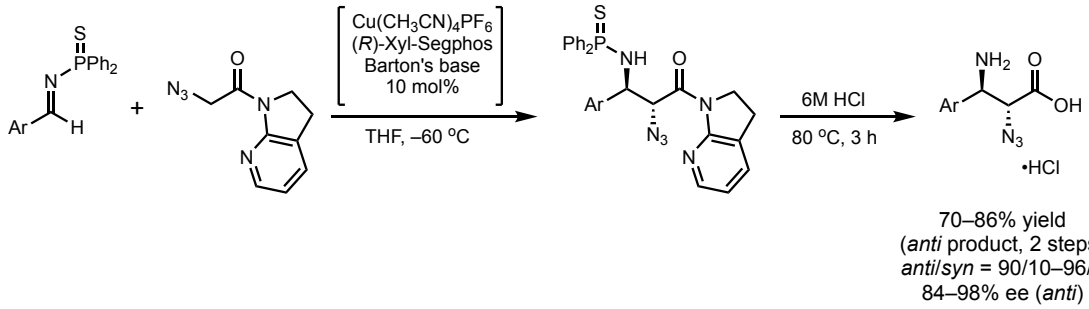

Scheme 12. Protocol for synthesis of α-azido-β-amino acids

Next, 7-azaindoline amides with different α-substituents were exploited in a direct catalytic asymmetric 1,6-conjugated addition to *p*-QMs (Scheme 13). This method provided an efficient way to synthesize chiral diarylmethine building blocks and further demonstrated the versatility of 7-azaindoline amides and soft Lewis acid/hard Brønsted base cooperative catalysis in asymmetric C–C bond forming reactions.

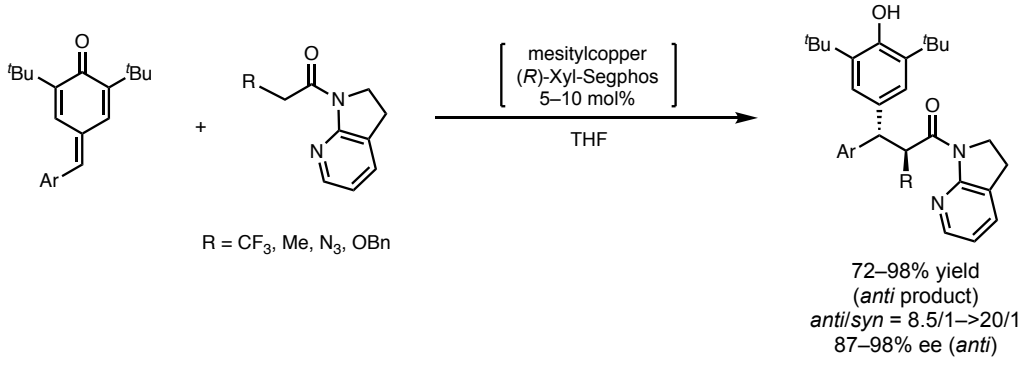

Scheme 13. Direct catalytic asymmetric 1,6-conjugated addition of amides to *p*-QMs

2. Chapter 2. Photocatalytic Functionalization of α-Oxy C(sp^3)–H Bond

2.1 Introduction

The past few years have witnessed profound advancement in photocatalysis, which has demonstrated the versatility in C–C and C–heteroatom bonds forming reactions.[22] Direct photoexcitation of organic substrates by visible light is unlikely to access since they can barely absorb visible light. However, the ability of photosensitizer to convert photoenergy in visible light into chemical energy, thereafter, activate organic molecules via single-electron transfer (SET) or energy transfer is of great interest to chemists and provides new possible entries to develop unprecedented chemical transformations. The merger of photoredox and transition metal catalysis has been exploited as a powerful cross-coupling platform forging C-C and C-heteroatom bonds since the pioneering studies carried out by MacMillan, Doyle and Molander were published in 2014 (Scheme 14).[23a,24a]

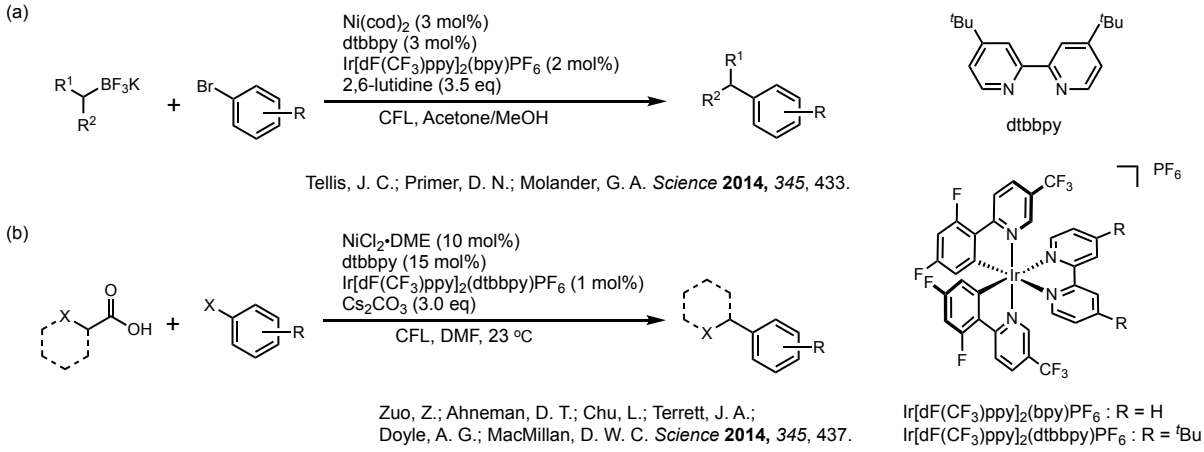

Scheme 14. Initial reports on photoredox/nickel dual catalysis

In this context, a diverse array of C(sp^2)–C(sp^3) and C(sp^3)–C(sp^3) bonds forming reactions has been well established wherein carboxylates,[23] trifluoroborates[24] and silicates[25] that can be activated by photosensitizers under visible light irradiation are employed as pronucleophiles instead of organometallic nucleophiles (Figure 17).

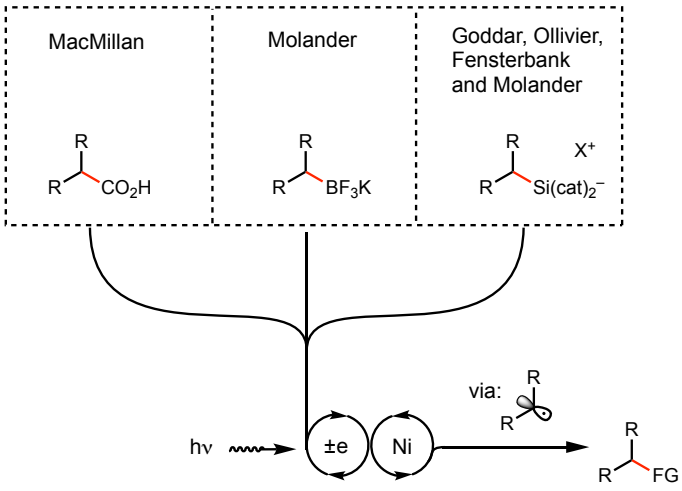

Figure 17. Dual photoredox nickel-catalyzed dual C–C forming reactions through oxidative radical formation

Besides C–C formation, photoredox/nickel dual catalysis has also been applied in C–X cross-coupling protocols (Scheme 15). The light-driven facile C(sp^2)–O cross-coupling was reported by MacMillan group (Scheme 15a).[26] C(sp^2)–N cross-coupling under mild conditions using synergetic iridium photoredox and nickel catalysis following the same blueprint was developed by Buchwald and Macmillan (Scheme 15b).[27] Highly reactive but elusive Ni(III) species, which are generated by SET process with excited iridium photocatalyst through reductive

quenching, are attributed for facile C–X reductive elimination event in these C(sp^2)–heteroatom bonds forming reactions. Meanwhile, Oderinde and Johannes reported photoredox/nickel-catalyzed cross-couplings of anilines and thiols with aryl halides (Scheme 15c and d).[28]

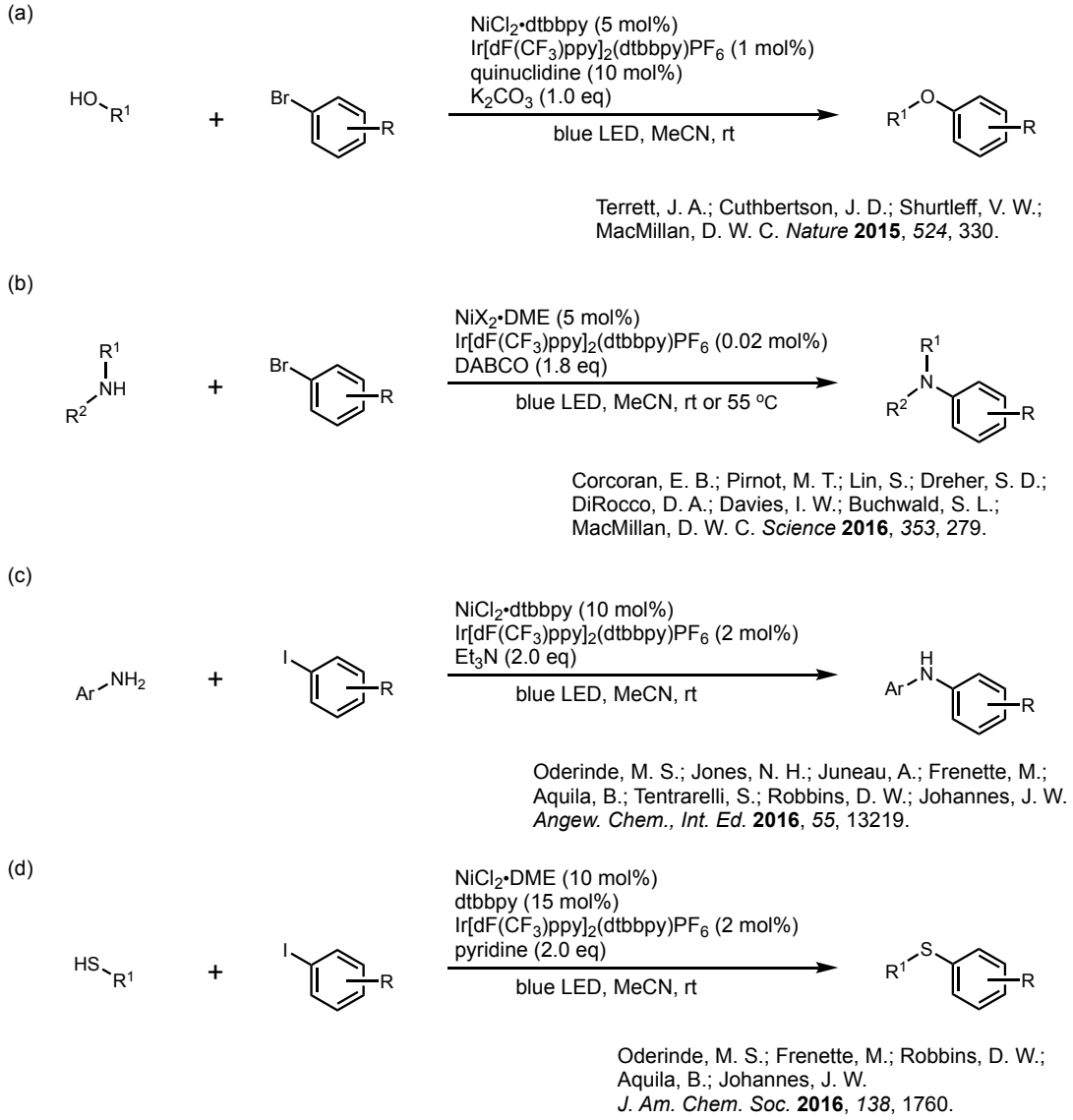

Scheme 15. Photoredox-mediated nickel-catalyzed C–X forming reactions

It is also worth noting that C(sp^3)–H bonds can be utilized as latent nucleophiles in a light-mediated cross-coupling reaction featuring a triple catalytic system orchestrating an iridium photocatalyst, a nickel catalyst and an organoamine hydrogen atom transfer (HAT) co-catalyst.[29]

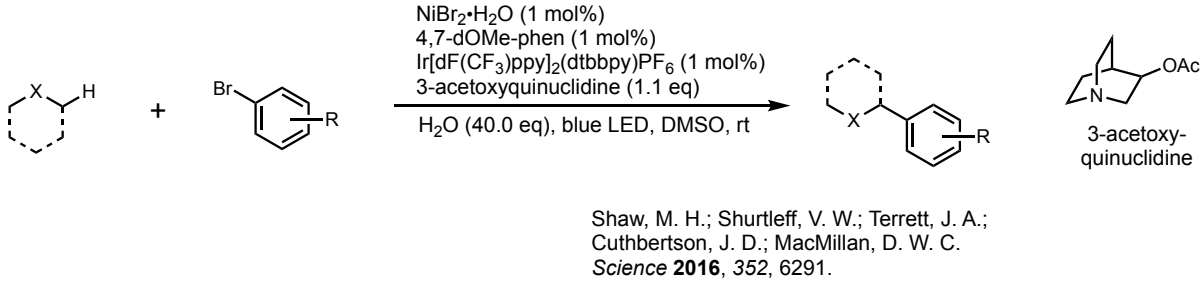

Shaw, M. H.; Shurtleff, V. W.; Terrett, J. A.; Cuthbertson, J. D.; MacMillan, D. W. C. Science 2016, 352, 6291.

Scheme 16. Photoredox, HAT nickel-catalyzed C–H arylation

In above-mentioned methodologies, the role of photocatalyst is to perform SET process to activate substrate, co-catalyst or manipulate transition metal valence. Although the photosensitization that could initiate a triplet-triplet energy transfer between light-harvest complex and transition metal complex had been recognized long time ago, until quite recently, attempts that exploited this phenomenon were made to accomplish nickel-catalyzed cross-couplings in combination of iridium photocatalysis. Cross-coupling of carboxylic acids with aryl bromides mediated by photosensitized dual catalysis of nickel and iridium was documented by MacMillan and co-workers (Scheme 17a).[30] Molander and co-workers developed photochemical nickel-catalyzed direct C(sp^3)–H arylation (Scheme 17b).[31] In both cases, generation of electronically excited nickel(II) triplet species through triplet-triplet energy transfer process was proposed as key factor.

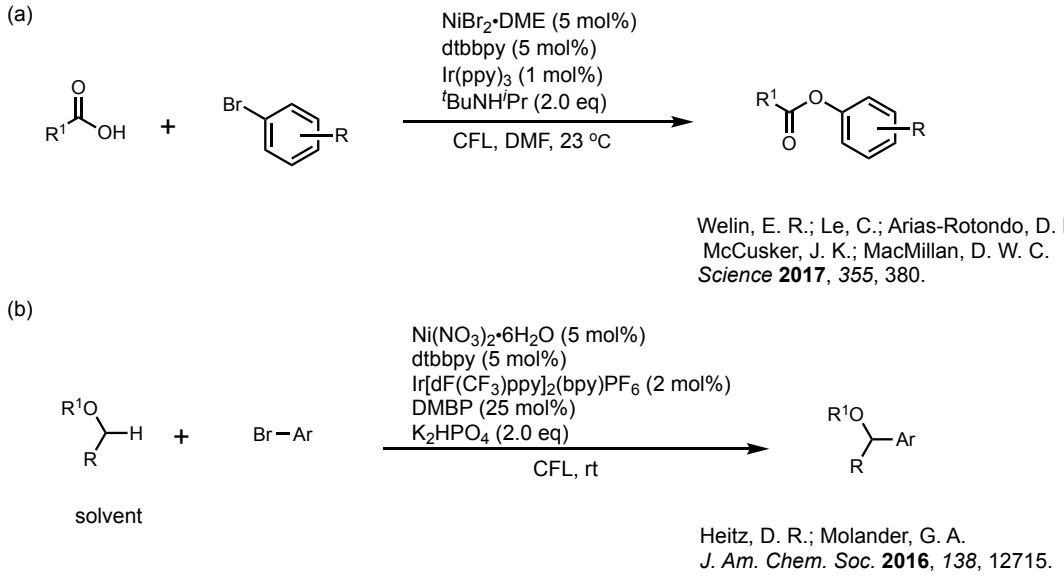

Scheme 17. Energy transfer-enabled nickel-catalyzed cross-couplings

Similar to the Molander's report of nickel-catalyzed direct C(sp^3)–H arylation, Doyle and co-workers reported direct C(sp^3)–H cross-coupling enabled by catalytic generation of chlorine radicals (Scheme 18).[32] Instead of energy transfer between iridium photocatalyst with nickel catalyst, Doyle proposed that photolysis of Ni(III) aryl chloride species, generated by SET from Ni(II) intermediate to iridium photocatalyst, facilitated the catalytic generation of chlorine radicals, which were responsible for C(sp^3)–H abstraction.

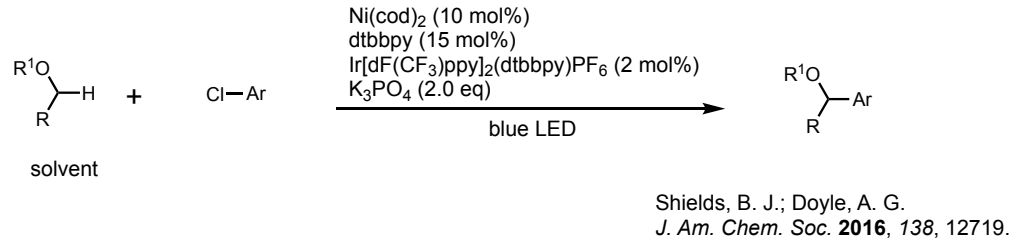

Scheme 18. Photochemical nickel-catalyzed C(sp^3)–H cross-coupling

2.2 Photocatalytic acylation of α-oxy C(sp^3)–H bond

Previously, successful realization of photocatalytic activation of α-oxy C(sp^3)–H in ethers has been demonstrated by the MacMillan's group using photoredox/HAT dual catalysis (Scheme 19).[33] Thiol and persulfate salt were employed as HAT co-catalyst respectively, collaborating with Ir photocatalysts to generate corresponding thiyl and sulfate radicals. These radicals reacted with ether substrates to give nucleophilic α-oxyalkyl radicals, which attacked electron-deficient substrates subsequently.

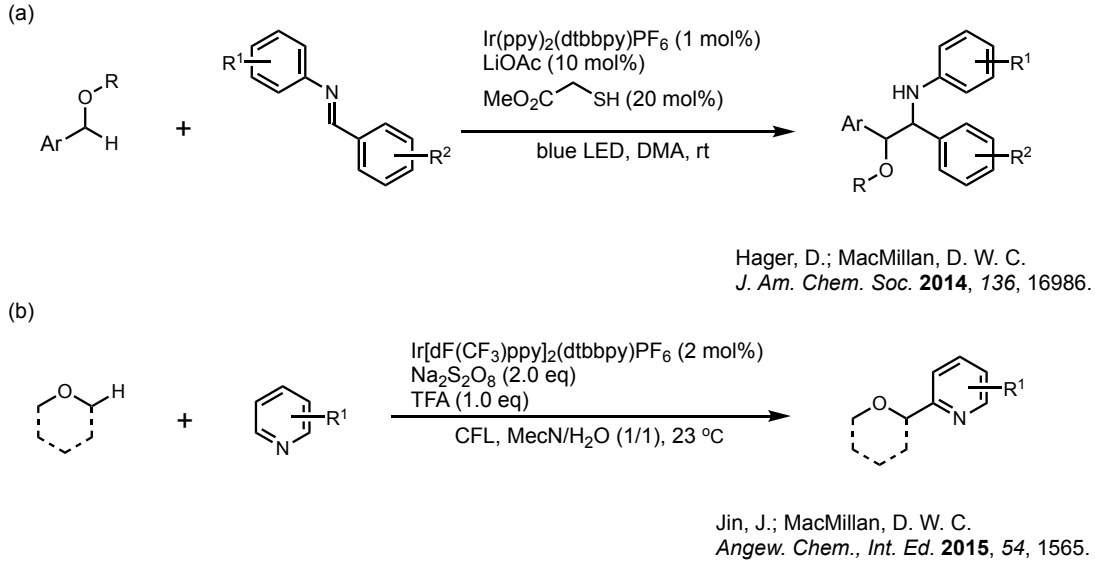

Scheme 19. α-Oxy C(sp^3)–H activation using photoredox/HAT dual catalysis

Although acylation reactions of carboxylic acids,[34] amines[35] and organotrifluoroborates[24h] by using light-driven Ir/Ni catalysis have been realized, direct α-oxy C(sp^3)–H acylation is still uncharted. Based on the reported literatures, I envisioned a direct α-oxy C(sp^3)–H acylation of ethers via synergistic Ir/Ni catalysis (Scheme 20).

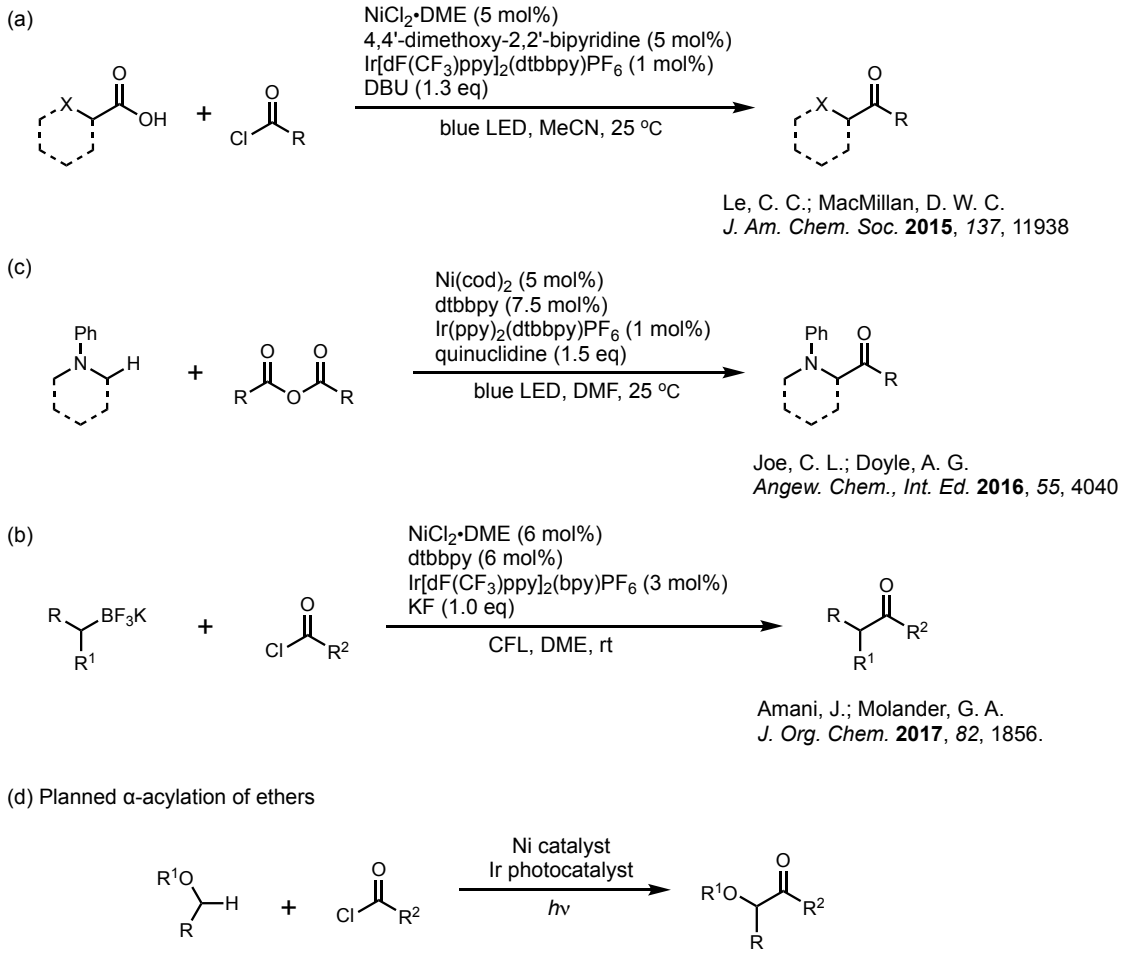

Scheme 20. Visible-light-mediated acylation reactions using Ir/Ni catalysis

2.2.1 Conditions screening

Table 7. Conditions screening[a]

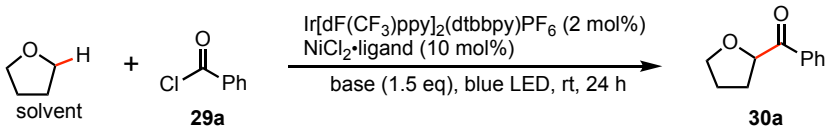

entry	ligand	concn (M)	base	yield[b] (%)
1	**L1**	0.05	K_2CO_3	31
2	**L1**	0.05	$KHCO_3$	34
3	**L1**	0.05	Cs_2CO_3	<10
4	**L1**	0.05	K_3PO_4	40
5	**L1**	0.05	K_2HPO_4	<10
6	**L1**	0.05	KH_2PO_4	<10
7	**L1**	0.05	DBU	<10
8	**L1**	0.05	Et_3N	<10
9	**L1**	0.05	Quinuclidine	<10
10	**L2**	0.05	K_3PO_4	66
11	**L3**	0.05	K_3PO_4	50
12	**L4**	0.05	K_3PO_4	28
13	**L5**	0.05	K_3PO_4	29
14	**L6**	0.05	K_3PO_4	25
15	**L7**	0.05	K_3PO_4	43
16	**L8**	0.05	K_3PO_4	33
17	**L2**	0.1	K_3PO_4	76
18	**L2**	0.2	K_3PO_4	77

[a] Reactions were carried out using 0.2 mmol acyl chloride **29a**.
[b] Determined by ^1H NMR using 1,3,5-trimethoxybenzene as an internal standard.

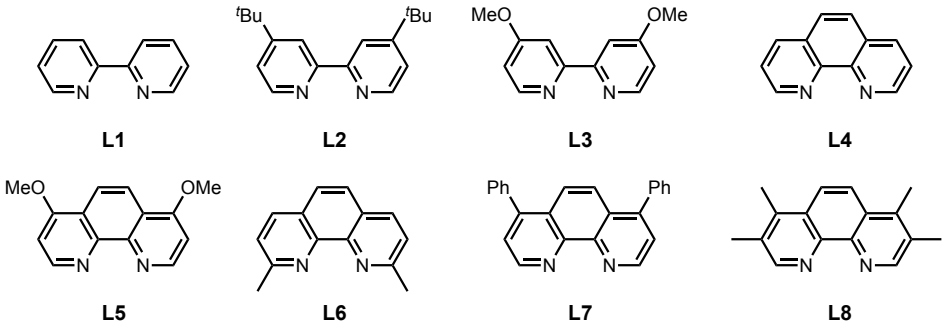

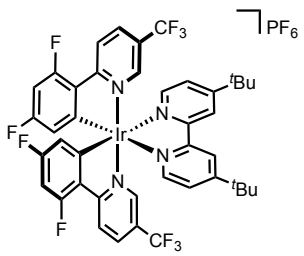

$Ir[dF(CF_3)ppy]_2(dtbbpy)PF_6$

Initially, I found that the acylation reaction of tetrahydrofuran (THF) with benzoyl chloride **29a** could occur in the presence of $NiCl_2$·**L1**, $Ir[dF(CF_3)ppy]_2(dtbbpy)PF_6$ and K_2CO_3 under irradiation of blue LEDs (Table 7, entry 1). Further screening of bases showed that potassium phosphate (K_3PO_4) could improve the yield (entry 4, 40%), and organoamines were proved to be ineffective for the reaction (entries 7–9). Next, I moved to examine ligand effect on this reaction (entries 10–16). Generally, 2,2'-bipyridine-derived ligands showed better reactivity than 1,10-phenanthroline-based ones. 4,4'-Di-*tert*-butyl-2,2'-bipyridine (**L2**) gave the highest yield (entry 10, 66%). Concentrated conditions could further improved reaction yield to 77% (entry 18).

2.2.2 Substrates scope

Table 8. Substrates scope[a]

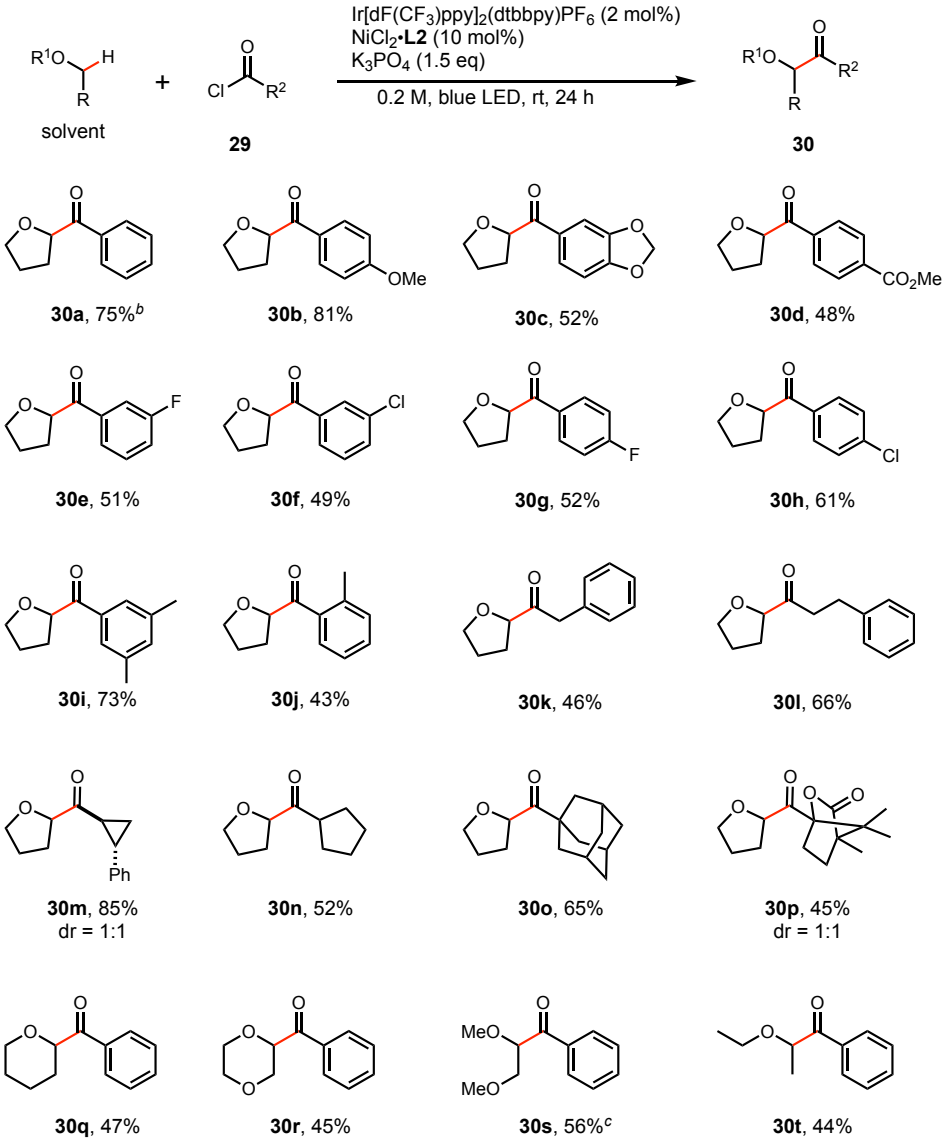

[a] Reactions were carried out using 0.4 mmol acyl chloride **29**. Isolated yield was reported.
[b] 69% yield was obtained from a 1.0 mmol scale reaction.
[c] Regioisomer (acylation on Me group) was isolated in 21% yield.

With the optimized conditions in hand, the scope of both the acyl chlorides and ethers were evaluated. As depicted in Table 8, a variety of benzoyl chlorides bearing electron-donating and -withdrawing groups was tested and able to couple with THF to deliver corresponding acylation products (**30b**–**d**). Halogen substitutions on the aromatic ring had no interference in the reactions (**30e**–**h**). Aliphatic acyl chlorides could undergo coupling reactions without troubles (**30k**–**p**). Reactions proceeded smoothly using coupling partner substrates that were mono or di-

substituted at alpha position (**30k**–**n**). Notably, a cyclopropane derivative was intact during the reaction and able to provide the corresponding ketone product in high yield (**30m**, 85%). The successful coupling reactions using bulky 1-adamantanecarbonyl chloride (**30o**) and structurally congested (*S*)-camphanic chloride (**30p**) showcased the robustness of this catalytic system and its capability of late-stage modification of complicated molecules. Finally, other cyclic (**30q**,**r**) and acyclic (**30k**,**t**) ethers besides THF could also be acylated under standard conditions, albeit in slightly lower yield.

2.2.3 Mechanistic study

To gain additional insight into the present α-oxy C(sp^3)–H functionalization of ethers, I next performed a kinetic isotope effect (KIE) study. The intermolecular competition experiment was carried out in a mixture of THF/THF-d_8 (1/1, v/v) (Figure 18a). Value of KIE was measured by ^{1}H NMR and ^{2}H NMR spectroscopy to be 2.4 indicating that C(sp^3)–H bond cleavage was involved in catalytic cycle. Given the fact that ethers possess relatively high oxidation potentials (for THF, E = 1.75 V vs SCE),[36] the cleavage of α-oxy C(sp^3)–H bond may not be feasible through SET/deprotonation process initiated by excited *Ir[dF(CF_3)ppy]$_2$(dtbbpy)PF_6 ($E_{1/2}^{*III/II}$ = 1.21 V vs SCE in MeCN).[37] Inspired by the recent publications of direct α-oxy C(sp^3)–H arylation from Molander and Doyle, I hypothesized that the generation of a chlorine radical via homolysis of an excited triplet state Ni(II) acyl chloride complex, which could be accessed through a triplet-triplet energy transfer from excited photosensitizer, [38-40] played an important role in this reaction in which the resulting chlorine radical would be sufficient to abstract the α-oxy hydrogen atom from THF (BDE of H–Cl: 102 kcal/mol, BDE of THF: 92 kcal/mol)[41] to produce a nucleophilic α-oxy radical.

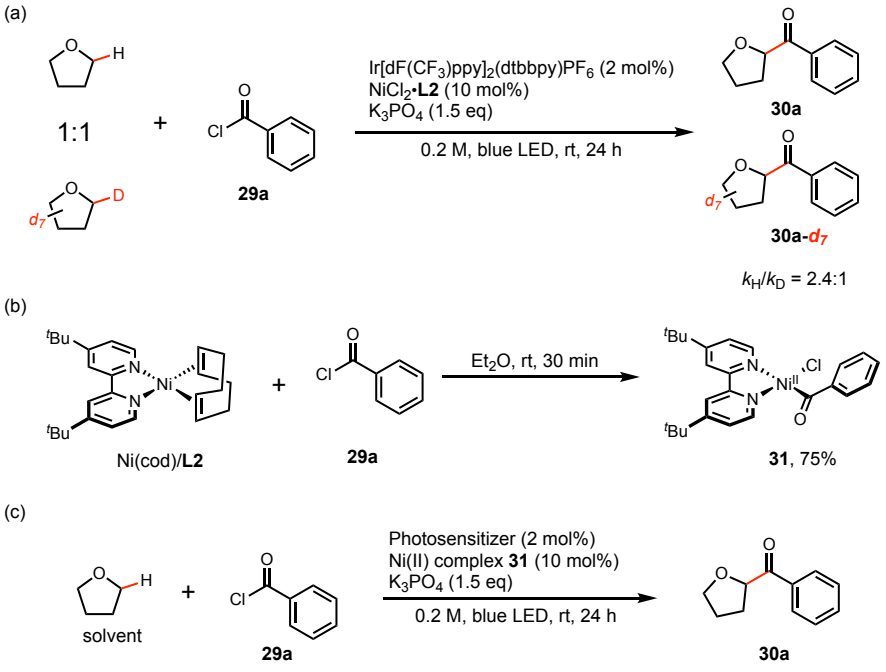

entry	photosensitizer	$E_{PC^*/PC}$ (V)	λ_{max}(emission) (nm)	E_T (kcal/mol)	yield (%)
1	Ir[dF(CF_3)ppy]$_2$(dtbbpy)PF_6	1.21	470	60.1	65
2	Ir(ppy)$_3$	0.31	518	55.2	trace
3	[9-MesAcr]ClO_4	2.05	590	–	trace
4	Ru(bpy)$_3Cl_2$	0.77	615	46.5	trace
5	none	–	–	–	trace

Figure 18. (a) Kinetic isotope effect experiment, (b) Synthesis of Ni(II) complex **31**, (C) Reactions of **31** with THF.

To validate this hypothesis, a series of experiments was performed. Firstly, Ni(II) acyl chloride complex **31** was synthesized from Ni(cod)/**L2** and benzoyl chloride **29a** (Figure 18b). I found that complex **31** could promote the reaction under blue LED irradiation using Ir[dF(CF_3)ppy]$_2$(dtbbpy)PF_6 photosensitizer that possessed a high triplet energy (Figure 18c, entry 1). In stark contrast, photosensitizers with lower triplet energy failed to facilitate the reactions efficiently, and only trace amount of product was observed in those cases (Figure 18c, entry 2-4). It's worth noting that the poor yield obtained from the reaction using [9-MesAcr]ClO_4, which has a much higher oxidation potential ($E_{1/2}^{*PC/PC}$ = 2.06 V vs SCE in MeCN),[42] implying that oxidation of Ni(II) to Ni(III) via SET might not be involved during the reaction (Figure 18c, entry 3). In control experiment, visible light failed to promote the reaction in the absence of photosensitizer meaning that triplet state of complex **31** could not be reached directly by using visible light irradiation (Figure 18c, entry 5). This result matched the observation from the UV-vis spectrum of complex **31** in which no detectable absorption showed in visible light region (400–600 nm) (Figure 19). However, an intense absorption band at UV region suggested that UV irradiation should promote an excitation of complex **31** into a higher energy excited singlet state that would lead to the excited triplet state after intersystem crossing and relaxations.

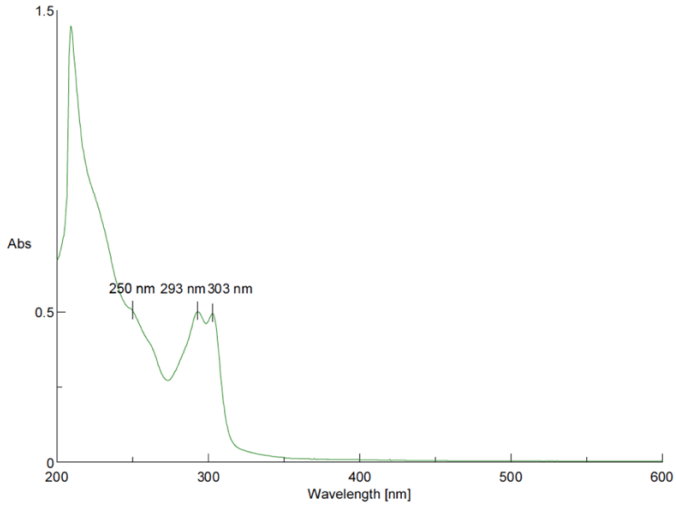

Figure 19. UV–vis spectrum of complex **31**

As the results shown in Scheme 21, the product was observed in 41% yield without a photosensitizer after 8 hours of UV (254 nm) irradiation. In the control reaction, no formation of the product was observed when the reaction was solely treated with UV (254 nm) irradiation in the absence of complex **31**. It is unlikely that a Ni(III) species is involved in catalytic cycle since UV irradiation alone can promote the reaction without using any oxidant.

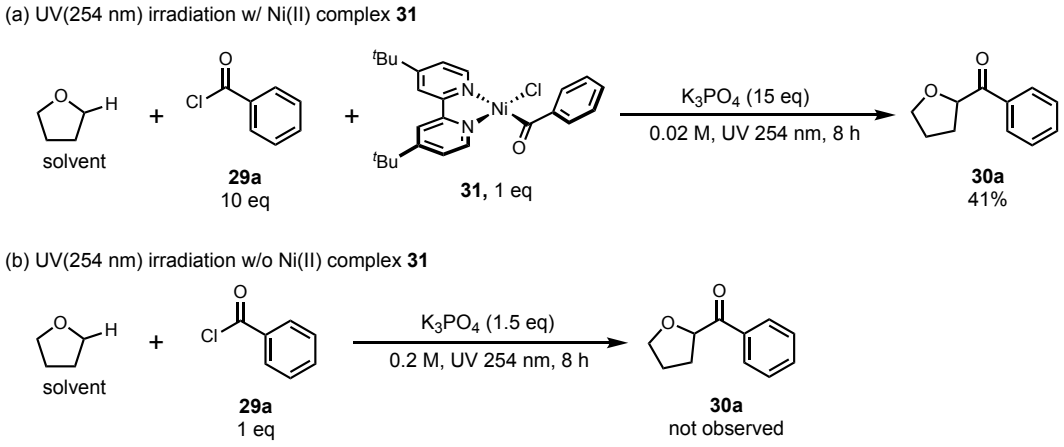

Scheme 21. α-Benzoylation of THF under UV (254 nm) irradiation

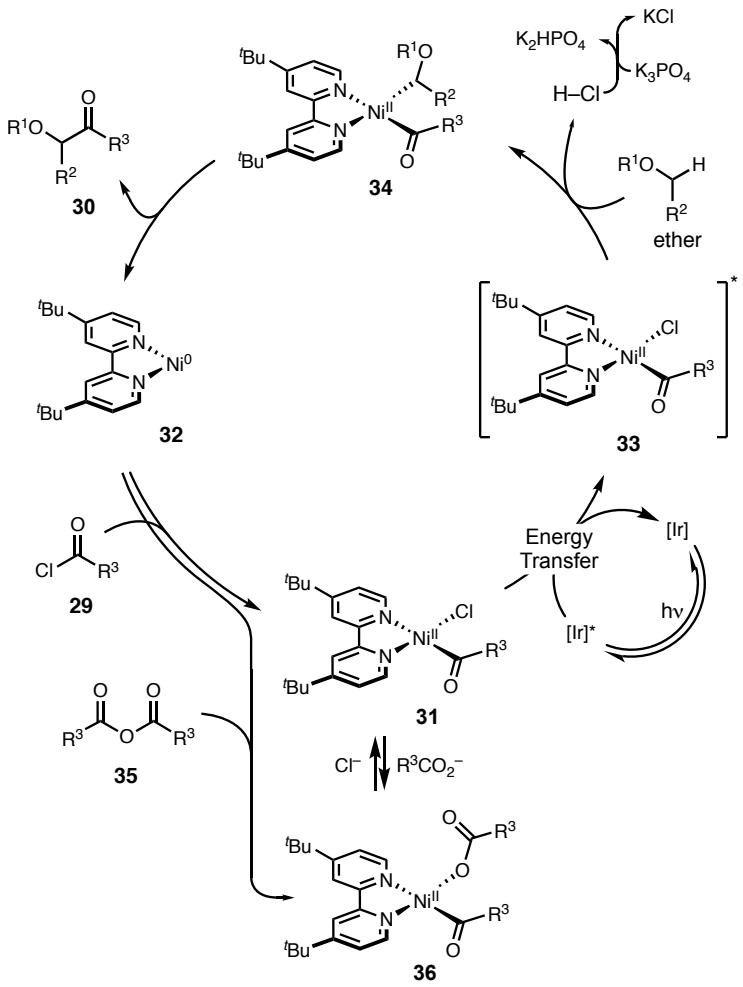

Figure 20. Plausible catalytic cycle

Based on above mentioned, a plausible catalytic cycle was proposed (Figure 20). Ni(II) intermediate (**31**) is generated after oxidative addition of an acyl chloride to Ni(0) (**32**). Ir photosensitizer serves as an energy shuttle, passing energy from its long-lived triplet state to Ni(II) intermediate (**31**) by engaging triplet-triplet energy transfer to produce triplet state Ni(II) (**33**). This pivotal intermediate is possible to undergo Ni–Cl homolysis. Yielded chlorine radical is able to withdraw the α-oxy hydrogen atom from THF to give α-oxy radical, subsequently captured by Ni catalyst to form intermediate **34**. Reductive elimination delivers corresponding ketone product and regenerates Ni(0) catalyst.

Besides acyl chlorides, anhydrides **35** and **37** could also be used as electrophiles for acylation under the same conditions when $NiCl_2$ was used as the Ni source, albeit in lower yield (Scheme 22a). $Ni(OAc)_2$ could mediate the acylation reaction of acyl chloride **29a**, however, $Ni(OAc)_2$ turned ineffective in the case that anhydride **35** was used for acylation. In contrast, the chloride additive (^{n}Bu$_4$NCl) facilitated the reaction of anhydride **35** using $Ni(OAc)_2$, indicating that Ni intermediate **36**, which was formed through oxidative addition of **35**, could transform into Ni complex **31** through ligand exchange and enter into the catalytic cycle. Although an energy transfer-based reaction mechanism was proposed, the electron transfer-based Ni(I)/Ni(III) catalytic cycle could not be completely ruled out. Further investigation involving transient absorption spectroscopic experiments is necessary to unveil the quenching pathway of the excited Ir photosensitizer.[43]

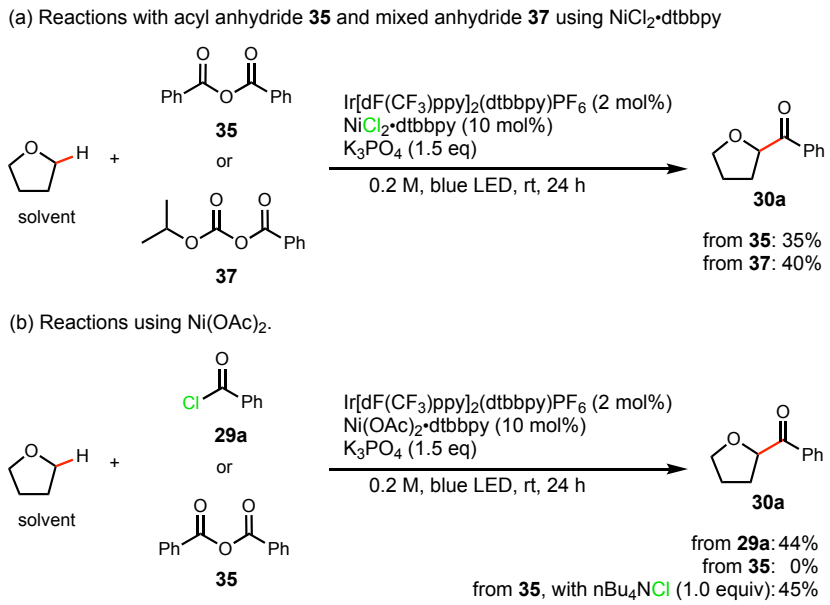

Scheme 22. Acylation using anhydrides

2.3 Asymmetric photocatalytic acylation of α-oxy C(sp^3)–H bond

An investigation on the asymmetric version of the photocatalytic acylation of α-oxy C(sp^3)–H bond was also engaged. The ligand screening for asymmetric acylation of α-oxy C(sp^3)–H bond was summarized in Figure 21.

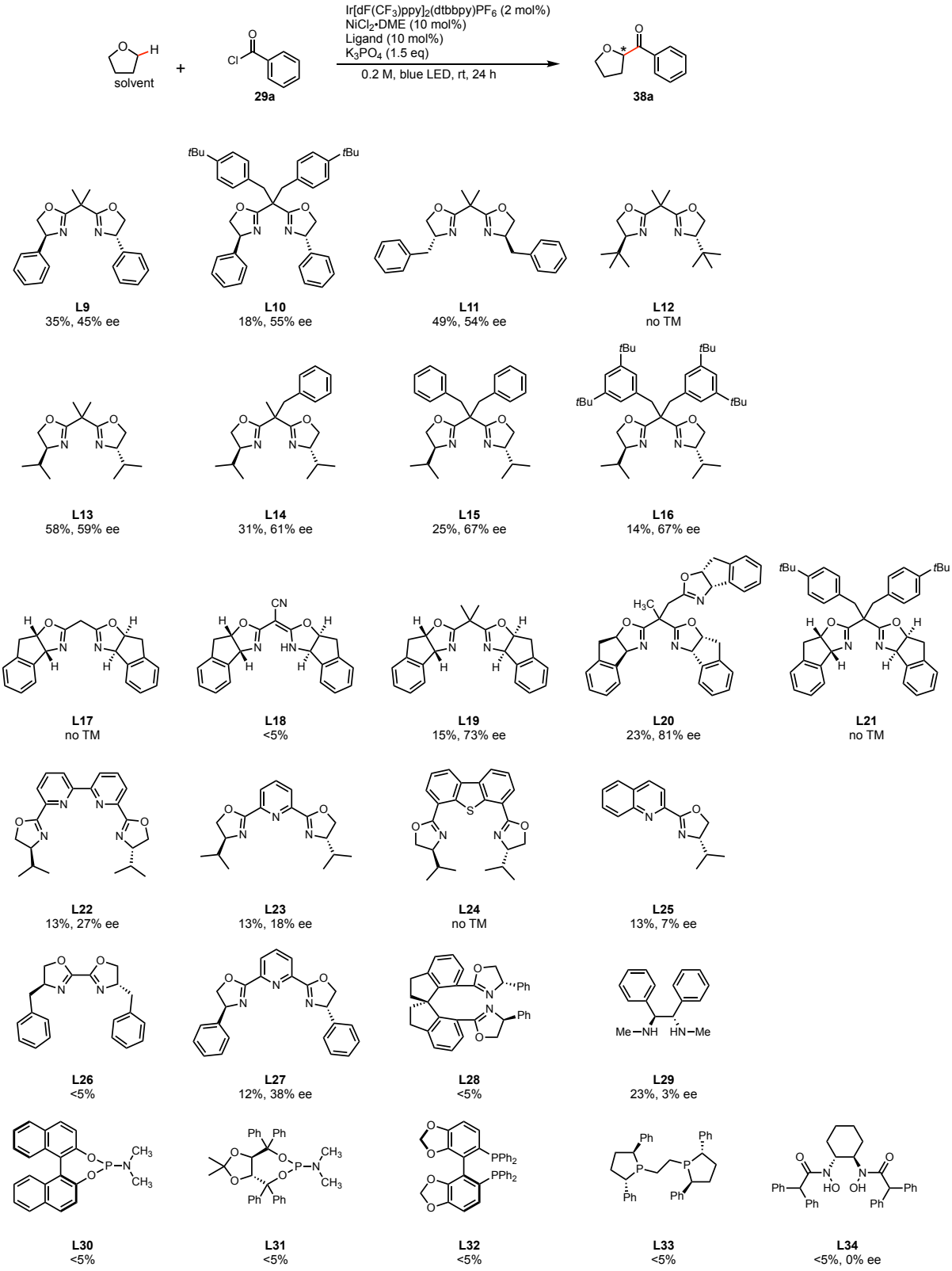

Figure 21. Ligand screening

In general, methylene bridged bis(oxazoline) ligands (BOX ligands) (**L9-21**) showed relatively better reactivity in the asymmetric acylation reaction. Neither shrunken nor expanded ring size on the backbone of the BOX ligands could bring beneficial effect in reactivity (**L22-28**). Other types of ligands gave inferior results (**L29-34**). **L13** provided the most balanced result (58% yield, 59% ee) and thus it was chosen for further conditions screening. Next, a survey of nickel source and base was conducted (Table 9). $NiCl_2$·DME was proved to be the best nickel source for the acylation reaction and the use of $KHCO_3$ slightly improved yield and enantioselectivity (entry 13).

Table 9. Conditions screening[a]

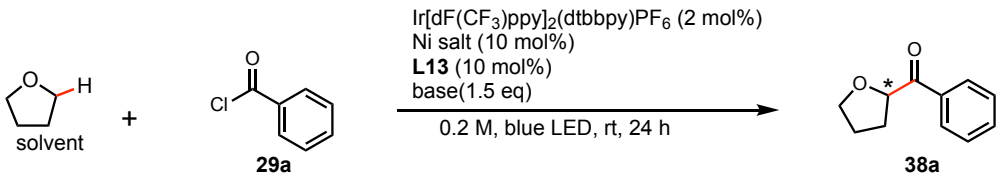

entry	Ni salt	base	yield[b] (%)	ee[c] (%)
1	$NiCl_2$•DME	K_3PO_4	58	59
2	$NiCl_2$•6H_2O	K_3PO_4	43	55
3	$Ni(OAc)_2$•4H_2O	K_3PO_4	33	50
4	$Ni(NO_3)_2$•6H_2O	K_3PO_4	0	–
5	$Ni(ClO_4)_2$•6H_2O	K_3PO_4	0	–
6	$Ni(acac)_2$	K_3PO_4	38	54
7	$Ni(OTf)_2$	K_3PO_4	0	–
8	$NiBr_2$	K_3PO_4	31	45
9	$Ni(cod)_2$	K_3PO_4	37	63
10	$NiCl_2$•DME	K_2HPO_4	60	52
11	$NiCl_2$•DME	KH_2PO_4	<5	–
12	$NiCl_2$•DME	K_2CO_3	<5	–
13	$NiCl_2$•DME	$KHCO_3$	73	64
14	$NiCl_2$•DME	Na_2CO_3	26	54
15	$NiCl_2$•DME	$NaHCO_3$	27	66
16	$NiCl_2$•DME	Li_2CO_3	37	46
17	$NiCl_2$•DME	Cs_2CO_3	24	64
18	$NiCl_2$•DME	CsF	30	67
19	$NiCl_2$•DME	$(NH_4)_2CO_3$	<5	–
20	$NiCl_2$•DME	NH_4HCO_3	10	66

[a] **29a**: 0.1 mmol.
[b] Determined by ^{1}H NMR using 1,3,5-trimethoxybenzene as an internal standard.
[c] Determined by chiral stationary phase HPLC analysis.

Subsequently, a handful of benzoyl chlorides with electron-withdrawing and donating substituents was examined under the conditions used in entry 13 (Table 10). Unfortunately, these reactions didn't show any promising results.

Table 10. Substrate scope[a]

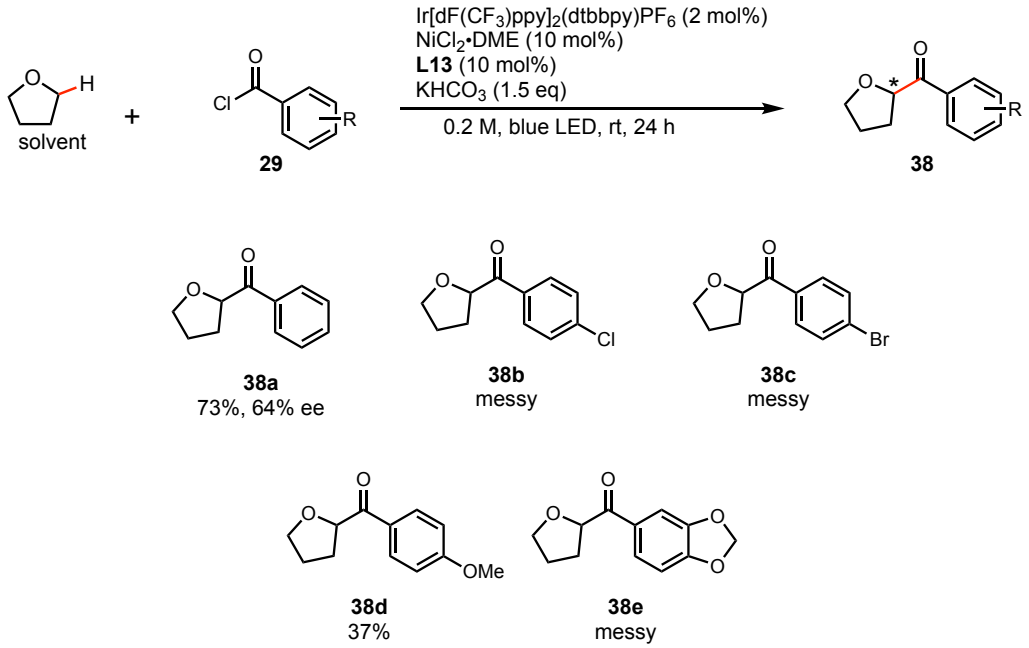

[a] Reactions were carried out using 0.1 mmol acyl chloride **29**. Yield was determined by ^{1}H NMR using 1,3,5-trimethoxybenzene as an internal standard. .

2.4 Photocatalytic arylation of α-oxy C(sp³)–H bond

Prior to the investigation of photocatalytic acylation of α-oxy C(sp³)–H bond, the project of photocatalytic arylation of α-oxy C(sp³)–H bond was also carried out. Since an identical arylation of α-oxy C(sp³)–H bond was published earlier by Molander,[31] this work was not able to be published. The project was summarized in the following Tables 11–13.

Table 11. Conditions screening

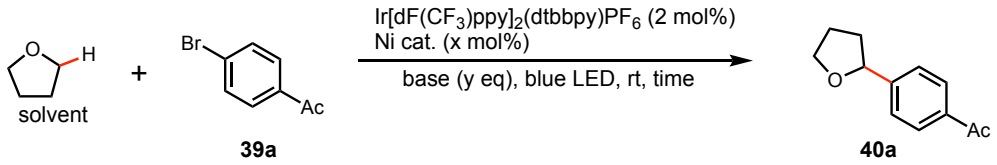

entry	Ni cat. (x mol%)	concn (M)	time (h)	base (y eq)	yield[c] (%)
1[a]	$NiCl_2$•**L1** (10)	0.2	24	Cs_2CO_3 (2)	34
2[a]	$NiCl_2$•**L2** (10)	0.2	24	Cs_2CO_3 (2)	34
3[a]	$NiCl_2$•**L3** (10)	0.2	24	Cs_2CO_3 (2)	0
4[a]	$NiCl_2$•**L4** (10)	0.2	24	Cs_2CO_3 (2)	0
5[a]	$NiCl_2$•**L5** (10)	0.2	24	Cs_2CO_3 (2)	0
6[a]	$NiCl_2$•**L6** (10)	0.2	24	Cs_2CO_3 (2)	0
7[b]	$NiCl_2$•**L1** (5)	0.05	12	Cs_2CO_3 (1.2)	74
8[b]	$NiCl_2$•**L1** (5)	0.05	12	K_2CO_3 (1.2)	68
9[b]	$NiCl_2$•**L1** (5)	0.05	12	$KHCO_3$ (1.2)	70
10[b]	$NiCl_2$•**L1** (5)	0.05	12	Na_2CO_3 (1.2)	62
11[b]	$NiCl_2$•**L1** (5)	0.05	12	$NaHCO_3$ (1.2)	50
12[b]	$NiCl_2$•**L1** (5)	0.05	12	K_3PO_4 (1.2)	47
13[b]	$NiCl_2$•**L1** (5)	0.05	12	K_2HPO_4 (1.2)	54
14[b]	$NiCl_2$•**L1** (5)	0.05	12	CsF (1.2)	32
15[b]	$NiCl_2$•**L1** (5)	0.05	12	CsOAc (1.2)	<10
16[b]	$NiCl_2$•**L1** (5)	0.05	12	DBU (1.2)	<10

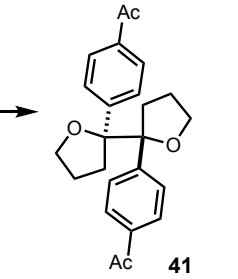

dimer as major product

[a] Reactions were carried out using 0.1 mmol **39a**.
[b] Reactions were carried out using 0.3 mmol **39a**.
[c] Determined by ^{1}H NMR using 1,3,5-trimethoxybenzene as an internal standard.

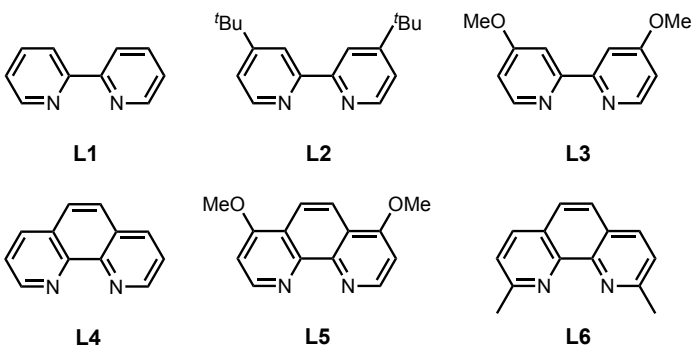

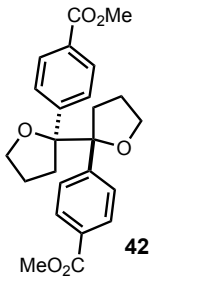

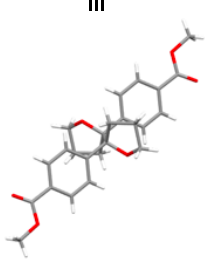

Table 12. Co-solvent effect[a]

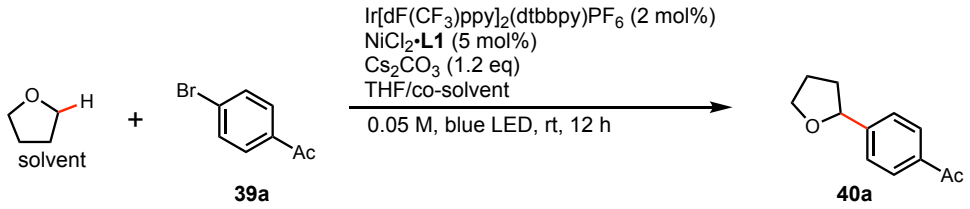

entry	THF/co-solvent (v/v)	yield[b] (%)
1	THF/DMF (1/3)	9
2	THF/DCM (1/3)	–
3	THF/Toluene (1/3)	<10
4	THF/DMF (11/1)	64
5	THF/DMF (5/1)	66
6	THF/MeOH (5/1)	0
7	THF/EtOAc (5/1)	72
8	THF/Acetone (5/1)	70
9	THF/Hexane (5/1)	59
10	THF/H_2O (11/1)	0

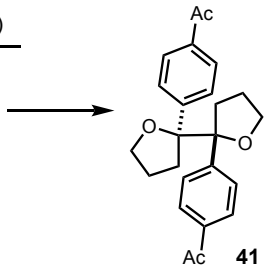

dimer as major product

[a] Reactions were carried out using 0.3 mmol **39a**.
[b] Determined by ^{1}H NMR using 1,3,5-trimethoxybenzene as an internal standard.

Table 13. Substrate scope[a]

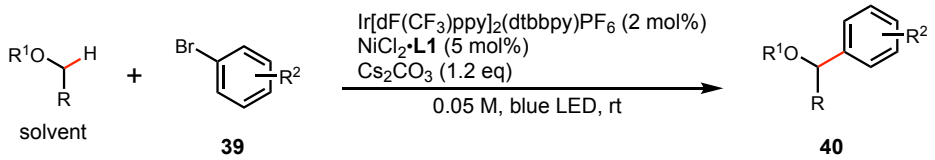

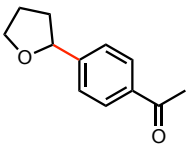

40a
72%, THF, 12 h

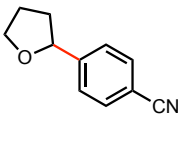

40b
72%, THF, 12 h

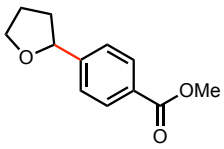

40c
70%, THF, 12 h

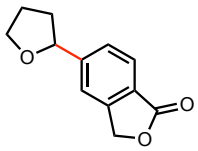

40d
73%, THF, 12 h

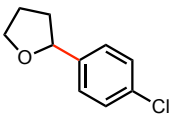

40e,63%, 10 mol% [Ni],
THF/Acetone 3:1, 24 h

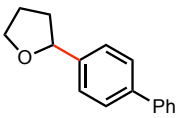

40f, 60%
THF/Acetone 3:1, 48 h

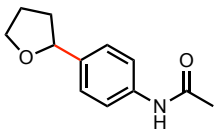

40g, 60%
THF/Acetone 3:1, 24 h

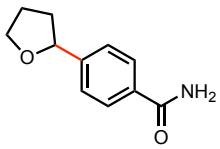

40h, 61%
THF/Acetone 3:1, 24 h

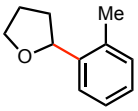

40i, 31%, 10 mol% [Ni],
THF/Acetone 3:1, 24 h

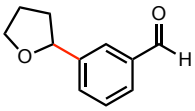

40j, 64%
THF/Acetone 3:1, 18 h

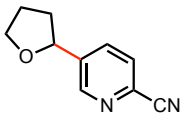

40k, 75%
THF/Acetone 3:1, 18 h

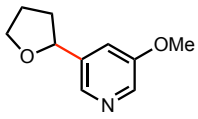

40l, 70%
THF/Acetone 3:1, 18 h

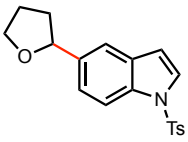

40m, 50%, 10 mol% [Ni],
THF/Acetone 3:1, 24 h

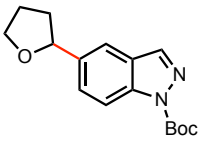

40n, 58%, 10 mol% [Ni],
THF/Acetone 3:1, 24 h

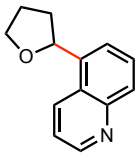

40o, 66%
THF/Acetone 3:1, 24 h

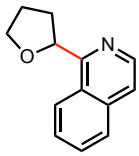

40p, 51%, 10 mol% [Ni],
THF/Acetone 3:1, 18 h

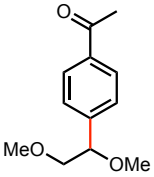

40q, 78%
DME, 12 h

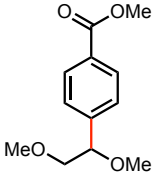

4r, 83%
DME, 12 h

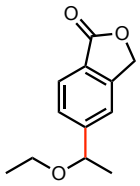

40s, 69%, 10 mol% [Ni],
Et_2O/Acetone 3:1, 24 h

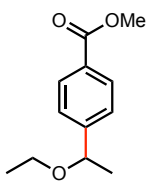

40t, 54%, 10 mol% [Ni],
Et_2O/Acetone 3:1, 24 h

[a] Reactions were carried out using 0.4 mmol **39a**. Isolated yield was reported.

2.5 Summary

In summary, direct α-oxy C(sp^3)–H acylation and arylation reactions via nickel and iridium dual catalysis have been developed in this chapter. These reactions demonstrate a unique approach of C(sp^3)–H functionalization incorporated with triplet state transition metal activation via energy transfer.

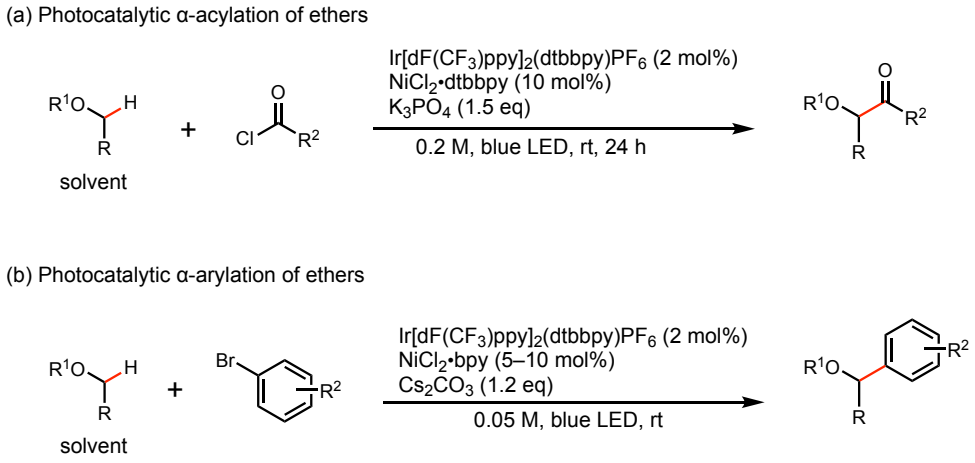

Scheme 23. Photocatalytic functionalization of α-oxy C(sp^3)–H bond

3. Experimental

3.1 General

Unless otherwise stated, reactions were run under an inert atmosphere (argon) and glassware using standard techniques for manipulating air-sensitive compounds. All glassware was oven-dried prior to use under an inert atmosphere of gas. Analytical thin-layer chromatography (TLC) was performed on precoated, glass-backed silica gel (Merck 60 F254). Visualization of the developed chromatogram was performed by UV absorbance or aqueous potassium permanganate. All work-up and purification procedures were carried out with reagent-grade solvents under ambient atmosphere.

3.2 Instrumentation

Infrared (IR) spectra were recorded on a HORIBA FT210 Fourier transform infrared spectrophotometer. UV-Vis spectra were recorded on a JASCO V-670 spectrophotometer. NMR was recorded on JEOL ECS-400, Bruker AVANCE III HD400 or Bruker AVANCE III 500 NMR spectrometers. Chemical shifts for proton are reported in parts per million downfield from tetramethylsilane and are referenced to residual protium in the NMR solvent (TMS in $CDCl_3$: δ 0.00 ppm; DMSO-d_6: δ 2.49; CD_3OD: δ 3.31 ppm; D_2O: δ 4.79 ppm). For ^{13}C NMR, chemical shifts were reported in the scale relative to NMR solvent ($CDCl_3$: δ 77.16 ppm; DMSO-d_6: δ 39.5; CD_3OD: δ 49.0 ppm) as an internal reference. For ^{13}C NMR in D_2O, chemical shifts were reported in the scale relative to TSP-d_4 (δ 0.00 ppm) as an external reference. For ^{19}F NMR, chemical shifts were reported in the scale relative δto $PhCF_3$ (δ –62.7680 ppm in $CDCl_3$) as an external reference. For ^{31}P NMR, chemical shifts were reported in the scale relative to $OP(OPh)_3$ (δ –17.6035 ppm in $CDCl_3$) as an external reference. NMR data are reported as follows: chemical shifts, multiplicity (s: singlet, d: doublet, dd: doublet of doublets, t: triplet, q: quartet, m: multiplet, br: broad signal), coupling constant (Hz), and integration. Single-crystal X-ray data were collected on a Rigaku R-AXIS RAPID II imaging plate area detector with graphite-monochromated Cu-Kα radiation. Optical rotation was measured using a 1 mL cell with a 1.0 dm path length on a JASCO polarimeter P-1030. High-resolution mass spectra (ESI TOF (+)) were measured on Thermo Fisher Scientific LTQ Orbitrap XL. HPLC analysis was conducted on a JASCO HPLC system equipped with Daicel chiral-stationary-phase columns (ø 0.46 cm x 25 cm). Preparative HPLC was conducted on a JASCO HPLC system equipped with Daicel chiral-stationary-phase columns (ø 2 cm x 25 cm). Reactions were carried out using 21 W blue LED (Grassy LeDiO RS122 Reef Blue V, spectrum see below) purchased from Volxjapan (www.volxjapan.co.jp).

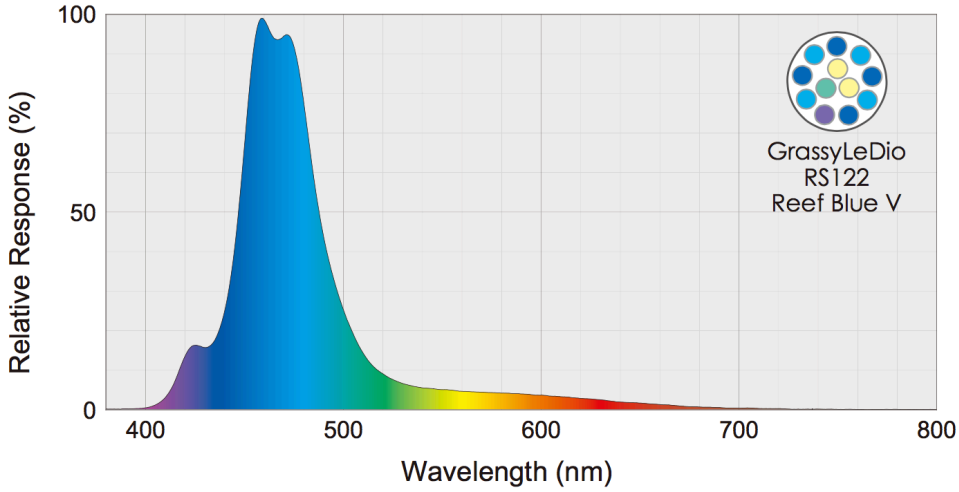

3.3 Materials

Unless otherwise noted, materials were purchased from commercial suppliers and were used without further purification. Anhydrous solvents were obtained either by filtration through drying columns (toluene, CH_2Cl_2, Et_2O, THF, DME, CH_3CN, EtOAc, DMF and hexane) on a GlassContour system. Anhydrous methanol and

acetone were purchased from Kanto Chemical Co., Inc.. Column chromatography was performed with silica gel Merck 60 (230-400 mesh ASTM), silica gel 60 N (spherical, neutral, 40-50 μm) from Kanto Chemical Co., Inc. and Wakogel® 50NH_2 (Catalog No. 231-02315) from Wako Pure Chemical Industries, Ltd.. Preparative TLC plates (1.05744.0001, PLC Silica gel 60 F_{254}) were purchased from Merck. 7-Azaindoline amides were prepared according to the reported literature α-N_3 amide **1a-d N_3** were prepared according to the reported literature *(since azides are capable of explosion, it is strongly recommended to apply standard safety rules and to use a safety shield)*.[5] DSC analysis indicated that **1-N_3** slowly started decomposition at 152.5 °C and released energy was 1619.86 mJ/mg. CCDC 1040789 contains the supplementary crystallographic data for **1-N_3**. *N*-thiophosphinoyl aldimines were prepared by following the reported procedure.[9] Chiral phosphine ligands were purchased from Sigma-Aldrich or TCI and used as received. Mesitylcopper was prepared by following the literature procedure[44] and handled in a glove box. 7-Azaindoline amides[5,6,19,21]and *p*-quinone methides[14a] were prepare by following reported procedures. $NiCl_2$·glyme and ligands were purchased from Sigma-Aldrich or TCI and used as received (stored under argon atmosphere on the bench top). The iridium photocatalyst, Ir[dF(CF_3)ppy]$_2$(dtbbpy)PF_6 was prepared from $IrCl_3$·xH_2O according to the reported procedure.[37] $NiCl_2$·ligand complexes were prepared from $NiCl_2$·glyme and corresponding ligands in 1.0 mmol scale by ultrasonication in CH_3CN, dried under reduced pressure and stored under argon atmosphere on the bench top.

3.4 Synthetic procedures for direct catalytic asymmetric Mannich-type reaction of α-azido 7-azaindoline amide

A flame-dried 20 mL test tube equipped with a magnetic stirring bar and 3-way glass stopcock was charged with amide **1-N_3** (61.0 mg, 0.3 mmol), corresponding *N*-thiophosphinoyl aldimine (0.36 mmol, 1.2 equiv). After evacuating for 5 min, the tube was backfilled with Ar and anhydrous THF (1.7 mL) was added via syringe with a stainless-steel needle at room temperature. Then the test tube was immersed into an electronically-controlled cooling bath at –60 °C with 2-propanol as medium.

To the solution was added the catalyst solution prepared as follows: A flame-dried 20 mL test tube equipped with a magnetic stirring bar and 3-way glass stopcock was charged with [Cu(CH_3CN)$_4$]PF_6 (11.2 mg, 0.03 mmol) and (*R*)-Xyl-Segphos (21.7 mg, 0.03 mmol) in a glove box. To the mixture was added anhydrous THF (1.0 mL) was added via syringe with a stainless-steel needle at room temperature. The resulting clear colorless solution was stirred for 1h at room temperature. After addition of the catalyst solution into the substrates, Barton's base (0.1 M in THF, 0.3 mL, 0.03 mmol) was subsequently added. Then the resulting solution was stirred at –60 °C for an indicated time. The reaction was quenched with AcOH (0.1 M in THF, 1 mL), then sat. NH_4Cl solution was added. The mixture was extracted with EtOAc, and the combined organic layers were washed with brine and dried over anhydrous Na_2SO_4. After filtration and concentration under reduced pressure, a small aliquot of the reaction crude was withdrawn for analyzing enatio exess of the major diastereoisomer using a chiral stationary phase HPLC. The residue was submitted to ^{1}H NMR analysis to determine the diastereomeric ratio. The diastereoisomers could be easily separated and purified by silica gel column chromatography (hexane/EtOAc, 5/1 to 1/1, Merck 60 (230-400 mesh ASTM)). The major diastereoisomer was subjected to acidic hydrolysis conditions using 6N HCl aq. solution (6 mL) at 80 °C. The reaction was monitored by ESI-LC/MS. After completion of the hydrolysis reaction, the reaction crude was transferred into a separatory funnel. The aqueous layer was washed by EtOAc twice and concentrated under reduced pressure. The crude mixture was loaded on a Wakogel® 50NH_2 (ca. 5~6 g) packed column and eluted with DCM/MeOH (1/2). As soon as 7-azaindoline was eluted off column completely, a 0.5 M HCl in DCM/MeOH(1/2) mixture solution was used for eluting the high polar *anti*-β-amino-α-azido acid off column. The fractions were collected and concentrated under reduced pressure to afford the corresponding *anti*-β-amino-α-azido acid.

(2*R*,3*R*)-3-Amino-2-azido-3-phenylpropanoic acid hydrochloride (6a).

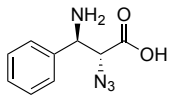

White powder; ^{1}H NMR (400 MHz, 300 K, CD_3OD): δ 7.54–7.50 (m, 2H), 7.45–7.42 (m, 3H), 4.96 (d, J = 4.4 Hz, 1H), 4.85 (d, J = 4.8 Hz, 1H); ^{13}C NMR (100 MHz, 300 K, CD_3OD): δ 169.5, 133.6, 130.9, 130.0, 129.6, 64.5, 56.0; IR (KBr): $\tilde{\nu}$ 2123, 1750 cm^{-1}; HRMS (ESI): *m/z* calculated for $C_9H_{11}O_2N_4$ $[M+H]^+$: 207.0877, found: 207.0878; $[\alpha]_D^{25}$ 46.9 (*c* 0.25, H_2O, 98% ee sample). Enantiomeric excess of the product was determined to be 98% ee by chiral stationary phase HPLC analysis (CHIRALPAK IA (ø 0.46 cm x 25 cm), hexane/2-propanol = 3/1, flow rate 1.0 mL/min, detection at 254 nm, t_R = 10.6 min (minor), 18.7 min (major)) of the Mannich product.

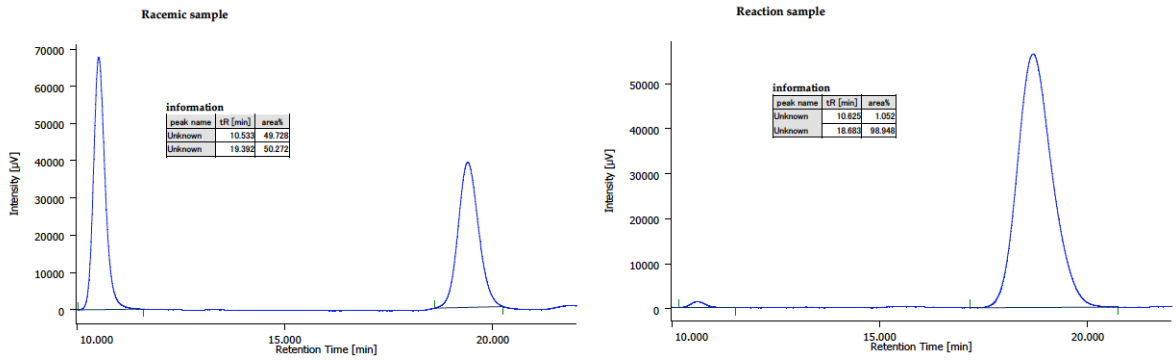

(2*R*,3*R*)-3-Amino-2-azido-3-(naphthalen-2-yl)propanoic acid hydrochloride (6b).

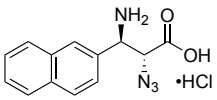

White powder; ^{1}H NMR (400 MHz, 300 K, CD_3OD): δ 8.04 (d, J = 1.6 Hz, 1H), 7.96–7.89 (m, 3H), 7.62 (dd, J = 8.8, 2.0 Hz, 1H), 7.58–7.54 (m, 2H), 5.04 (br, 2H); ^{13}C NMR (100 MHz, 300 K, CD_3OD): δ 169.6, 135.1, 134.3, 130.9, 129.8, 129.6, 129.3, 128.8, 128.3, 127.9, 126.2, 64.5, 56.2; IR (KBr): $\tilde{\nu}$ 2131, 1741 cm^{-1}; HRMS (ESI): *m/z* calculated for $C_{13}H_{13}O_2N_4$ $[M+H]^+$: 257.1033, found: 257.1035; $[\alpha]_D^{26}$ 34.0 (*c* 0.15, H_2O, 94% ee sample). Enantiomeric excess of the product was determined to be 94% ee by chiral stationary phase HPLC analysis (CHIRALPAK IA (ø 0.46 cm x 25 cm), hexane/2-propanol = 3/1, flow rate 1.0 mL/min, detection at 254 nm, t_R = 14.1 min (minor), 22.0 min (major)) of the Mannich product.

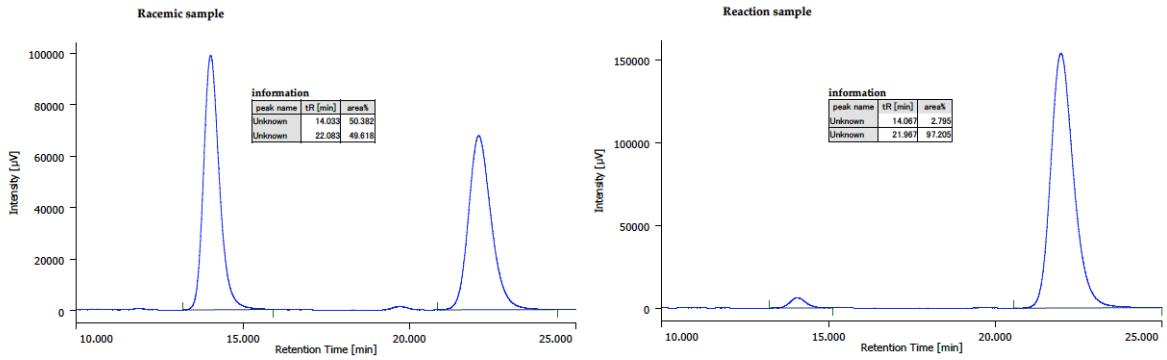

(2*R*,3*R*)-3-Amino-2-azido-3-(4-methoxyphenyl)propanoic acid hydrochloride (6c).

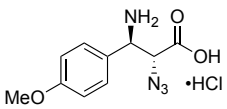

White powder; ^{1}H NMR (400 MHz, 300 K, CD_3OD): δ 7.47–7.43 (m, 2H), 6.99–6.95 (m, 2H), 4.92 (d, J = 4.4 Hz, 1H), 4.80 (d, J = 4.8 Hz, 1H), 3.81 (s, 3H); ^{13}C NMR (100 MHz, 300 K, CD_3OD): δ 169.5, 162.2, 131.0, 125.3, 115.2, 64.6, 55.9, 55.6; IR (KBr): $\tilde{\nu}$ 2125, 1735 cm^{-1}; HRMS (ESI): *m/z* calculated for $C_{10}H_{11}O_3N_4Na_2$ $[M+Na_2]^+$: 281.0621, found: 281.0621; $[\alpha]_D^{25}$ 27.8 (*c* 0.25, H_2O, 98% ee sample). Enantiomeric excess of the

product was determined to be 98% ee by chiral stationary phase HPLC analysis (CHIRALPAK IA (ø 0.46 cm x 25 cm), hexane/2-propanol = 3/1, flow rate 1.0 mL/min, detection at 254 nm, t_R = 13.9 min (minor), 27.1 min (major)) of the Mannich product.

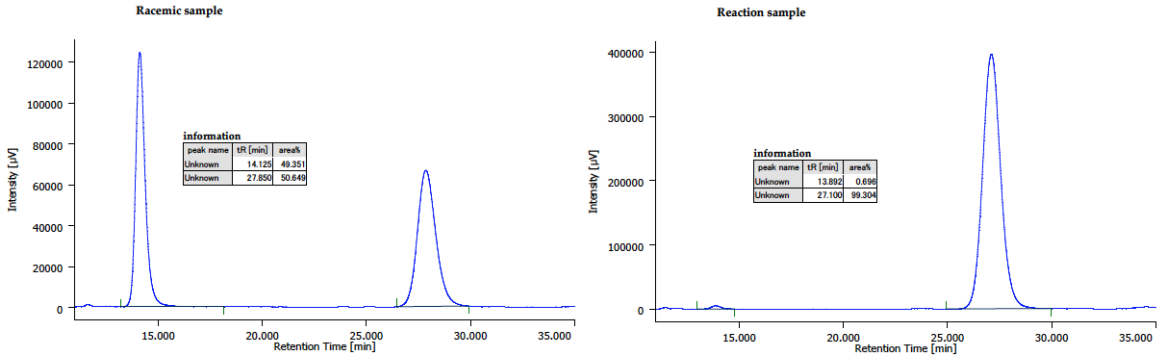

(2*R*,3*R*)-3-Amino-2-azido-3-(3-methoxyphenyl)propanoic acid hydrochloride (6d).

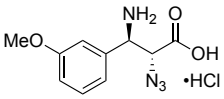

White powder; ^{1}H NMR (400 MHz, 300 K, D_2O): δ 7.47–7.43 (m, 1H), 7.13–7.10 (m, 3H), 4.99 (d, *J* = 4.9 Hz, 1H), 4.95 (d, *J* = 4.6 Hz, 1H), 3.88 (s, 3H); ^{13}C NMR (100 MHz, 300 K, D_2O): δ 173.4, 162.0, 135.9, 133.3, 123.4, 118.5, 116.4, 66.7, 58.4, 57.5; IR (KBr): $\tilde{\nu}$ 2136, 1684 cm^{-1}; HRMS (ESI): *m/z* calculated for $C_{10}H_{13}O_3N_4$ $[M+H]^+$: 237.0982, found: 237.0983; $[\alpha]_D^{26}$ 48.5 (*c* 0.25, H_2O, 92% ee sample). Enantiomeric excess of the product was determined to be 92% ee by chiral stationary phase HPLC analysis (CHIRALPAK IA (ø 0.46 cm x 25 cm), hexane/2-propanol = 3/1, flow rate 1.0 mL/min, detection at 254 nm, t_R = 10.5 min (minor), 14.9 min (major)) of the Mannich product.

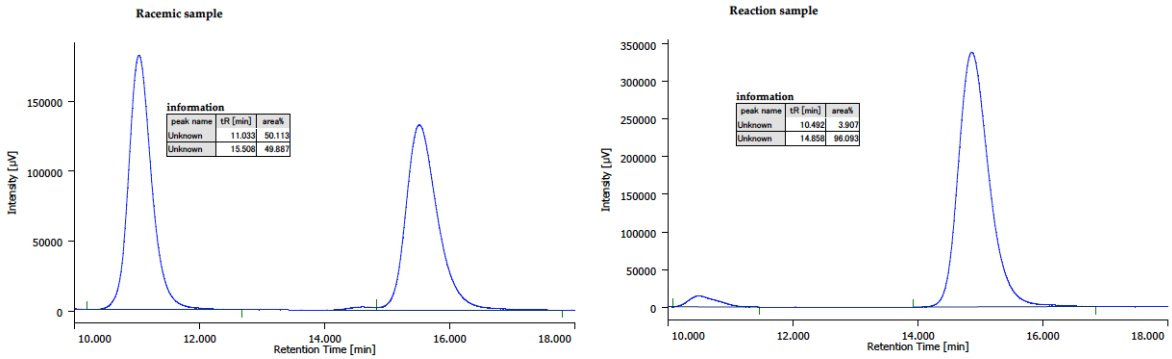

(2*R*,3*R*)-3-Amino-2-azido-3-(4-chlorophenyl)propanoic acid hydrochloride (6e).

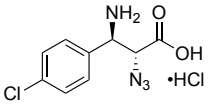

White powder; ^{1}H NMR (400 MHz, 300 K, D_2O): δ 7.52–7.46 (m, 4H), 4.98 (d, *J* = 4.6 Hz, 1H), 4.95 (d, *J* = 4.6 Hz, 1H); ^{13}C NMR (100 MHz, 300 K, CD_3OD): δ 169.3, 137.1, 132.4, 131.3, 130.1, 64.3, 55.3; IR (KBr): $\tilde{\nu}$ 2132, 1732 cm^{-1}; HRMS (ESI): *m/z* calculated for $C_9H_{10}O_2N_4Cl$ $[M+H]^+$: 241.0487, found: 241.0488; $[\alpha]_D^{26}$ 42.2 (*c* 0.25, H_2O, 97% ee sample). Enantiomeric excess of the product was determined to be 97% ee by chiral stationary phase HPLC analysis (CHIRALPAK IA (ø 0.46 cm x 25 cm), hexane/2-propanol = 3/1, flow rate 1.0 mL/min, detection at 254 nm, t_R = 13.3 min (minor), 26.3 min (major)) of the Mannich product.

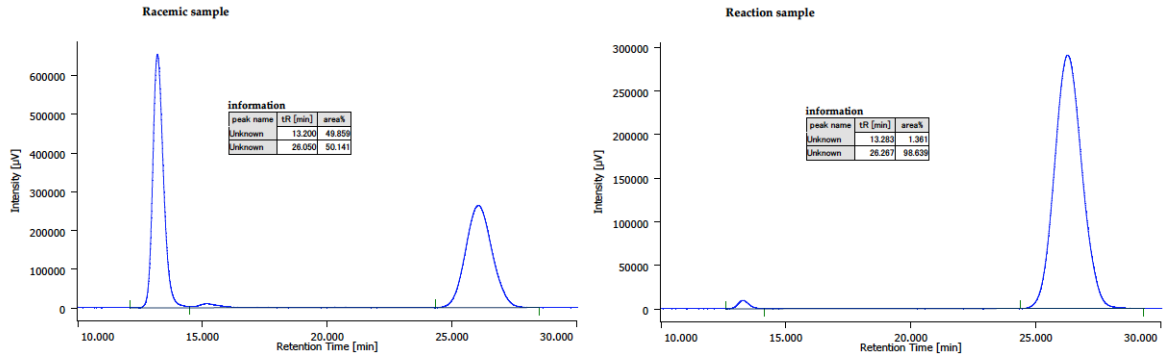

(2*R*,3*R*)-3-Amino-2-azido-3-(3-chlorophenyl)propanoic acid hydrochloride (6f).

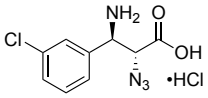

White powder; ^{1}H NMR (400 MHz, 300 K, D_2O): δ 7.57–7.52 (m, 2H), 7.49–7.41 (m, 2H), 5.03 (d, *J* = 4.6 Hz, 1H), 4.96 (d, *J* = 4.6 Hz, 1H); ^{13}C NMR (100 MHz, 300 K, D_2O): δ 173.2, 137.1, 136.3, 133.5, 133.0, 130.8, 129.4, 66.5, 57.0; IR (KBr): $\tilde{\nu}$ 2136, 1685 cm^{-1}; HRMS (ESI): *m/z* calculated for $C_9H_{10}O_2N_4Cl$ $[M+H]^+$: 241.0487, found: 241.0492; $[\alpha]_D^{26}$ 59.9 (*c* 0.25, H_2O, 95% ee sample). Enantiomeric excess of the product was determined to be 95% ee by chiral stationary phase HPLC analysis (CHIRALPAK IA (ø 0.46 cm x 25 cm), hexane/2-propanol = 3/1, flow rate 1.0 mL/min, detection at 254 nm, t_R = 10.2 min (minor), 13.8 min (major)) of the Mannich product.

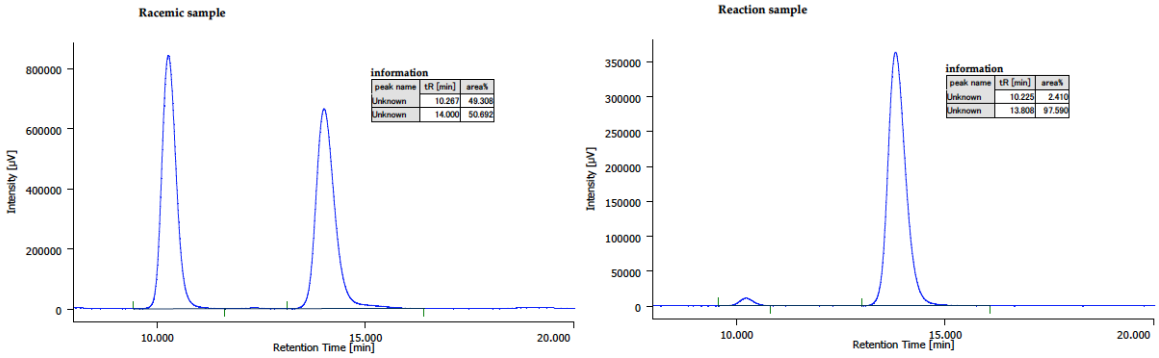

(2*R*,3*R*)-3-Amino-2-azido-3-(2-chlorophenyl)propanoic acid hydrochloride (6g).

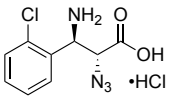

White powder; ^{1}H NMR (400 MHz, 300 K, D_2O): δ 7.79–7.74 (m, 1H), 7.61–7.56 (m, 1H), 7.52–7.45 (m, 2H), 5.46 (d, *J* = 5.6 Hz, 1H), 5.09 (d, *J* = 5.9 Hz, 1H); ^{13}C NMR (100 MHz, 300 K, D_2O): δ 173.3, 136.5, 134.4, 133.2, 132.3, 131.8, 130.8, 65.6, 53.4; IR (KBr): $\tilde{\nu}$ 2121, 1732 cm^{-1}; HRMS (ESI): *m/z* calculated for $C_9H_{10}O_2N_4Cl$ $[M+H]^+$: 241.0487, found: 241.0490; $[\alpha]_D^{26}$ 16.5 (*c* 0.25, H_2O, 89% ee sample). Enantiomeric excess of the product was determined to be 89% ee by chiral stationary phase HPLC analysis (CHIRALPAK IA (ø 0.46 cm x 25 cm), hexane/2-propanol = 3/1, flow rate 1.0 mL/min, detection at 254 nm, t_R = 12.6 min (minor), 13.8 min (major)) of the Mannich product.

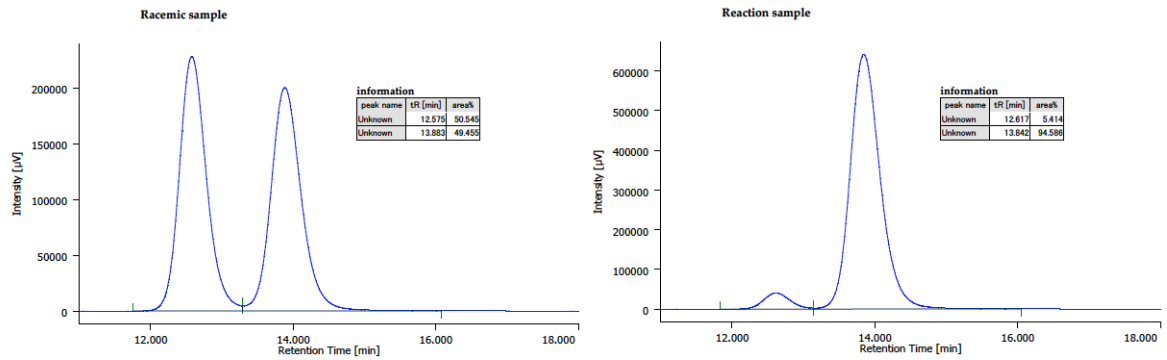

(2*R*,3*R*)-3-Amino-2-azido-3-(4-fluorophenyl)propanoic acid hydrochloride (6h).

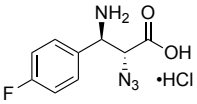

White powder; ^{1}H NMR (400 MHz, 300 K, D_2O): δ 7.56–7.51 (m, 2H), 7.26–7.20 (m, 2H), 5.02 (d, *J* = 4.6 Hz, 1H), 4.98 (d, *J* = 4.9 Hz, 1H); ^{13}C NMR (100 MHz, 300 K, D_2O): δ 173.3, 166.2 (d, *J* = 247.2 Hz), 133.1 (d, *J* = 8.8 Hz), 130.4 (d, *J* = 3.7 Hz), 118.9 (d, *J* = 22.0 Hz), 66.7, 56.9; ^{19}F NMR (376 MHz, 300 K, D_2O): δ –111.7; IR (KBr): $\tilde{\nu}$ 2134, 1758 cm^{-1}; HRMS (ESI): *m/z* calculated for $C_9H_{10}O_2N_4F$ $[M+H]^+$: 225.0782, found: 225.0784; $[\alpha]_D^{26}$ 59.7 (*c* 0.25, H_2O, 98% ee sample). Enantiomeric excess of the product was determined to be 98% ee by chiral stationary phase HPLC analysis (CHIRALPAK IA (ø 0.46 cm x 25 cm), hexane/2-propanol = 3/1, flow rate 1.0 mL/min, detection at 254 nm, t_R = 12.5 min (minor), 24.3 min (major)) of the Mannich product.

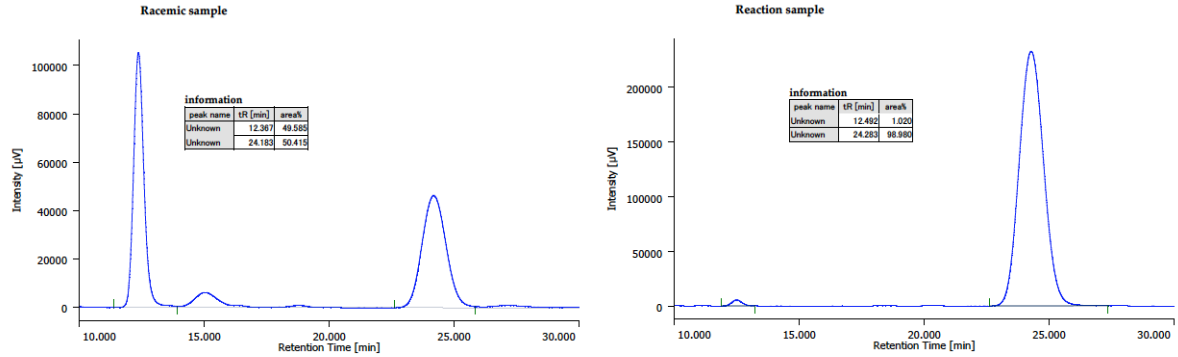

(2*R*,3*R*)-3-Amino-2-azido-3-(2-fluorophenyl)propanoic acid hydrochloride (6i).

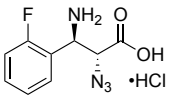

White powder; ^{1}H NMR (400 MHz, 300 K, D_2O): δ 7.64–7.52 (m, 2H), 7.35–7.25 (m, 2H), 5.23 (d, *J* = 5.6 Hz, 1H), 5.03 (d, *J* = 5.2 Hz, 1H); ^{13}C NMR (100 MHz, 300 K, D_2O): δ 173.5, 164.4 (d, *J* = 245.7 Hz), 135.2 (d, *J* = 8.8 Hz), 132.5 (d, *J* = 2.2 Hz), 127.9 (d, *J* = 2.9 Hz), 121.7 (d, *J* = 12.4 Hz), 119.0 (d, *J* = 21.9 Hz), 66.1, 51.6 (d, *J* = 2.9 Hz); ^{19}F NMR (376 MHz, 300 K, D_2O): δ –116.7; IR (KBr): $\tilde{\nu}$ = 2124, 1746 cm^{-1}; HRMS (ESI): *m/z* calculated for $C_9H_{10}O_2N_4F$ $[M+H]^+$: 225.0782, found: 225.0782; $[\alpha]_D^{26}$ 57.1 (*c* 0.25, H_2O, 96% ee sample). Enantiomeric excess of the product was determined to be 96% ee by chiral stationary phase HPLC analysis (CHIRALPAK IA (ø 0.46 cm x 25 cm), hexane/2-propanol = 3/1, flow rate 1.0 mL/min, detection at 254 nm, t_R = 11.0 min (minor), 13.5 min (major)) of the Mannich product.

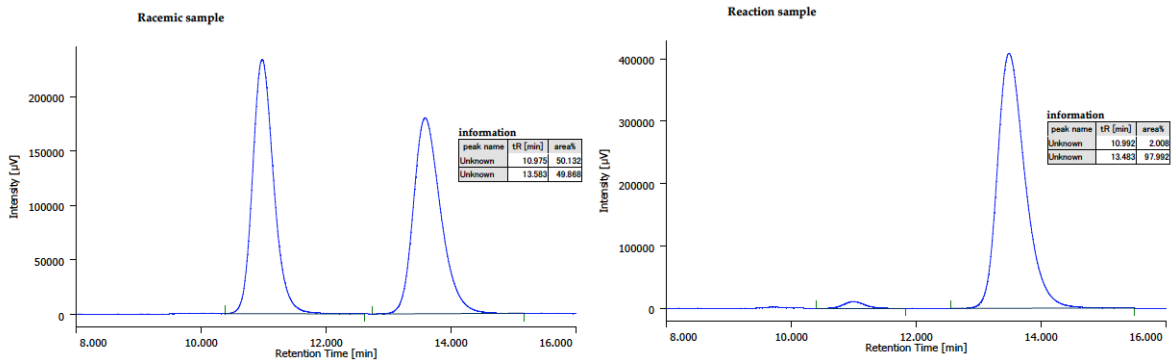

(2*R*,3*R*)-3-Amino-2-azido-3-(4-bromophenyl)propanoic acid hydrochloride (6j).

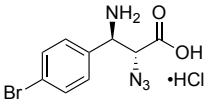

White powder; ^{1}H NMR (400 MHz, 300 K, D_2O): δ 7.67 (d, *J* = 8.6 Hz, 2H), 7.41 (d, *J* = 8.6 Hz, 2H), 4.98 (d, *J* = 4.8 Hz, 1H), 4.94 (d, *J* = 4.6 Hz, 1H); ^{13}C NMR (100 MHz, 300 K, D_2O): δ 173.4, 135.0, 133.5, 132.6, 126.6, 66.7, 57.1; IR (KBr): $\tilde{\nu}$ 2128, 1725 cm^{-1}; HRMS (ESI): *m/z* calculated for $C_9H_{10}O_2N_4Br$ $[M+H]^+$: 284.9982, found: 284.9985; $[\alpha]_D^{27}$ 48.1 (*c* 0.15, H_2O, 97% ee sample). Enantiomeric excess of the product was determined to be 97% ee by chiral stationary phase HPLC analysis (CHIRALPAK IA (ø 0.46 cm x 25 cm), hexane/2-propanol = 3/1, flow rate 1.0 mL/min, detection at 254 nm, t_R = 13.5 min (minor), 25.6 min (major)) of the Mannich product.

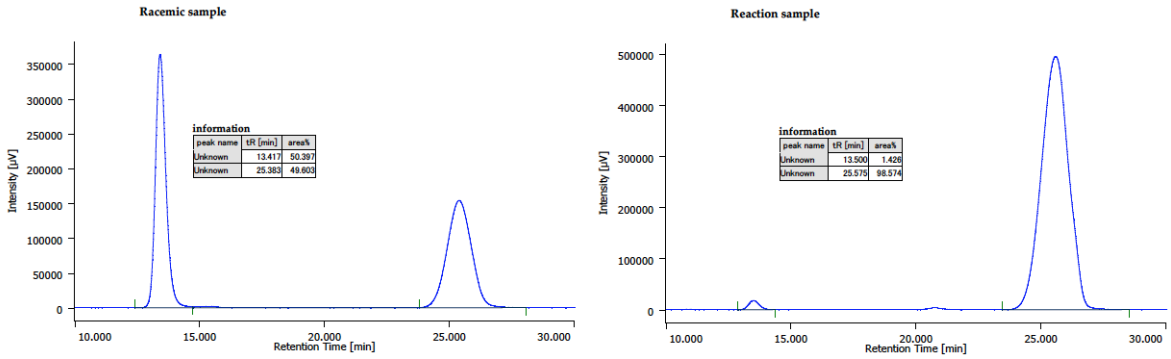

(2*R*,3*R*)-3-Amino-2-azido-3-(2-bromophenyl)propanoic acid hydrochloride (6k).

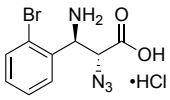

White powder; ^{1}H NMR (400 MHz, 300 K, D_2O): δ 7.78 (dd, *J* = 8.0, 1.2 Hz, 1H), 7.75 (dd, *J* = 8.0, 1.6 Hz, 1H), 7.41 (ddd, *J* = 8.0, 7.3, 1.6 Hz, 1H), 5.36 (d, *J* = 6.1 Hz, 1H), 4.89 (d, *J* = 5.9 Hz, 1H); ^{13}C NMR (100 MHz, 300 K, D_2O): δ 173.3, 136.6, 134.6, 134.1, 131.7, 131.4, 127.0, 65.8, 55.9; IR (KBr): $\tilde{\nu}$ 2119, 1731 cm^{-1}; HRMS (ESI): *m/z* calculated for $C_9H_{10}O_2N_4Br$ $[M+H]^+$: 284.9982, found: 284.9987; $[\alpha]_D^{26}$ –0.4 (*c* 0.15, H_2O, 84% ee sample). Enantiomeric excess of the product was determined to be 84% ee by chiral stationary phase HPLC analysis (CHIRALPAK ID (ø 0.46 cm x 25 cm), hexane/2-propanol = 3/1, flow rate 2.0 mL/min, detection at 254 nm, t_R = 21.5 min (minor), 25.2 min (major)) of the Mannich product.

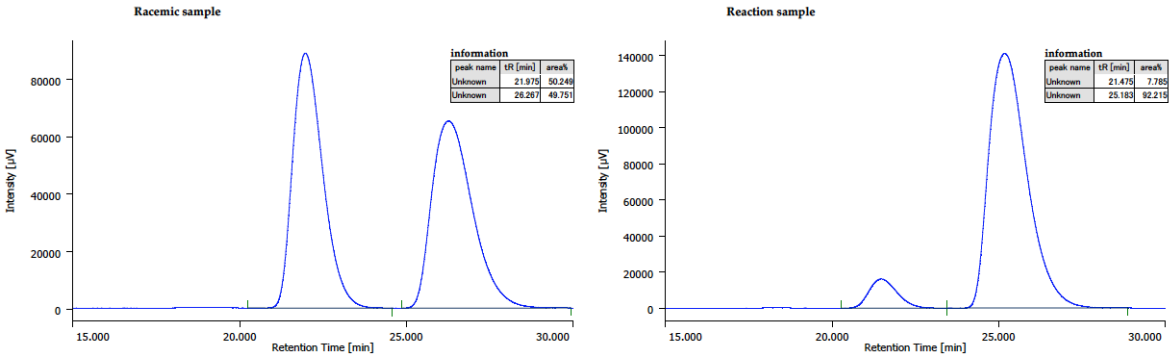

(2*R*,3*R*)-3-Amino-2-azido-3-(3-(trifluoromethyl)phenyl)propanoic acid hydrochloride (6l).

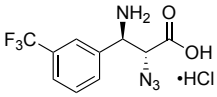

White powder; ^{1}H NMR (400 MHz, 300 K, D_2O): δ 7.86–7.82 (m, 2H), 7.76–7.74 (m, 1H), 7.69–7.65 (m, 1H), 5.09 (m, 2H); ^{13}C NMR (100 MHz, 300 K, D_2O): δ 173.2, 135.3, 134.7, 133.4 (q, J = 32.5 Hz), 132.8, 129.8 (q, J = 3.7 Hz), 127.7 (q, J = 3.9 Hz), 125.9 (q, J = 270.0 Hz), 66.5, 57.2; ^{19}F NMR (376 MHz, 300 K, D_2O): δ –62.6; IR (KBr): $\tilde{\nu}$ 2133, 1736 cm^{-1}; HRMS (ESI): *m/z* calculated for $C_{10}H_{10}O_2N_4F_3$ $[M+H]^+$: 275.0750, found: 275.0750; $[\alpha]_D^{26}$ 53.4 (*c* 0.25, H_2O, 95% ee sample). Enantiomeric excess of the product was determined to be 95% ee by chiral stationary phase HPLC analysis (CHIRALPAK IA (ø 0.46 cm x 25 cm), hexane/2-propanol = 3/1, flow rate 1.0 mL/min, detection at 254 nm, t_R = 8.6 min (minor), 10.2 min (major)) of the Mannich product.

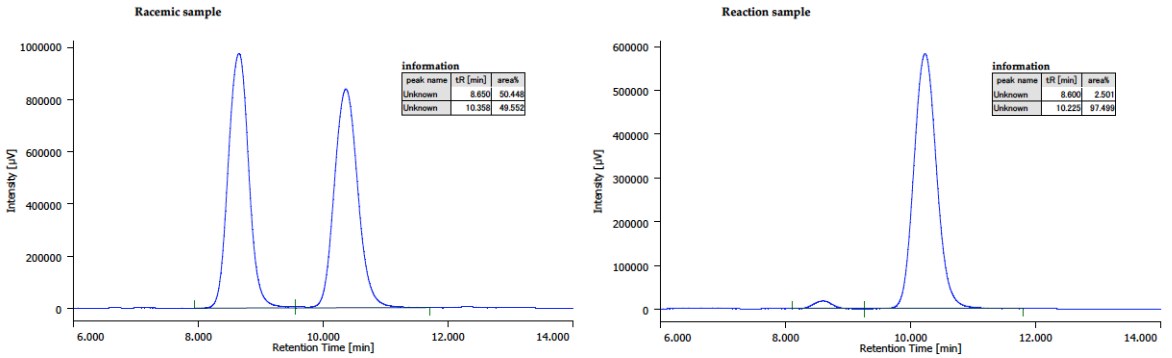

(2*R*,3*S*)-3-Amino-2-azido-3-(furan-2-yl)propanoic acid hydrochloride (6m).

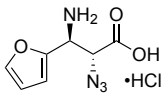

Brownish powder; ^{1}H NMR (400 MHz, 300 K, CD_3OD): δ 7.63–7.62 (m, 1H), 6.63–6.62 (m, 1H), 6.51–6.49 (m, 1H), 5.05 (d, J = 4.4 Hz, 1H), 4.89–4.87 (m, 1H); ^{13}C NMR (100 MHz, 300 K, CD_3OD): δ 169.3, 146.8, 145.2, 112.1, 112.0, 63.4, 50.3; IR (KBr): $\tilde{\nu}$ 2126, 1748 cm^{-1}; HRMS (ESI): *m/z* calculated for $C_7H_9O_3N_4$ $[M+H]^+$: 197.0669, found: 197.0672; $[\alpha]_D^{26}$ 44.9 (*c* 0.25, H_2O, 95% ee sample). Enantiomeric excess of the product was determined to be 95% ee by chiral stationary phase HPLC analysis (CHIRALPAK IA (ø 0.46 cm x 25 cm), hexane/2-propanol = 3/1, flow rate 1.0 mL/min, detection at 254 nm, t_R = 11.0 min (minor), 16.6 min (major)) of the Mannich product.

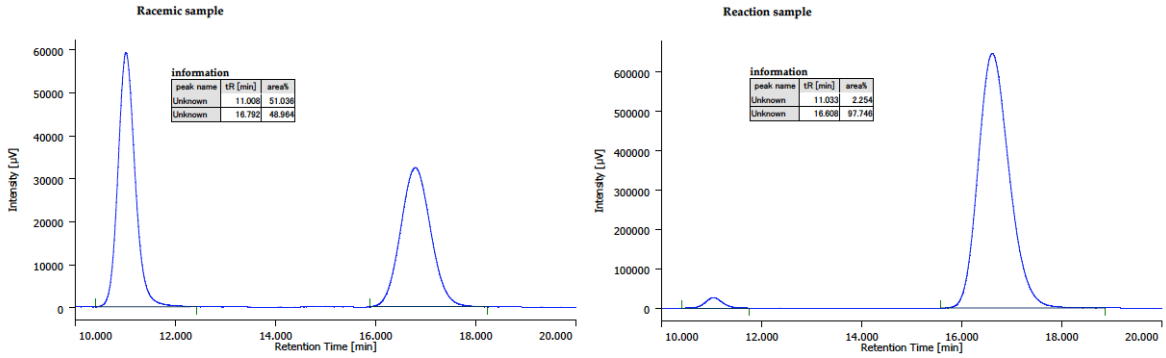

(2*R*,3*R*)-3-Amino-2-azido-3-(thiophen-3-yl)propanoic acid hydrochloride (6n).

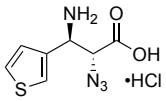

Brownish powder; ^{1}H NMR (400 MHz, 300 K, CD_3OD): δ 7.66 (ddd, *J* = 3.0, 1.2, 0.4 Hz, 1H), 7.51 (dd, *J* = 4.8, 2.8 Hz, 1H), 7.26 (dd, *J* = 5.2, 1.2 Hz, 1H), 5.04 (d, *J* = 4.0 Hz, 1H), 4.95 (d, *J* = 4.0 Hz, 1H); ^{13}C NMR (100 MHz, 300 K, CD_3OD): δ = 169.5, 133.9, 128.2, 127.9, 127.3, 64.3, 52.0; IR (KBr): $\tilde{\nu}$ 2125, 1749 cm^{-1}; HRMS (ESI): *m/z* calculated for $C_7H_9O_2N_4S$ $[M+H]^+$: 213.0441, found: 213.0443; $[\alpha]_D^{26}$ 48.1 (*c* 0.25, H_2O, 98% ee sample). Enantiomeric excess of the product was determined to be 98% ee by chiral stationary phase HPLC analysis (CHIRALPAK IA (ø 0.46 cm x 25 cm), hexane/2-propanol = 3/1, flow rate 1.0 mL/min, detection at 254 nm, t_R = 13.4 min (minor), 33.6 min (major)) of the Mannich product.

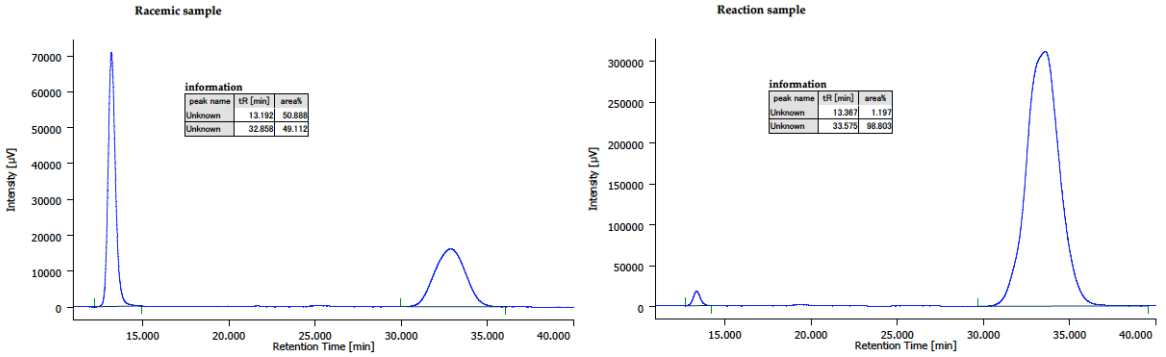

***N*-((1*R*,2*R*)-2-Azido-1-(4-chlorophenyl)-3-(2,3-dihydro-1*H*-pyrrolo[2,3-*b*]pyridin-1-yl)-3-oxopropyl)-*P*,*P*-diphenylphosphinothioic amide (5e).**

A flame-dried 100 mL test tube equipped with a magnetic stirring bar and 3-way glass stopcock was charged with $[Cu(CH_3CN)_4]PF_6$ (93.2 mg, 0.25 mmol) and (*R*)-Xyl-Segphos (180.7 mg, 0.25 mmol) in a glove box. After evacuating for 5 min, the tube was backfilled with Ar and anhydrous THF (5.0 mL) was added via syringe with a stainless-steel needle at room temperature. The resulting clear colorless solution was stirred for 1h at room temperature. After addition of a solution mixture of amide **1a** (1.02 g, 5.0 mmol) and *N*-thiophosphinoyl aldimine **2e** (2.13g, 6.0 mmol) in THF (20.0 mL) via cannulation, the test tube was immersed into an electronically-controlled cooling bath at –60 °C with 2-propanol as medium. After stirring 5 min, Barton's base (50 μL, 0.25 mmol) was subsequently added. Then the resulting mixture was stirred at –60 °C for 24h. The reaction was quenched with 1N HCl. The mixture was extracted with EtOAc, and the combined organic layers were washed with brine and dried over anhydrous Na_2SO_4. After filtration and concentration under reduced pressure, to the reaction crude was added 2-propanol for recrystallization upon heating. The mixture was settled at room temperature overnight. 2.40 g of the product **5e** (86% yield in enatiopure form) was isolated by vacuum filtration and dried under reduced pressure.

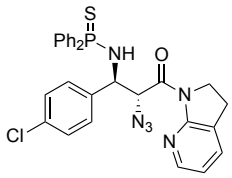

White solid, m. p.: 174–175 °C; ^{1}H NMR (400 MHz, 300 K, $CDCl_3$): δ 7.99 (dd, *J* = 5.2, 1.2 Hz, 1H), 7.70–7.57 (m, 4H), 7.46 (dd, *J* = 7.2, 1.2 Hz, 1H), 7.40–7.34 (m, 2H), 7.30–7.20 (m, 8H), 6.88 (dd, *J* = 7.2, 4.8 Hz, 1H), 5.98 (d, *J* = 7.6 Hz, 1H), 5.08–4.98 (m, 2H), 4.18 (ddd, *J* = 12.0, 10.4, 5.6 Hz, 1H), 3.93 (ddd, *J* = 12.0, 10.4, 7.2 Hz, 1H), 3.09–2.89 (m, 2H); ^{13}C NMR (100 MHz, 300 K, $CDCl_3$): δ 168.1, 155.0, 145.6, 139.26, 139.24, 135.4, 135.1, 134.6, 134.4, 134.1, 133.65, 131.55, 131.44, 131.41, 131.1, 131.0, 128.8, 128.7, 128.35, 128.27, 128.22, 128.1, 126.9, 119.3, 63.2, 63.1, 57.2, 46.3, 24.3; ^{31}P NMR (162 MHz, 300 K, $CDCl_3$): δ 58.1; IR ($CHCl_3$ film): $\tilde{\nu}$ 2108, 1659 cm^{-1}; HRMS (ESI): *m/z* calculated for $C_{28}H_{25}N_6OClPS$ $[M+Na]^+$: 559.1231, found: 559.1235; $[\alpha]_D^{26}$ –107.0 (*c* 0.25, $CHCl_3$, >99% ee sample).

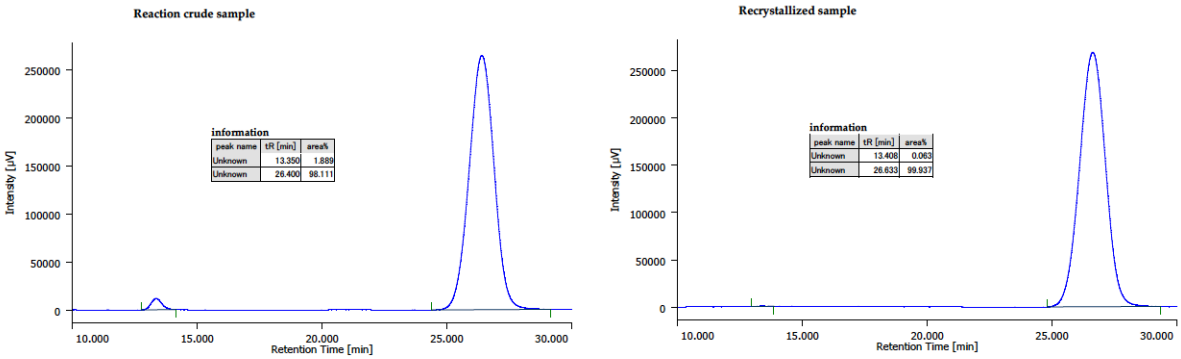

***N*-((3*R*,4*R*,*E*)-4-azido-5-(2,3-dihydro-1*H*-pyrrolo[2,3-*b*]pyridin-1-yl)-1-(4-fluorophenyl)-5-oxopent-1-en-3-yl)-*P*,*P*-diphenylphosphinothioic amide (5o).**

Compound **5o** was prepared according to General Procedure. 61.0 mg of Amide **1a** (0.3 mmol) and 131.5 mg of **3o** (0.36 mmol, 1.2 equiv) were used with 20 mol% $[Cu(CH_3CN)_4]PF_6$ (22.4 mg, 0.06 mmol), (*R*)- Xyl-Segphos (43.4 mg, 0.06 mmol) and Barton's base (0.1 M in THF, 0.6 mL, 0.06 mmol) in THF (0.1 M). After stirring at –60 °C for 48h, the reaction was quenched. Purification by silica gel chromatography (hexane/EtOAc, 5/1 to 1/1) and preparative HPLC afforded major diastereoisomer (*anti*) **5o** (106 mg, 62%).

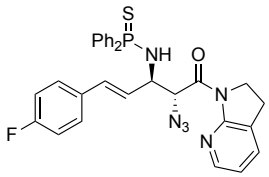

Viscous foam; ^{1}H NMR (400 MHz, 300 K, $CDCl_3$): δ 7.91–7.85 (m, 5H), 7.47–7.35 (m, 7H), 7.18–7.15 (m, 2H), 6.94 (t, *J* = 4.8 Hz, 2H), 6.87 (dd, *J* = 7.4, 5.4 Hz, 1H), 6.41 (d, *J* = 15.6 Hz, 1H), 6.14 (dd, *J* = 15.9, 7.6 Hz, 1H), 5.92 (d, *J* = 6.4 Hz, 1H), 4.76–4.69 (m, 1H), 4.26–4.16 (m, 2H), 4.06–3.99 (m, 1H), 3.13–2.97 (m, 2H); ^{13}C NMR (125 MHz, 300 K, $CDCl_3$): δ 167.8, 163.4, 161.4, 154.8, 146.0, 135.6, 135.1, 134.8, 134.3, 134.2, 132.65, 132.63, 131.9, 131.64, 131.55, 131.46, 131.43, 131.41, 131.3, 128.34, 128.30, 128.23, 128.19, 128.12, 127.52, 126.27, 126.4, 119.0, 115.3, 115.2, 63.7, 63.6, 55.8, 46.0, 24.2; ^{19}F NMR (376 MHz, 300 K, $CDCl_3$): δ –114.3; ^{31}P NMR (162 MHz, 300 K, $CDCl_3$): δ 57.8; IR ($CHCl_3$ film): $\tilde{\nu}$ 2108, 1658 cm^{-1}; HRMS (ESI): *m/z* calculated for $C_{30}H_{27}ON_6FPS$ $[M+H]^+$: 569.1683, found: 569.1689; $[\alpha]_D^{25}$ –48.0 (*c* 0.45, $CHCl_3$, >99% ee sample). Enantiomeric excess of the product was determined to be 92% ee by chiral stationary phase HPLC analysis (CHIRALPAK IE (ø 0.46 cm x 25 cm), hexane/2-propanol = 3/1, flow rate 1.0 mL/min, detection at 254 nm, t_R = 30.2 min (major), 33.6 min (minor)).

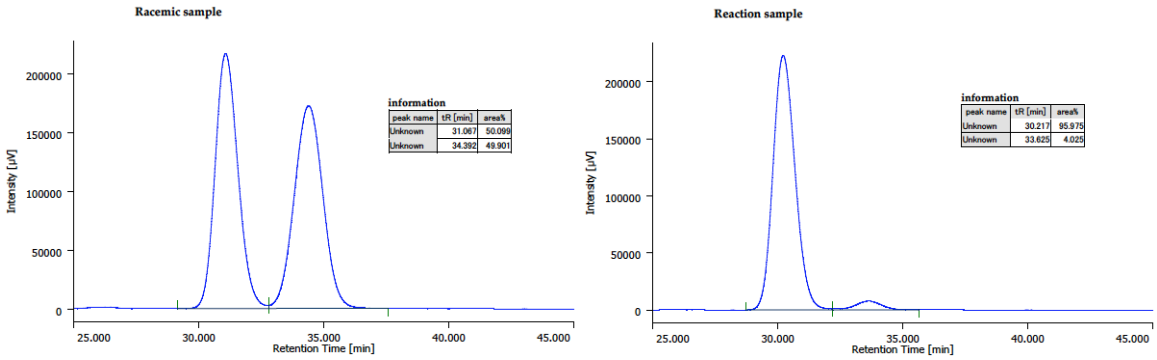

***N*-((2*R*,3*R*,*E*)-2-Azido-1-(2,3-dihydro-1*H*-pyrrolo[2,3-*b*]pyridin-1-yl)-1-oxooct-4-en-3-yl)-*P*,*P*-diphenylphosphinothio-ic amide (5p).**

Compound **5p** was prepared according to General Procedure. 61.0 mg of Amide **1a** (0.3 mmol) and 112.8 mg of **3p** (0.36 mmol, 1.2 equiv) were used with 20 mol% $[Cu(CH_3CN)_4]PF_6$ (22.4 mg, 0.06 mmol), (*R*)-DM-SEGPHOS (43.4 mg, 0.06 mmol) and Barton's base (0.1 M in THF, 0.6 mL, 0.06 mmol) in THF (0.1 M). After stirring at –60 °C for 48h, the reaction was quenched. Purification by silica gel chromatography (hexane/EtOAc, 5/1 to 1/1) and preparative HPLC afforded major diastereoisomer (*anti*) **5p** (106 mg, 62%).

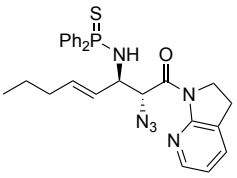

Viscous foam; ^{1}H NMR (400 MHz, 300 K, $CDCl_3$): δ 7.90–7.81 (m, 5H), 7.46–7.32 (m, 7H), 6.85 (dd, *J* = 6.8, 4.8 Hz, 1H), 5.79 (d, *J* = 6.8 Hz, 1H), 5.60–5.48 (m, 2H), 4.58–4.49 (m, 1H), 4.22–4.15 (m, 1H), 4.09–3.99 (m, 2H), 3.12–2.96 (m, 2H), 1.90 (dd, *J* = 13.2, 7.2 Hz, 2H), 1.33–1.23 (m, 2H), 0.82 (t, *J* = 7.2 Hz, 3H); ^{13}C NMR (125 MHz, 300 K, $CDCl_3$): δ 168.2, 155.0, 146.1, 135.8, 135.5, 135.0, 134.9, 134.7, 134.2, 131.8, 131.7, 131.48, 131.46, 131.44, 131.41, 131.39, 131.36, 128.36, 128.32, 128.25, 128.21, 126.31, 119.0, 63.92, 63.87, 55.8, 46.1, 34.4, 24.3, 22.2, 13.7; ^{31}P NMR (162 MHz, 300 K, $CDCl_3$): δ 57.6; IR ($CHCl_3$ film): $\tilde{\nu}$ 2108, 1659 cm^{-1}; HRMS (ESI): *m/z* calculated for $C_{27}H_{30}ON_6PS$ $[M+H]^+$: 517.1934, found: 517.1921; $[\alpha]_D^{25}$ –15.2 (*c* 0.85, $CHCl_3$, >99% ee sample). Enantiomeric excess of the product was determined to be 96% ee by chiral stationary phase HPLC analysis (CHIRALPAK IE (ø 0.46 cm x 25 cm), hexane/2-propanol = 3/1, flow rate 1.0 mL/min, detection at 254 nm, t_R = 25.3 min (major), 29.6 min (minor)).

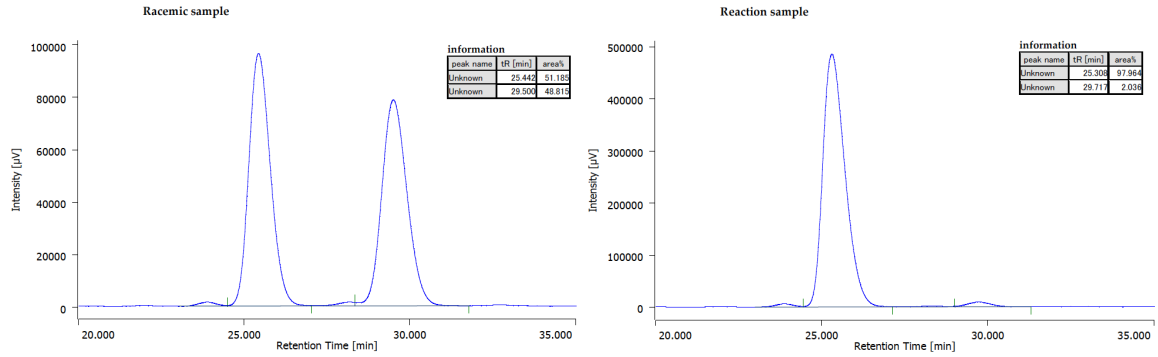

Synthesis of enatiopure anti-β-amino-α-azido acid 6e from 5e.

Anti-β-amino-α-azido acid **6e** was synthesized using the identical procedure described in General Procedures. A mixture of enatiopure **5e** (559.0 mg, 1.0 mmol) and 6N HCl (20 mL) was stirred at stirred at 80 °C for 5h. 255

mg (92%) of *anti*-β-amino-α-azido acid **6e** was obtained after purification. $[\alpha]_D^{26}$ 96.4 (*c* 0.25, H_2O, >99% ee sample).

Synthesis of enatiopure anti-β-amino-α-azido acid 6e from 9.

A 50 mL flask equipped with a magnetic stirring bar and a 3-way glass stopcock was charged with compound **9** (291 mg, 1.0 mmol) and 6N HCl (20 mL). The resulting mixture was vigorously stirred at 80 °C for 6h. After completion of the reaction, the reaction mixture was concentrated under reduced pressure to afford compound **6e** (276 mg) in quantitive yield without further purification.

(2*R*,3*R*)-2,3-Diamino-3-(4-chlorophenyl)propanoic acid dihydrochloride (7).

A 20 mL flask equipped with a magnetic stirring bar and a 3-way glass stopcock was charged with *anti*-β-amino-α-azido acid **6e** (27.7 mg, 0.1 mmol) and EtOAc (1 mL). To the above solution was added palladium on carbon (5% w/w, 21.3 mg, 0.01 mmol), and the mixture was vigorously stirred under H_2 (1 atm) for 4 h at room temperature. The EtOAc was evaporated, and water was added to reaction crude. Filtration through a Celite® pad, followed by addition of an extra amount of 1N HCl aq., and concentration under reduced pressure gave *anti*-α,β-diamino acid dihydrochloride **7** as a white powder (27 mg, 94%) without further purification.

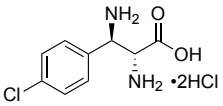

White powder; ^{1}H NMR (400 MHz, 300 K, D_2O): δ 7.66–7.59 (m, 4H), 4.83 (d, J = 10.8 Hz, 1H), 4.49 (d, J = 12.2 Hz, 1H); ^{13}C NMR (100 MHz, 300 K, D_2O): δ 171.9, 139.5, 133.2, 132.5, 132.2, 56.5, 56.2; IR (KBr): $\tilde{\nu}$ 3396, 1743 cm^{-1}; HRMS (ESI): *m/z* calculated for $C_9H_{12}O_2N_2Cl$ $[M+H]^+$: 215.0582, found: 215.0583; $[\alpha]_D^{27}$ 34.6 (*c* 0.25, H_2O).

(3*R*,4*R*)-3-Azido-4-(4-chlorophenyl)azetidin-2-one (8).

A 20 mL screw-capped test tube equipped with a magnetic stirring bar was charged with $NaHCO_3$ (117.6 mg, 1.4 mmol), MsCl (24 μL, 0.3 mmol) and CH_3CN (1 mL). Then the test tube was sealed and heated to 90 °C. After stirring 5 min at 90 °C, *anti*-β-amino-α-azido acid **6e** (55.4 mg, 0.2 mmol) was added. The resulting mixture was vigorously stirred at 80 °C for 12h. The reaction mixture was diluted with CH_3CN and filtered through a Celite® pad, and the filtrate was concentrated under reduced pressure. The residue was purified by silica gel chromatography (hexane/EtOAc, 3/1 to 2/1) to afford compound **8**, 17 mg (38%).

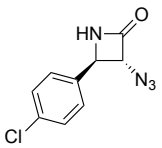

White solid; ^{1}H NMR (400 MHz, 300 K, $CDCl_3$): δ 7.41–7.38 (m, 2H), 7.32–7.29 (m, 2H), 6.46 (br, 1H), 4.58 (d, J = 2.0 Hz, 1H), 4.36 (br, 1H); ^{13}C NMR (100 MHz, 300 K, $CDCl_3$): δ 164.7, 135.8, 135.1, 129.5, 127.2, 73.8, 58.8; IR ($CHCl_3$ film): $\tilde{\nu}$ 2118, 1769 cm^{-1}; HRMS (ESI): *m/z* calculated for $C_9H_8N_4OCl$ $[M+H]^+$: 223.0381, found: 223.0382; $[\alpha]_D^{25}$ 120.8 (*c* 0.25, $CHCl_3$).

Methyl (2*R*,3*R*)-3-amino-2-azido-3-(4-chlorophenyl)propanoate hydrochloride (9).

A 100 mL flask equipped with a magnetic stirring bar and a 3-way glass stopcock was charged with amide **5e** (1.12 g, 2.0 mmol) and 2N HCl in MeOH solution (40 mL). The resulting mixture was vigorously stirred at 70 °C for 24h. The reaction was monitored by ESI-LC/MS. After completion of the reaction, the reaction mixture was concentrated under reduced pressure, and 4N HCl in EtOAc was added to the reaction crude for recrystallization. The mixture was settled at 5 °C overnight. 513 mg of the product **9** (88% yield) was isolated by vacuum filtration, rinsed with CH_2Cl_2 and dried under reduced pressure.

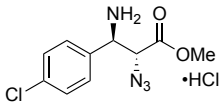

White fluffy crystal, m. p.: 163–165 °C; ^{1}H NMR (400 MHz, 300 K, CD_3OD): δ 7.47 (br, 4H), 4.99 (d, J = 4.8 Hz, 1H), 4.88 (d, J = 4.8 Hz, 1H), 3.75 (s, 3H); ^{13}C NMR (100 MHz, 300 K, CD_3OD): δ 168.5, 137.2, 132.2, 131.3, 130.2, 64.4, 55.2, 53.7; IR (KBr): $\tilde{\nu}$ 2132, 1737 cm^{-1}; HRMS (ESI): *m/z* calculated for $C_{10}H_{12}O_2N_4Cl$ $[M+H]^+$: 255.0643, found: 255.0644; $[\alpha]_D^{26}$ 91.4 (*c* 0.25, MeOH).

Methyl (2*R*,3*R*)-2-azido-3-((*S*)-2-(((benzyloxy)carbonyl)amino)-3-methylbutanamido)-3-(4-chlorophenyl) propanoate (10).

A 50 mL flask equipped with a magnetic stirring bar and a 3-way glass stopcock was charged with **9** (145.6 mg, 0.5 mmol), Cbz-L-Val-OH (125.6 mg, 0.5 mmol), PyBOP (260.2.6 mg, 0.5 mmol) and anhydrous HOBt (67.6.6 mg, 0.5 mmol). To the above mixture was added anhydrous DMF (5 mL) and DIPEA (262 μL, 1.5 mmol). The resulting mixture was vigorously stirred at room temperature for 3h. The reaction mixture was diluted with 5 mL EtOAc, quenched with 1N HCl aq. and the biphasic mixture was extracted with EtOAc. The combined organic was washed with sat. aq. $NaHCO_3$ and dried over anhydrous Na_2SO_4. After evaporation of the solvent under reduced pressure, the residue was purified by silica gel chromatography (hexane/EtOAc, 3/1) to afford compound **10**, 219 mg (90%).

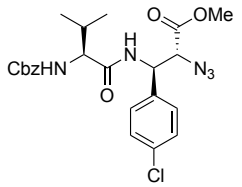

White solid, m. p.: 159–161 °C; ^{1}H NMR (400 MHz, 300 K, $CDCl_3$): δ 7.38–7.20 (m, 9H), 6.89 (br, 1H), 5.49 (dd, J = 8.4, 4.8 Hz, 1H), 5.22 (br, 1H), 5.14–5.07 (m, 2H), 4.49 (br, 1H), 4.00 (dd, J = 6.4, 4.8 Hz, 1H), 3.70 (s, 3H), 2.21–2.12 (m, 1H), 1.00 (d, J = 6.4 Hz, 3H), 0.93 (d, J = 6.4 Hz, 3H); ^{13}C NMR (100 MHz, 300 K, $CDCl_3$): δ 170.9, 168.1, 156.5, 136.0, 134.7, 134.5, 128.9, 128.7, 128.5, 128.2, 128.0, 67.1, 64.7, 60.6, 53.2, 52.8, 30.7, 19.2, 17.8; IR ($CHCl_3$ film): $\tilde{\nu}$ 2120, 1721 cm^{-1}; HRMS (ESI): *m/z* calculated for $C_{23}H_{26}N_5O_5ClNa$ $[M+Na]^+$: 510.1515, found: 510.1507; $[\alpha]_D^{27}$ –4.4 (*c* 0.25, $CHCl_3$).

Methyl (2*R*,3*R*)-2-amino-3-((*S*)-2-(((benzyloxy)carbonyl)amino)-3-methylbutanamido)-3-(4-chlorophenyl) propanoate (11).

A 20 mL test tube equipped with a magnetic stirring bar and a 3-way glass stopcock was charged with **10** (48.8 mg, 0.1 mmol), 1.26% Pd/Fibroin (9.8 mg, 20%wt to compound **10**), and anhydrous MeOH (1 mL). The mixture was vigorously stirred under H_2 (1 atm) for 4 h at room temperature. The reaction mixture was filtered through a Celite® pad, and the filtrate was concentrated under reduced pressure. The residue was purified by silica gel chromatography (CH_2Cl_2/MeOH, 15/1) to afford compound **11**, 35 mg (75%).

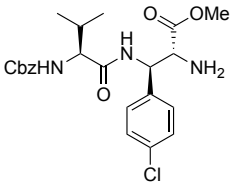

White solid, m. p.: 179–181 °C; ^{1}H NMR (400 MHz, 300 K, $CDCl_3$): δ 7.41–7.29 (m, 6H), 7.23–7.10 (m, 4H), 5.36–5.32 (m, 2H), 5.15–5.06 (m, 2H), 4.05–4.02 (m, 1H), 3.73 (br, 1H), 3.66 (s, 3H), 2.21–2.13 (m, 1H), 0.99 (d, J = 6.8 Hz, 3H), 0.91 (d, J = 6.6 Hz, 3H); ^{13}C NMR (100 MHz, 300 K, $CDCl_3$): δ 173.3, 170.6, 156.6, 136.3, 136.0, 134.0, 128.9, 128.7, 128.40, 128.36, 128.3, 67.3, 60.9, 58.1, 54.1, 52.3, 30.8, 19.5, 17.9; IR ($CHCl_3$ film): $\tilde{\nu}$ 3019, 1721, 1677 cm^{-1}; HRMS (ESI): *m/z* calculated for $C_{23}H_{29}N_3O_5Cl$ $[M+H]^+$: 462.1790, found: 462.1787; $[\alpha]_D^{25}$ –8.6 (*c* 0.25, $CHCl_3$).

3.5 Synthetic procedures for direct catalytic asymmetric 1,6-conjugate addition of 7-azaindoline amides to *para*-quinone methides

A flame-dried 20 mL test tube equipped with a magnetic stirring bar and 3-way glass stopcock was charged with corresponding amide **1** (0.2 mmol) and *p*-quinone methide (0.24 mmol, 1.2 equiv). After evacuating for 5 min, the tube was backfilled with Ar.

To the reaction test tube was added the catalyst solution prepared as follows at corresponding temperature (for the reaction of **1-CF$_3$** at 25 °C; **1-Me** at 0 °C; **1-N$_3$** at – 40 °C; **1-OBn** at 25 °C.) : A flame-dried 20 mL test tube equipped with a magnetic stirring bar and 3-way glass stopcock was charged with mesitylcopper (1.8 mg, 0.01 mmol, 5 mol % or 3.6 mg, 0.02 mmol, 10 mol %) and (*R*)-Xyl-Segphos (7.2 mg, 0.01 mmol, 5 mol % or 14.5 mg, 0.02 mmol, 10 mol %) in a glove box. To the mixture was added anhydrous THF (0.6 mL for the reactions of **1-CF$_3$**, **1-Me**, **1-OBn** or 2 mL for that of **1-N$_3$**) was added via syringe with a stainless-steel needle at room temperature.

The reaction was stirred at indicated temperature for 24 h. The reaction was quenched with AcOH (0.1 M in THF, 0.2 mL), then sat. NH_4Cl solution was added. The mixture was extracted with EtOAc, and the combined organic layers were washed with brine and dried over anhydrous Na_2SO_4. After filtration and concentration under reduced pressure, a small aliquot of the reaction crude was withdrawn for analyzing enatio exess of the major diastereoisomer using a chiral stationary phase HPLC. The residue was submitted to ^{1}H NMR analysis to determine the diastereomeric ratio and then purified by automated flash column chromatography (Biotage Isolera One) with pre-packed silica gel column.

(*S*)-2-((*R*)-(3,5-Di-*tert*-butyl-4-hydroxyphenyl)(phenyl)methyl)-1-(2,3-dihydro-1*H*-pyrrolo[2,3-*b*]pyridin-1-yl)-3,3,3-trifluoropropan-1-one (20a):

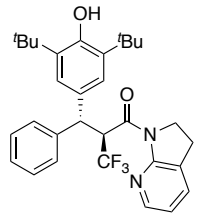

Obtained in 97% yield (3.06 g, 6.0 mmol gram-scale reaction in 20 mL THF); pink solid; m.p. : 185–187 °C; ^{1}H NMR (400 MHz, 300 K, $CDCl_3$): δ 8.30–8.24 (m, 1H), 7.55–7.49 (m, 2H), 7.43–7.40 (m, 1H), 7.35–7.30 (m, 2H), 7.23–7.18 (m, 1H), 7.03–6.93 (m, 4H), 4.93 (s, 1H), 4.63 (d, J = 11.8 Hz, 1H), 3.96–3.88 (m, 1H), 3.58–3.50 (m, 1H), 2.91–2.81 (m, 1H), 2.69–2.59 (m, 1H), 1.17 (s, 18H); ^{13}C NMR (100 MHz, 300 K, $CDCl_3$): δ 165.78 (q, J = 2.9 Hz), 155.17, 152.31, 145.97, 141.37, 135.27, 134.04, 131.29, 128.43, 128.29, 126.67, 126.37, 125.28 (q, J = 280.8 Hz), 124.85, 118.63, 51.47 (q, J = 24.4 Hz), 51.02 (br), 45.75, 34.10, 30.01, 23.60; ^{19}F NMR (376 MHz, 300 K, $CDCl_3$): δ –62.78 (d, J = 7.7 Hz); IR ($CHCl_3$ film): $\tilde{\nu}$ 3640, 1664, 1591, 1426, 1157, 755 cm^{-1}; HRMS

(ESI): *m/z* calculated for $C_{31}H_{36}F_3N_2O_2$ $[M+H]^+$: 525.2723, found: 525.2723; $[\alpha]_D^{26}$ –87.6 (*c* 1.0, $CHCl_3$, 97% ee sample). Enantiomeric excess of the product was determined to be 97% ee by chiral stationary phase HPLC analysis (CHIRALCEL OD-3 (*ø* 0.46 cm x 25 cm), hexane/2-propanol = 49/1, flow rate 1.0 mL/min, detection at 254 nm, t_R = 7.5 min (major), 10.6 min (minor)).

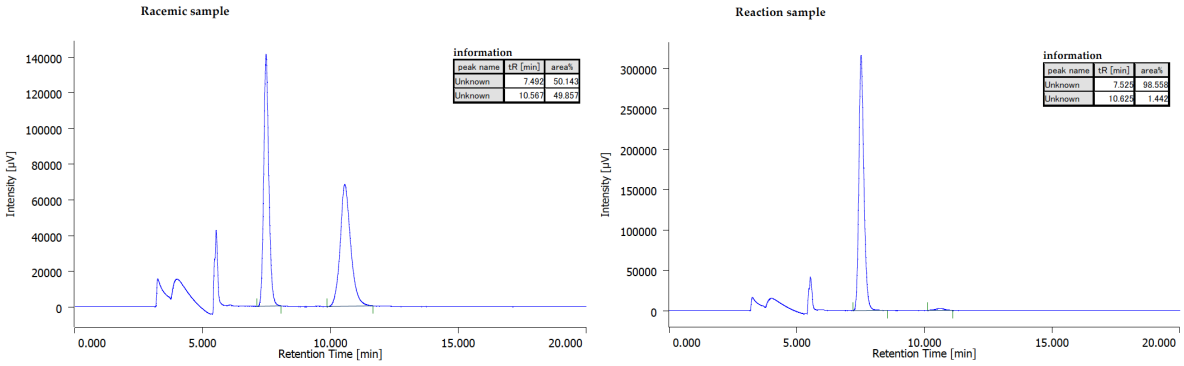

Methyl 4-((1*R*,2*S*)-1-(3,5-di-*tert*-butyl-4-hydroxyphenyl)-2-(2,3-dihydro-1*H*-pyrrolo[2,3-*b*]pyridine-1-carbonyl)-3,3,3-trifluoropropyl)benzoate (20b):

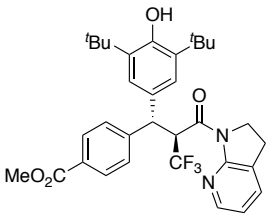

Obtained in 95% yield (111.0 mg); viscous foam; ^{1}H NMR (400 MHz, 300 K, $CDCl_3$): δ 8.30–8.28 (m, 1H), 8.03–8.00 (m, 2H), 7.60–7.57 (m, 2H), 7.44 (dq, *J* = 7.5, 1.4 Hz, 1H), 7.09–6.95 (m, 4H), 4.98 (s, 1H), 4.70 (d, *J* = 11.7 Hz, 1H), 3.98–3.90 (m, 1H), 3.89 (s, 3H), 3.59–3.52 (m, 1H), 2.93–2.84 (m, 1H), 2.71–2.62 (m, 1H), 1.17 (s, 18H); ^{13}C NMR (100 MHz, 300 K, $CDCl_3$): δ 166.97, 165.35 (br), 155.10, 152.54, 146.71, 145.97, 135.53, 134.18, 130.38, 129.86, 128.60, 128.34, 126.42, 125.17 (q, *J* = 281.9 Hz), 124.85, 118.79, 52.01, 51.17 (q, *J* = 24.6 Hz), 50.83 (br), 45.78, 34.14, 29.99, 23.60; ^{19}F NMR (376 MHz, 300 K, $CDCl_3$): δ –62.83 (d, *J* = 7.1 Hz); IR ($CHCl_3$ film): $\tilde{\nu}$ 3638, 1665, 1600, 1426, 757 cm^{-1}; HRMS (ESI): *m/z* calculated for $C_{33}H_{38}F_3N_2O_4$ $[M+H]^+$: 583.2278, found: 583.2275; $[\alpha]_D^{26}$ –43.4 (*c* 1.1, $CHCl_3$, 96% ee sample). Enantiomeric excess of the product was determined to be 96% ee by chiral stationary phase HPLC analysis (CHIRALCEL OD-H (*ø* 0.46 cm x 25 cm), hexane/2-propanol = 49/1, flow rate 1.0 mL/min, detection at 254 nm, t_R = 14.0 min (major), 24.0 min (minor)).

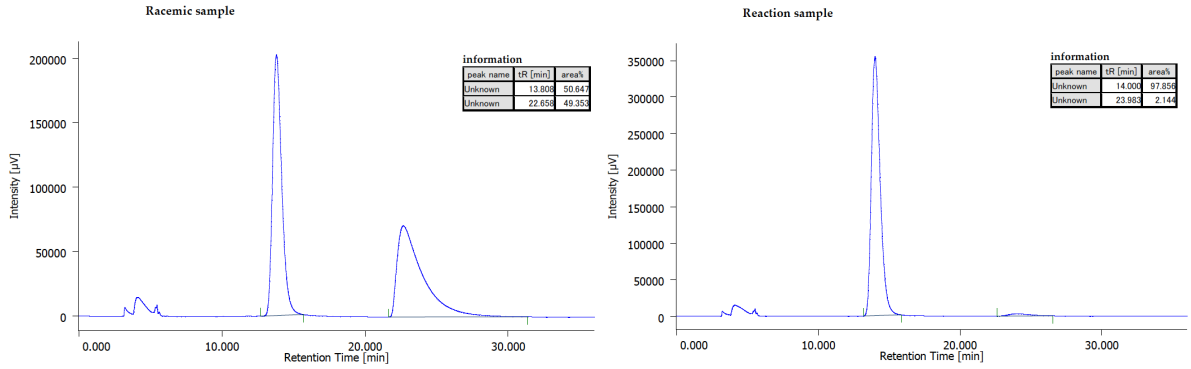

4-((1*R*,2*S*)-1-(3,5-Di-*tert*-butyl-4-hydroxyphenyl)-2-(2,3-dihydro-1*H*-pyrrolo[2,3-*b*]pyridine-1-carbonyl)-3,3,3-trifluoropropyl)benzonitrile (20c):

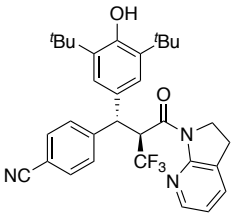

Obtained in 92% yield (101.4 mg); viscous foam; ^{1}H NMR (400 MHz, 300 K, $CDCl_3$): δ 8.29 (dd, *J* = 5.2, 1.6 Hz, 1H), 7.65–7.59 (m, 4H), 7.47 (dd, *J* = 7.4, 1.5 Hz, 1H), 7.08–6.95 (m, 4H), 5.02 (s, 1H), 4.71 (d, *J* = 11.8 Hz, 1H), 4.00–3.92 (m, 1H), 3.61–3.53 (m, 1H), 2.96–2.87 (m, 1H), 2.75–2.65 (m, 1H), 1.17 (s, 18H); ^{13}C NMR (100 MHz, 300 K, $CDCl_3$): δ 164.95 (q, *J* = 3.0 Hz), 155.02, 152.72, 146.99, 145.96, 135.78, 134.29, 132.37, 129.88, 129.07, 126.48, 125.06 (q, *J* = 282.4 Hz), 124.69, 118.91, 118.89, 110.60, 50.96 (q, *J* = 24.5 Hz), 50.79, 45.79, 34.16, 29.96, 23.58; ^{19}F NMR (376 MHz, 300 K, $CDCl_3$): δ –62.82 (d, *J* = 7.5 Hz); IR ($CHCl_3$ film): $\tilde{\nu}$ 3638, 2230, 1665, 1592, 1426, 758 cm^{-1}; HRMS (ESI): *m/z* calculated for $C_{32}H_{35}F_3N_3O_2$ $[M+H]^+$: 550.2676, found: 550.2674; $[\alpha]_D^{26}$ –65.6 (*c* 1.0, $CHCl_3$, 92% ee sample). Enantiomeric excess of the product was determined to be 92% ee by chiral stationary phase HPLC analysis (CHIRALCEL OD-H (ø 0.46 cm x 25 cm), hexane/2-propanol = 49/1, flow rate 1.0 mL/min, detection at 254 nm, t_R = 20.0 min (major), 30.7 min (minor)).

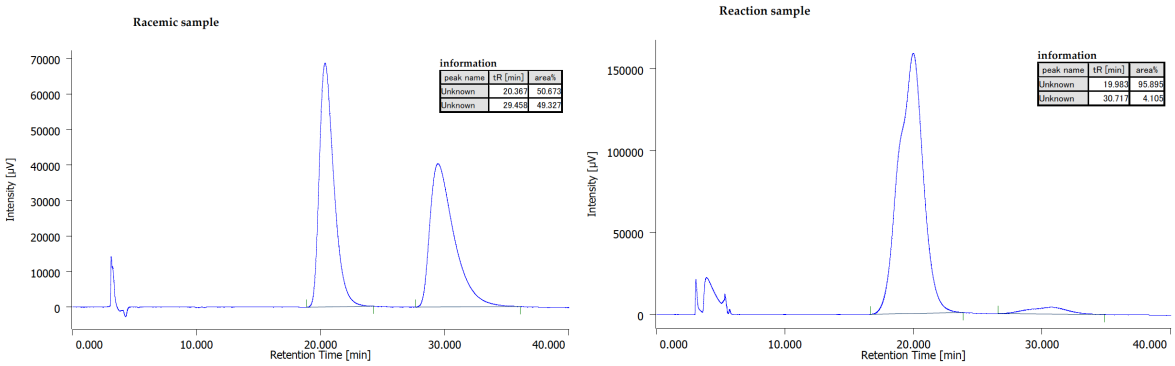

(*S*)-2-((*R*)-(3,5-Di-*tert*-butyl-4-hydroxyphenyl)(4-(trifluoromethyl)phenyl)methyl)-1-(2,3-dihydro-1*H*-pyrrolo[2,3-*b*]pyridin-1-yl)-3,3,3-trifluoropropan-1-one (20d):

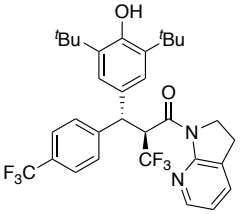

Obtained in 96% yield (113.5 mg); viscous foam; ^{1}H NMR (400 MHz, 300 K, $CDCl_3$): δ 8.30–8.27 (m, 1H), 7.64–7.58 (m, 4H), 7.46–7.42 (m, 1H), 7.10–6.95 (m, 4H), 4.99 (s, 1H), 4.72 (d, *J* = 11.8 Hz, 1H), 3.99–3.91 (m, 1H), 3.60–3.52 (m, 1H), 2.94–2.85 (m, 1H), 2.73–2.63 (m, 1H), 1.18 (s, 18H); ^{13}C NMR (100 MHz, 300 K, $CDCl_3$): δ 165.25 (q, *J* = 3.3 Hz), 155.11, 152.63, 145.98, 145.58, 135.65, 134.23, 130.41, 128.94 (q, *J* = 32.4 Hz), 128.62, 126.47, 125.49 (q, *J* = 3.8 Hz), 125.17 (q, *J* = 282.0 Hz), 124.76, 124.26 (q, *J* = 271.9 Hz), 118.85, 51.21 (q, *J* = 24.5 Hz), 50.72 (br), 45.79, 34.16, 29.99, 23.60; ^{19}F NMR (376 MHz, 300 K, $CDCl_3$): δ –62.39, –62.78 (d, *J* = 7.6 Hz); IR ($CHCl_3$ film): $\tilde{\nu}$ 3639, 1664, 1592, 1426, 762 cm^{-1}; HRMS (ESI): *m/z* calculated for $C_{32}H_{35}F_6N_2O_2$ $[M+H]^+$: 593.2597, found: 593.2591; $[\alpha]_D^{26}$ –83.0 (*c* 1.0, $CHCl_3$, 95% ee sample). Enantiomeric excess of the product was determined to be 95% ee by chiral stationary phase HPLC analysis (CHIRALCEL OD-H (ø 0.46 cm x 25 cm), hexane/2-propanol = 49/1, flow rate 1.0 mL/min, detection at 254 nm, t_R = 7.7 min (major), 10.7 min (minor)).

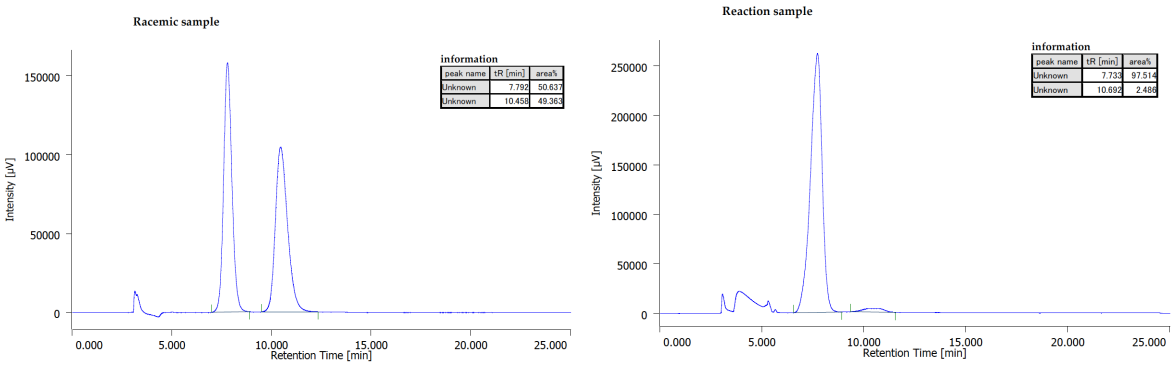

(*S*)-2-((*R*)-(3,5-Di-*tert*-butyl-4-hydroxyphenyl)(4-nitrophenyl)methyl)-1-(2,3-dihydro-1*H*-pyrrolo[2,3-*b*]pyridin-1-yl)-3,3,3-trifluoropropan-1-one (20e):

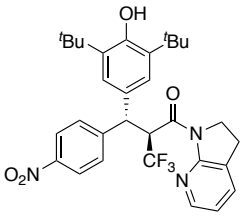

Obtained in 93% yield (106.3 mg); viscous foam; ^{1}H NMR (400 MHz, 300 K, $CDCl_3$): δ 8.30 (dd, *J* = 5.2, 1.6 Hz, 1H), 8.22–8.18 (m, 2H), 7.69–7.64 (m, 2H), 7.49–7.46 (m, 1H), 7.12–7.04 (m, 1H), 7.01–6.97 (m, 3H), 5.03 (s, 1H), 4.78 (d, *J* = 11.8 Hz, 1H), 4.02–3.94 (m, 1H), 3.62–3.55 (m, 1H), 2.97–2.89 (m, 1H), 2.77–2.67 (m, 1H), 1.18 (s, 18H); ^{13}C NMR (100 MHz, 300 K, $CDCl_3$): δ 164.85 (q, *J* = 3.2 Hz), 155.01, 152.79, 149.11, 146.78, 145.98, 135.86, 134.33, 129.70, 129.12, 126.51, 125.07 (q, *J* = 281.9 Hz), 124.70, 123.84, 118.97, 51.01 (q, *J* = 24.6 Hz), 50.54 (br), 45.81, 34.17, 29.96, 23.59; ^{19}F NMR (376 MHz, 300 K, $CDCl_3$): δ –62.82 (d, *J* = 7.6 Hz); IR ($CHCl_3$ film): $\tilde{\nu}$ 3638, 1665, 1595, 1523, 758 cm^{-1}; HRMS (ESI): *m/z* calculated for $C_{31}H_{35}F_3N_3O_4$ $[M+H]^+$: 570.2574, found: 570.2579; $[\alpha]_D^{26}$ –53.1 (*c* 1.0, $CHCl_3$, 93% ee sample). Enantiomeric excess of the product was determined to be 93% ee by chiral stationary phase HPLC analysis (CHIRALCEL OD-H (ø 0.46 cm x 25 cm), hexane/2-propanol = 49/1, flow rate 1.0 mL/min, detection at 254 nm, t_R = 7.5 min (major), 10.6 min (minor)).

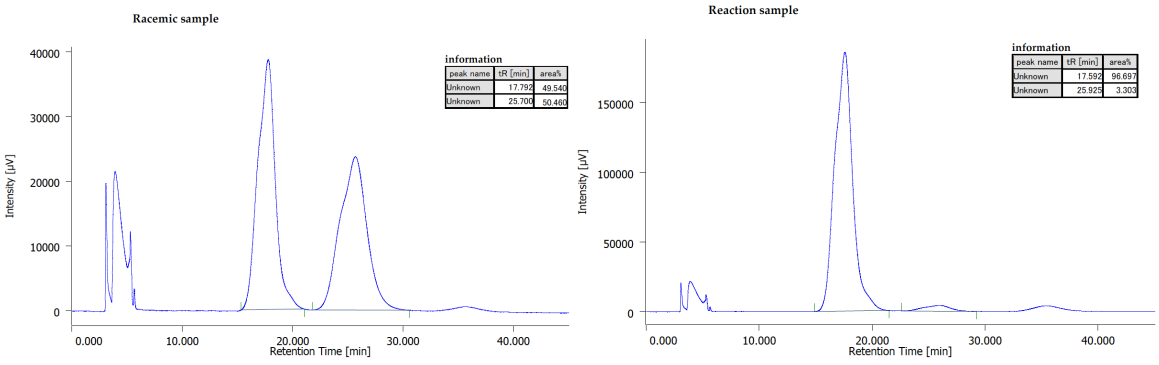

(*S*)-2-((*S*)-Benzo[*d*][1,3]dioxol-5-yl(3,5-di-*tert*-butyl-4-hydroxyphenyl)methyl)-1-(2,3-dihydro-1*H*-pyrrolo[2,3-*b*]pyridin-1-yl)-3,3,3-trifluoropropan-1-one (20f):

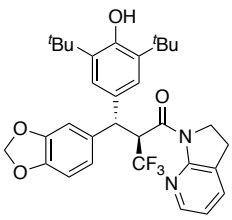

Obtained in 93% yield (105.6 mg); viscous foam; ^{1}H NMR (400 MHz, 300 K, $CDCl_3$): δ 8.29–8.26 (m, 1H), 7.44–7.40 (m, 1H), 6.99–6.85 (m, 6H), 6.76 (d, J = 7.9 Hz, 1H), 5.91 (q, J = 1.5 Hz, 2H), 4.95 (s, 1H), 4.58 (d, J = 11.8 Hz, 1H), 3.97–3.89 (m, 1H), 3.58–3.50 (m, 1H), 2.92–2.83 (m, 1H), 2.71–2.61 (m, 1H), 1.18 (s, 18H); ^{13}C NMR (100 MHz, 300 K, $CDCl_3$): δ 165.67 (br), 155.15, 152.33, 147.57, 146.27, 146.01, 135.38, 135.37, 134.09, 131.51, 126.38, 125.28 (q, J = 282.0 Hz), 124.59, 121.44, 118.68, 108.62, 108.19, 100.88, 51.56 (q, J = 24.2 Hz), 50.61 (br), 45.74, 34.11, 30.02, 23.59; ^{19}F NMR (376 MHz, 300 K, $CDCl_3$): δ –62.77 (d, J = 7.7 Hz); IR ($CHCl_3$ film): $\tilde{\nu}$ 3640, 1664, 1599, 1426, 760 cm^{-1}; HRMS (ESI): *m/z* calculated for $C_{32}H_{36}F_3N_2O_4$ $[M+H]^+$: 569.2622, found: 569.2620; $[\alpha]_D^{26}$ –114.5 (*c* 1.0, $CHCl_3$, 98% ee sample). Enantiomeric excess of the product was determined to be 98% ee by chiral stationary phase HPLC analysis (CHIRALCEL OD-H (ø 0.46 cm x 25 cm), hexane/2-propanol = 49/1, flow rate 1.0 mL/min, detection at 254 nm, t_R = 13.1 min (major), 30.6 min (minor)).

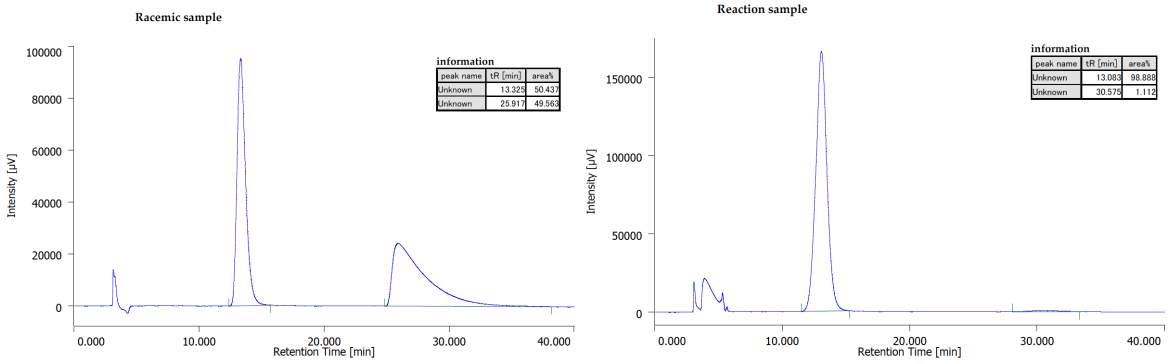

(*S*)-2-((*R*)-(3,5-Di-*tert*-butyl-4-hydroxyphenyl)(naphthalen-2-yl)methyl)-1-(2,3-dihydro-1*H*-pyrrolo[2,3-*b*]pyridin-1-yl)-3,3,3-trifluoropropan-1-one (20g):

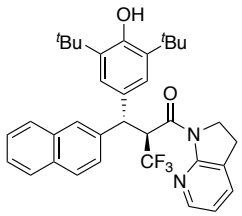

Obtained in 98% yield (112.3 mg); viscous foam; ^{1}H NMR (400 MHz, 300 K, $CDCl_3$): δ 8.32 (dd, J = 5.2, 1.5 Hz, 1H), 7.93–7.92 (m, 1H), 7.84–7.76 (m, 3H), 7.69 (dd, J = 8.6, 1.8 Hz, 1H), 7.46–7.35 (m, 3H), 7.17–7.04 (m, 3H), 6.94 (dd, J = 7.4, 5.1 Hz, 1H), 4.93 (s, 1H), 4.83 (d, J = 11.7 Hz, 1H), 3.97–3.89 (m, 1H), 3.60–3.52 (m, 1H), 2.88–2.79 (m, 1H), 2.68–2.59 (m, 1H), 1.16 (s, 18H); ^{13}C NMR (100 MHz, 300 K, $CDCl_3$): δ 165.72 (br), 155.17, 152.33, 145.95, 138.89, 135.34, 134.09, 133.55, 132.39, 131.19, 128.02, 127.86, 127.53, 127.09, 126.41, 126.29, 125.91, 125.54, 125.33 (q, J = 281.9 Hz), 124.87, 118.69, 51.34 (q, J = 24.3 Hz), 51.09 (br), 45.77, 34.09, 29.99, 23.57; ^{19}F NMR (376 MHz, 300 K, $CDCl_3$): δ –62.74 (d, J = 7.5 Hz); IR ($CHCl_3$ film): $\tilde{\nu}$ 3639, 1664, 1593, 1426, 759 cm^{-1}; HRMS (ESI): *m/z* calculated for $C_{35}H_{38}F_3N_2O_2$ $[M+H]^+$: 575.2872, found: 575.2871; $[\alpha]_D^{26}$ –100.2 (*c* 1.0, $CHCl_3$, 97% ee sample). Enantiomeric excess of the product was determined to be 97% ee by chiral stationary phase HPLC analysis (CHIRALCEL OD-H (ø 0.46 cm x 25 cm), hexane/2-propanol = 49/1, flow rate 1.0 mL/min, detection at 254 nm, t_R = 9.9 min (major), 21.6 min (minor)).

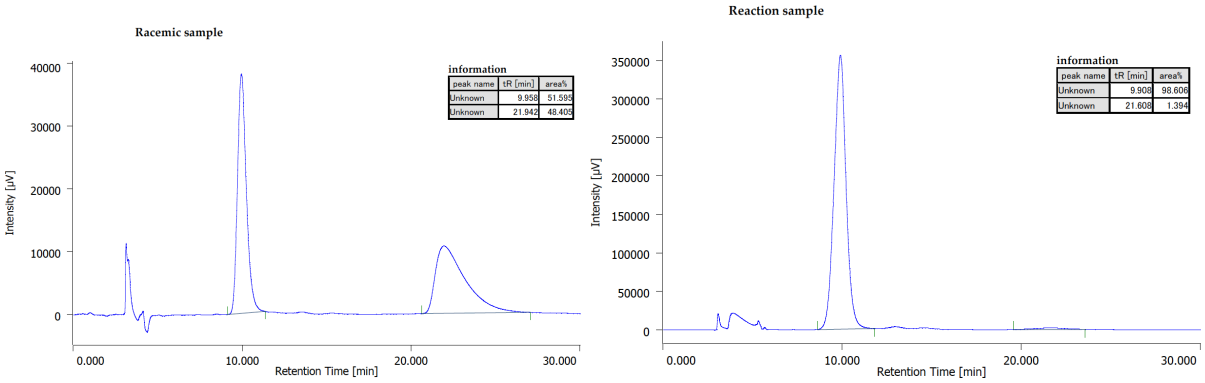

(*S*)-2-((*S*)-(3,5-Di-*tert*-butyl-4-hydroxyphenyl)(2-fluorophenyl)methyl)-1-(2,3-dihydro-1*H*-pyrrolo[2,3-*b*]pyridin-1-yl)-3,3,3-trifluoropropan-1-one (20h):

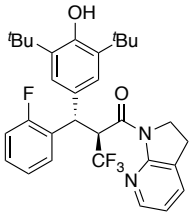

Obtained in 96% yield (104.2 mg); viscous foam; ^{1}H NMR (400 MHz, 300 K, $CDCl_3$): δ 8.28–8.26 (m, 1H), 7.60 (td, *J* = 7.5, 1.9 Hz, 1H), 7.44–7.40 (m, 1H), 7.22–7.08 (m, 3H), 7.05 (s, 2H), 7.03–6.96 (m, 1H), 6.94 (dd, *J* = 7.4, 5.1 Hz, 1H), 4.96 (s, 1H), 4.95 (d, *J* = 12.1 Hz, 1H), 3.97–3.89 (m, 1H), 3.60–3.53 (m, 1H), 2.92–2.82 (m, 1H), 2.70–2.60 (m, 1H), 1.18 (s, 18H); ^{13}C NMR (100 MHz, 300 K, $CDCl_3$): δ 165.55 (br), 160.57 (d, *J* = 246.0 Hz), 155.12, 152.49, 146.01, 135.38, 134.07, 130.35, 129.97, 128.46 (d, *J* = 13.8 Hz), 128.33 (d, *J* = 8.4 Hz), 126.33, 125.27 (q, *J* = 281.9 Hz), 125.10 (d, *J* = 2.0 Hz), 124.01 (d, *J* = 3.5 Hz), 118.72, 115.91 (d, *J* = 23.0 Hz), 50.09 (q, *J* = 24.5 Hz), 45.83, 44.41 (br), 34.12, 30.02, 23.64; ^{19}F NMR (376 MHz, 300 K, $CDCl_3$): δ –63.48 (d, *J* = 7.4 Hz), –116.22; IR ($CHCl_3$ film): $\tilde{\nu}$ 3639, 1665, 1601, 1427, 758 cm^{-1}; HRMS (ESI): *m/z* calculated for $C_{31}H_{35}F_4N_2O_2$ $[M+H]^+$: 543.2629, found: 543.2631; $[\alpha]_D^{26}$ –85.8 (*c* 1.0, $CHCl_3$, 96% ee sample). Enantiomeric excess of the product was determined to be 97% ee by chiral stationary phase HPLC analysis (CHIRALCEL OD-H (ø 0.46 cm x 25 cm), hexane/2-propanol = 49/1, flow rate 1.0 mL/min, detection at 254 nm, t_R = 8.8 min (major), 13.5 min (minor)).

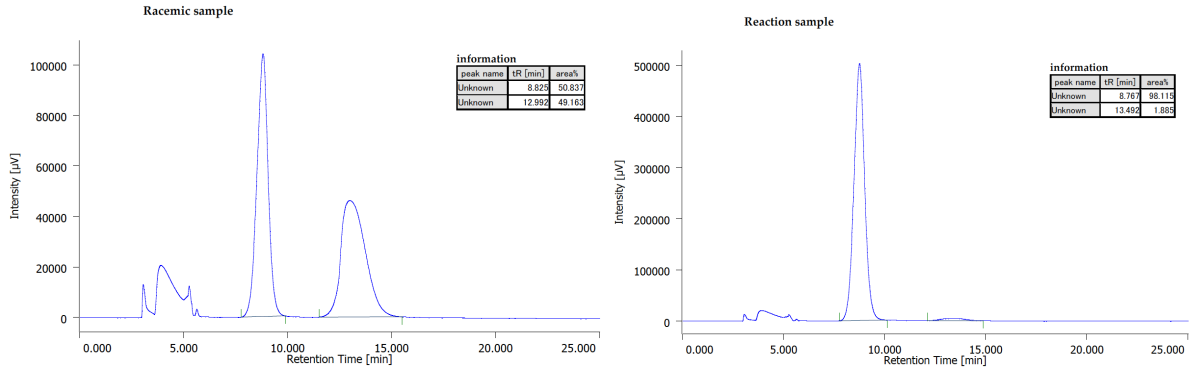

(*S*)-2-((*S*)-(3,5-Di-*tert*-butyl-4-hydroxyphenyl)(3-fluorophenyl)methyl)-1-(2,3-dihydro-1*H*-pyrrolo[2,3-*b*]pyridin-1-yl)-3,3,3-trifluoropropan-1-one (20i):

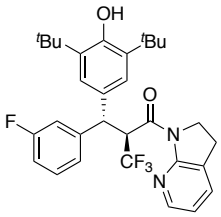

Obtained in 94% yield (101.9 mg); viscous foam; ^{1}H NMR (400 MHz, 300 K, $CDCl_3$): δ 8.30–8.27 (m, 1H), 7.44–7.41 (m, 1H), 7.30–7.20 (m, 3H), 7.02–6.87 (m, 5H), 4.98 (s, 1H), 4.64 (d, J = 11.7 Hz, 1H), 3.97–3.89 (m, 1H), 3.58–3.50 (m, 1H), 2.92–2.83 (m, 1H), 2.71–2.61 (m, 1H), 1.18 (s, 18H); ^{13}C NMR (100 MHz, 300 K, $CDCl_3$): δ 165.38 (q, J = 3.1 Hz), 162.78 (d, J = 245.3 Hz), 155.10, 152.51, 145.99, 144.01 (d, J = 7.0 Hz), 135.48, 134.15, 130.68, 129.89 (d, J = 8.3 Hz), 126.40, 125.20 (q, J = 281.9 Hz), 124.78, 124.03 (d, J = 2.7 Hz), 118.76, 115.22 (d, J = 21.7 Hz), 113.61 (d, J = 21.2 Hz), 51.34 (q, J = 24.4 Hz), 50.58 (br), 45.75, 34.13, 29.99, 23.58; ^{19}F NMR (376 MHz, 300 K, $CDCl_3$): δ –62.86 (d, J = 7.6 Hz), –113.12—113.16 (m); IR ($CHCl_3$ film): $\tilde{\nu}$ 3638, 1665, 1592, 1427, 758 cm^{-1}; HRMS (ESI): *m/z* calculated for $C_{31}H_{35}F_4N_2O_2$ $[M+H]^+$: 543.2629, found: 543.2629; $[\alpha]_D^{26}$ –89.8 (*c* 1.0, $CHCl_3$, 97% ee sample). Enantiomeric excess of the product was determined to be 97% ee by chiral stationary phase HPLC analysis (CHIRALCEL OD-H (ø 0.46 cm x 25 cm), hexane/2-propanol = 49/1, flow rate 1.0 mL/min, detection at 254 nm, t_R = 8.5 min (major), 12.3 min (minor)).

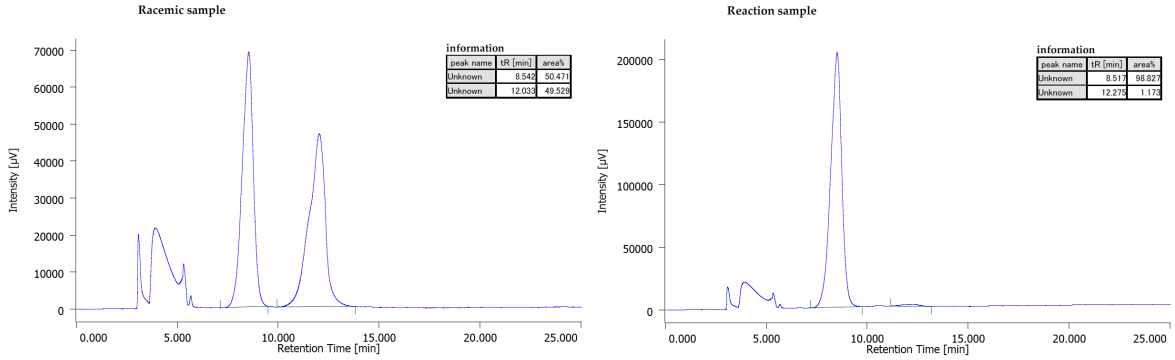

(*S*)-2-((*R*)-(3,5-Di-*tert*-butyl-4-hydroxyphenyl)(4-fluorophenyl)methyl)-1-(2,3-dihydro-1*H*-pyrrolo[2,3-*b*]pyridin-1-yl)-3,3,3-trifluoropropan-1-one (20j):

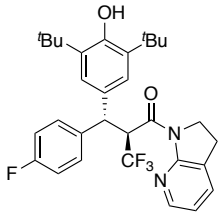

Obtained in 96% yield (104.6 mg); viscous foam; ^{1}H NMR (400 MHz, 300 K, $CDCl_3$): δ 8.29–8.26 (m, 1H), 7.49–7.41 (m, 3H), 7.05–6.91 (m, 6H), 4.95 (s, 1H), 4.64 (d, J = 11.7 Hz, 1H), 3.97–3.89 (m, 1H), 3.59–3.51 (m, 1H), 2.92–2.83 (m, 1H), 2.70–2.60 (m, 1H), 1.18 (s, 18H); ^{13}C NMR (100 MHz, 300 K, $CDCl_3$): δ 165.58 (q, J = 2.9 Hz), 161.70 (d, J = 244.7 Hz), 155.12, 152.39, 145.94, 137.19 (d, J = 3.3 Hz), 135.40, 134.11, 131.10, 129.74 (d, J = 7.9 Hz), 126.40, 125.22 (q, J = 281.9 Hz), 124.73, 118.71, 115.28 (d, J = 21.3 Hz), 51.56 (q, J = 24.2 Hz), 50.16 (br), 45.76, 34.12, 30.00, 23.59; ^{19}F NMR (376 MHz, 300 K, $CDCl_3$): δ –62.70 (d, J = 7.7 Hz), –116.41—116.49 (m); IR ($CHCl_3$ film): $\tilde{\nu}$ 3638, 1665, 1593, 1426, 762 cm^{-1}; HRMS (ESI): *m/z* calculated for $C_{31}H_{35}F_4N_2O_2$ $[M+H]^+$: 543.2629, found: 543.2628; $[\alpha]_D^{26}$ –80.8 (*c* 1.0, $CHCl_3$, 96% ee sample). Enantiomeric excess of the product was determined to be 96% ee by chiral stationary phase HPLC analysis (CHIRALCEL OD-H (ø 0.46 cm x 25 cm), hexane/2-propanol = 49/1, flow rate 1.0 mL/min, detection at 254 nm, t_R = 8.4 min (major), 11.4 min (minor)).

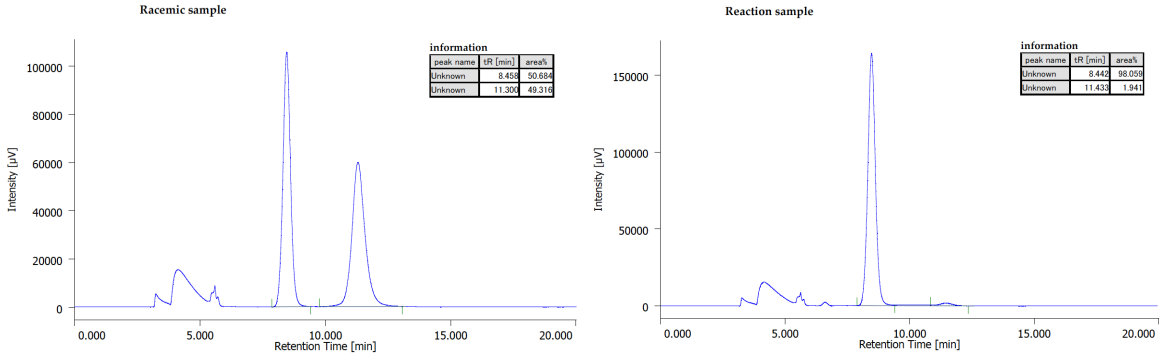

(*S*)-2-((*S*)-(2-Chlorophenyl)(3,5-di-*tert*-butyl-4-hydroxyphenyl)methyl)-1-(2,3-dihydro-1*H*-pyrrolo[2,3-*b*]pyridin-1-yl)-3,3,3-trifluoropropan-1-one (20k):

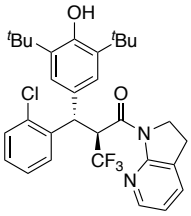

Obtained in 94% yield (104.7 mg); white solid; m.p. : 177–179 °C; ^{1}H NMR (400 MHz, 300 K, $CDCl_3$): δ 8.29 (dd, *J* = 5.2, 1.5 Hz, 1H), 7.79 (d, *J* = 7.9 Hz, 1H), 7.45–7.41 (m, 1H), 7.35–7.29 (m, 2H), 7.13 (td, *J* = 7.7, 1.6 Hz, 1H), 7.08 (br, 1H), 7.03 (s, 2H), 6.96 (dd, *J* = 7.4, 5.1 Hz, 1H), 5.33 (d, *J* = 11.8 Hz, 1H), 4.95 (s, 1H), 3.98–3.90 (m, 1H), 3.55–3.48 (m, 1H), 2.92–2.83 (m, 1H), 2.69–2.60 (m, 1H), 1.17 (s, 18H); ^{13}C NMR (100 MHz, 300 K, $CDCl_3$): δ 165.36 (br), 155.19, 152.44, 145.93, 138.74, 135.22, 134.16, 133.93, 129.99, 129.74, 128.94, 127.69, 126.55, 126.48, 125.36, 125.25 (q, *J* = 282.0 Hz), 50.71 (q, *J* = 23.4 Hz), 45.79, 45.61 (br), 34.10, 30.02, 23.60; ^{19}F NMR (376 MHz, 300 K, $CDCl_3$): δ –63.00 (d, *J* = 7.5 Hz); IR ($CHCl_3$ film): $\tilde{\nu}$ 3638, 1666, 1591, 1426, 759 cm^{-1}; HRMS (ESI): *m/z* calculated for $C_{31}H_{35}ClF_3N_2O_2$ $[M+H]^+$: 559.2334, found: 559.2337; $[\alpha]_D^{26}$ –119.0 (*c* 1.1, $CHCl_3$, 97% ee sample). Enantiomeric excess of the product was determined to be 97% ee by chiral stationary phase HPLC analysis (CHIRALCEL OD-H (ø 0.46 cm x 25 cm), hexane/2-propanol = 49/1, flow rate 1.0 mL/min, detection at 254 nm, t_R = 8.7 min (major), 11.1 min (minor)).

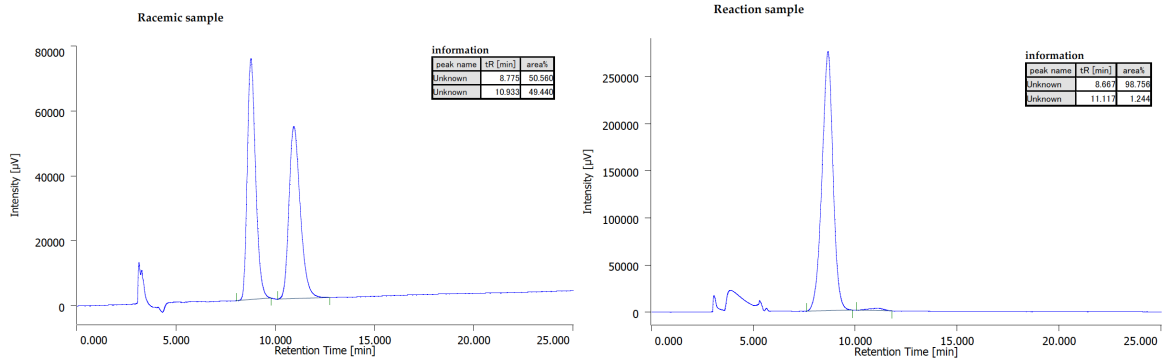

(*S*)-2-((*S*)-(3-Chlorophenyl)(3,5-di-*tert*-butyl-4-hydroxyphenyl)methyl)-1-(2,3-dihydro-1*H*-pyrrolo[2,3-*b*]pyridin-1-yl)-3,3,3-trifluoropropan-1-one (20l):

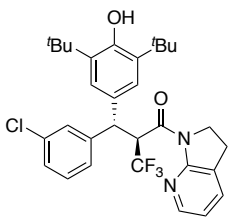

Obtained in 95% yield (106.3 mg); viscous foam; ^{1}H NMR (400 MHz, 300 K, $CDCl_3$): δ 8.31–8.28 (m, 1H), 7.50 (t, J = 1.9 Hz, 1H), 7.45–7.39 (m, 2H), 7.27 (t, J = 7.8 Hz, 1H), 7.21–7.17 (m, 1H), 7.02–6.93 (m, 4H), 4.97 (s, 1H), 4.61 (d, J = 11.7 Hz, 1H), 3.97–3.89 (m, 1H), 3.57–3.49 (m, 1H), 2.92–2.83 (m, 1H), 2.70–2.60 (m, 1H), 1.18 (s, 18H); ^{13}C NMR (100 MHz, 300 K, $CDCl_3$): δ 165.33 (q, J = 2.9 Hz), 155.07, 152.52, 145.97, 143.46, 135.46, 134.14, 134.11, 130.47, 129.68, 128.64, 126.89, 126.41, 126.38, 125.16 (q, J = 281.9 Hz), 124.84, 118.76, 51.29 (q, J = 24.4 Hz), 50.54 (br), 45.74, 34.13, 29.98, 23.57; ^{19}F NMR (376 MHz, 300 K, $CDCl_3$): δ –62.84 (d, J = 7.8 Hz); IR ($CHCl_3$ film): $\tilde{\nu}$ 3638, 1666, 1594, 1426, 761 cm^{-1}; HRMS (ESI): *m/z* calculated for $C_{31}H_{35}ClF_3N_2O_2$ $[M+H]^+$: 559.2334, found: 559.2332; $[\alpha]_D^{26}$ –72.0 (*c* 1.0, $CHCl_3$, 96% ee sample). Enantiomeric excess of the product was determined to be 96% ee by chiral stationary phase HPLC analysis (CHIRALCEL OD-H (ø 0.46 cm x 25 cm), hexane/2-propanol = 49/1, flow rate 1.0 mL/min, detection at 254 nm, t_R = 8.6 min (major), 12.3 min (minor)).

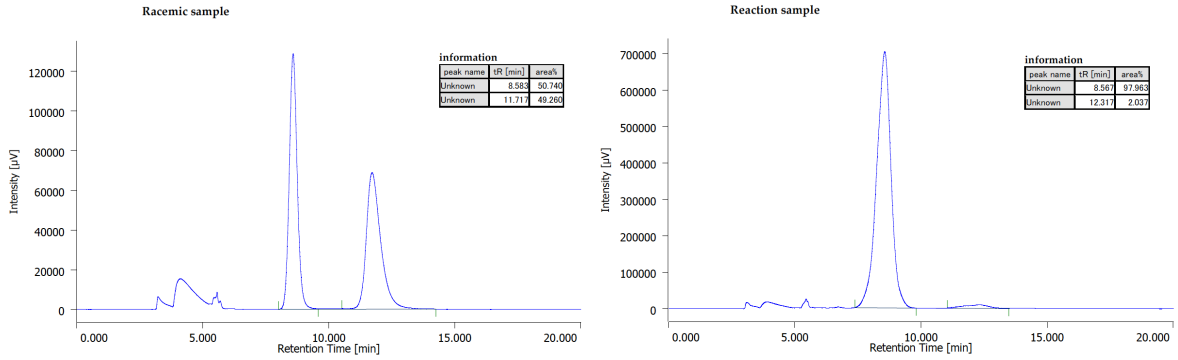

(*S*)-2-((*R*)-(4-Chlorophenyl)(3,5-di-*tert*-butyl-4-hydroxyphenyl)methyl)-1-(2,3-dihydro-1*H*-pyrrolo[2,3-*b*]pyridin-1-yl)-3,3,3-trifluoropropan-1-one (20m):

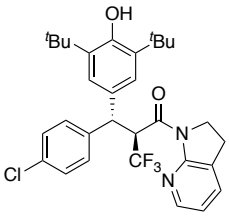

Obtained in 93% yield (104.9 mg); viscous foam; ^{1}H NMR (400 MHz, 300 K, $CDCl_3$): δ 8.28–8.26 (m, 1H), 7.45–7.40 (m, 3H), 7.32–7.25 (m, 2H), 6.99–6.91 (m, 4H), 4.96 (s, 1H), 4.62 (d, J = 11.8 Hz, 1H), 3.97–3.89 (m, 1H), 3.58–3.51 (m, 1H), 2.92–2.83 (m, 1H), 2.71–2.61 (m, 1H), 1.17 (s, 18H); ^{13}C NMR (100 MHz, 300 K, $CDCl_3$): δ 165.44 (q, J = 3.1 Hz), 155.10, 152.45, 145.95, 140.01, 135.46, 134.13, 132.44, 130.81, 129.61, 128.61, 126.40, 125.18 (q, J = 281.7 Hz), 124.69, 118.74, 51.34 (q, J = 24.4 Hz), 50.28 (br), 45.76, 34.12, 29.99, 23.58; ^{19}F NMR (376 MHz, 300 K, $CDCl_3$): δ –62.70 (d, J = 7.6 Hz); IR ($CHCl_3$ film): $\tilde{\nu}$ 3638, 1665, 1593, 1426, 758 cm^{-1}; HRMS (ESI): *m/z* calculated for $C_{31}H_{35}ClF_3N_2O_2$ $[M+H]^+$: 559.2334, found: 559.2337; $[\alpha]_D^{26}$ –63.7 (*c* 1.0, $CHCl_3$, 96% ee sample). Enantiomeric excess of the product was determined to be 96% ee by chiral stationary phase HPLC analysis (CHIRALCEL OD-H (ø 0.46 cm x 25 cm), hexane/2-propanol = 49/1, flow rate 1.0 mL/min, detection at 254 nm, t_R = 8.4 min (major), 11.2 min (minor)).

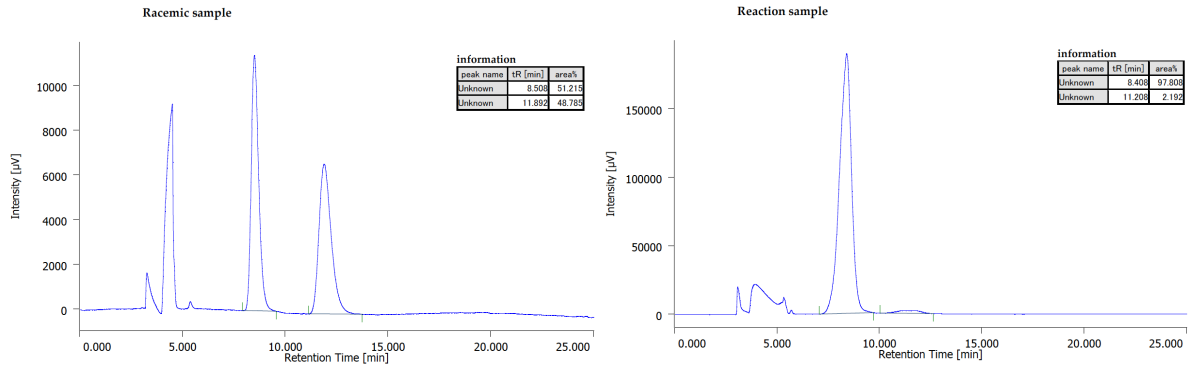

(*S*)-2-((*S*)-(2-Bromophenyl)(3,5-di-*tert*-butyl-4-hydroxyphenyl)methyl)-1-(2,3-dihydro-1*H*-pyrrolo[2,3-*b*]pyridin-1-yl)-3,3,3-trifluoropropan-1-one (20n):

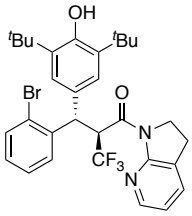

Obtained in 95% yield (114.7 mg); viscous foam; ^{1}H NMR (400 MHz, 300 K, $CDCl_3$): δ 8.30–8.27 (m, 1H), 7.81–7.78 (m, 1H), 7.53 (dd, *J* = 8.0, 1.3 Hz, 1H), 7.42 (dd, *J* = 7.4, 1.6 Hz, 1H), 7.38–7.33 (m, 1H), 7.12–7.02 (m, 4H), 6.95 (dd, *J* = 7.4, 5.1 Hz, 1H), 5.31 (d, *J* = 11.8 Hz, 1H), 4.95 (s, 1H), 3.97–3.89 (m, 1H), 3.54–3.47 (m, 1H), 2.91–2.82 (m, 1H), 2.68–2.59 (m, 1H), 1.17 (s, 18H); ^{13}C NMR (100 MHz, 300 K, $CDCl_3$): δ 165.28 (br), 155.19, 152.46, 145.91, 140.35, 135.22, 134.19, 133.34, 129.69, 129.06, 128.00, 127.20, 126.49, 125.39, 125.29 (q, *J* = 282.2 Hz), 124.85, 118.70, 50.87 (q, *J* = 24.8 Hz), 48.46 (br), 45.78, 34.11, 30.02, 23.59; ^{19}F NMR (376 MHz, 300 K, $CDCl_3$): δ –62.85 (d, *J* = 7.1 Hz); IR ($CHCl_3$ film): $\tilde{\nu}$ 3637, 1666, 1591, 1425, 759 cm^{-1}; HRMS (ESI): *m/z* calculated for $C_{31}H_{35}BrF_3N_2O_2$ $[M+H]^+$: 603.1829, found: 603.1827; $[\alpha]_D^{26}$ –130.0 (*c* 1.0, $CHCl_3$, 96% ee sample). Enantiomeric excess of the product was determined to be 96% ee by chiral stationary phase HPLC analysis (CHIRALCEL OD-H (ø 0.46 cm x 25 cm), hexane/2-propanol = 49/1, flow rate 1.0 mL/min, detection at 254 nm, t_R = 8.8 min (major), 10.7 min (minor)).

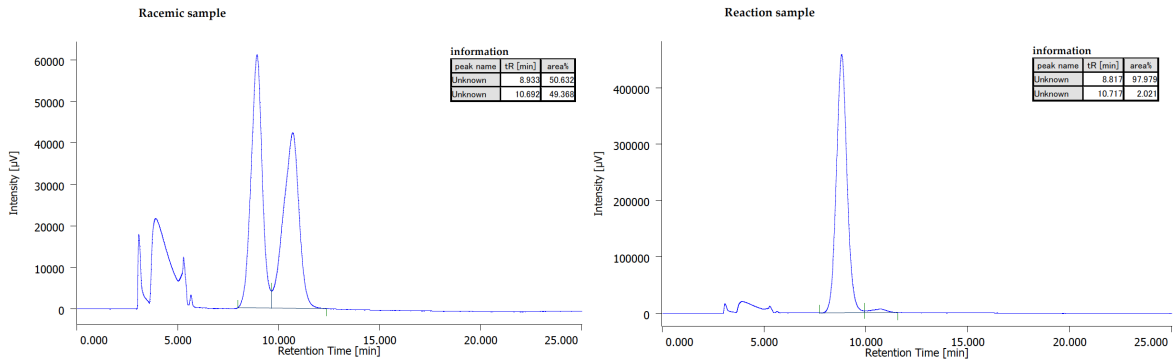

(*S*)-2-((*S*)-(3-Bromophenyl)(3,5-di-*tert*-butyl-4-hydroxyphenyl)methyl)-1-(2,3-dihydro-1*H*-pyrrolo[2,3-*b*]pyridin-1-yl)-3,3,3-trifluoropropan-1-one (20o):

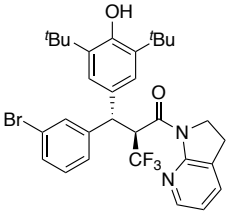

Obtained in 94% yield (113.2 mg); viscous foam; ^{1}H NMR (400 MHz, 300 K, $CDCl_3$): δ 8.31–8.28 (m, 1H), 7.67 (t, *J* = 1.8 Hz, 1H), 7.47–7.41 (m, 2H), 7.36–7.33 (m, 1H), 7.21 (t, *J* = 7.8 Hz, 1H), 7.01–6.90 (m, 4H), 4.98 (s, 1H), 4.59 (d, *J* = 11.6 Hz, 1H), 3.97–3.89 (m, 1H), 3.56–3.48 (m, 1H), 2.92–2.82 (m, 1H), 2.70–2.59 (m, 1H), 1.18 (s, 18H); ^{13}C NMR (100 MHz, 300 K, $CDCl_3$): δ 165.29 (q, *J* = 3.2 Hz), 155.05, 152.52, 145.95, 143.72, 135.44, 134.15, 131.57, 130.38, 129.98, 129.80, 126.84, 126.37, 125.15 (q, *J* = 282.0 Hz), 124.87, 122.40, 118.75, 51.29 (q, *J* = 24.5 Hz), 50.50 (br), 45.73, 34.12, 29.97, 23.56; ^{19}F NMR (376 MHz, 300 K, $CDCl_3$): δ –62.84 (d, *J* = 7.3 Hz); IR ($CHCl_3$ film): $\tilde{\nu}$ 3638, 1665, 1592, 1426, 760 cm^{-1}; HRMS (ESI): *m/z* calculated for $C_{31}H_{35}BrF_3N_2O_2$ $[M+H]^+$: 603.1829, found: 603.1834; $[\alpha]_D^{26}$ –62.7 (*c* 1.0, $CHCl_3$, 96% ee sample). Enantiomeric excess of the product was determined to be 96% ee by chiral stationary phase HPLC analysis (CHIRALCEL OD-H (ø 0.46 cm x 25 cm), hexane/2-propanol = 49/1, flow rate 1.0 mL/min, detection at 254 nm, t_R = 7.5 min (major), 10.6 min (minor)).

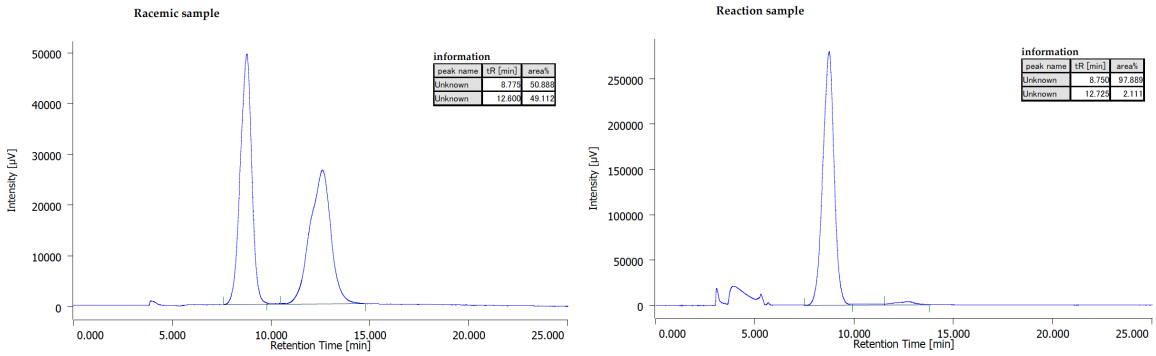

(*S*)-2-((*R*)-(4-Bromophenyl)(3,5-di-*tert*-butyl-4-hydroxyphenyl)methyl)-1-(2,3-dihydro-1*H*-pyrrolo[2,3-*b*]pyridin-1-yl)-3,3,3-trifluoropropan-1-one (20p):

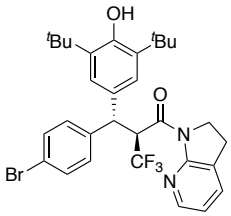

Obtained in 94% yield (113.9 mg); viscous foam; ^{1}H NMR (400 MHz, 300 K, $CDCl_3$): δ 8.27 (dd, *J* = 5.2, 1.5 Hz, 1H), 7.47–7.35 (m, 5H), 7.00–6.91 (m, 4H), 4.96 (s, 1H), 4.61 (d, *J* = 11.8 Hz, 1H), 3.98–3.90 (m, 1H), 3.59–3.51 (m, 1H), 2.93–2.84 (m, 1H), 2.71–2.62 (m, 1H), 1.17 (s, 18H); ^{13}C NMR (100 MHz, 300 K, $CDCl_3$): δ 165.41 (br), 155.09, 152.46, 145.95, 140.54, 135.47, 134.13, 131.56, 130.73, 129.98, 126.40, 125.17 (q, *J* = 281.9 Hz), 124.67, 120.56, 118.74, 51.27 (q, *J* = 24.4 Hz), 50.34 (br), 45.76, 34.12, 29.99, 23.59; ^{19}F NMR (376 MHz, 300 K, $CDCl_3$): δ –62.73 (d, *J* = 7.6 Hz); IR ($CHCl_3$ film): $\tilde{\nu}$ 3637, 1665, 1593, 1426, 760 cm^{-1}; HRMS (ESI): *m/z* calculated for $C_{31}H_{35}BrF_3N_2O_2$ $[M+H]^+$: 603.1829, found: 603.1832; $[\alpha]_D^{26}$ –58.2 (*c* 1.0, $CHCl_3$, 96% ee sample). Enantiomeric excess of the product was determined to be 96% ee by chiral stationary phase HPLC analysis (CHIRALCEL OD-H (ø 0.46 cm x 25 cm), hexane/2-propanol = 49/1, flow rate 1.0 mL/min, detection at 254 nm, t_R = 8.6 min (major), 12.1 min (minor)).

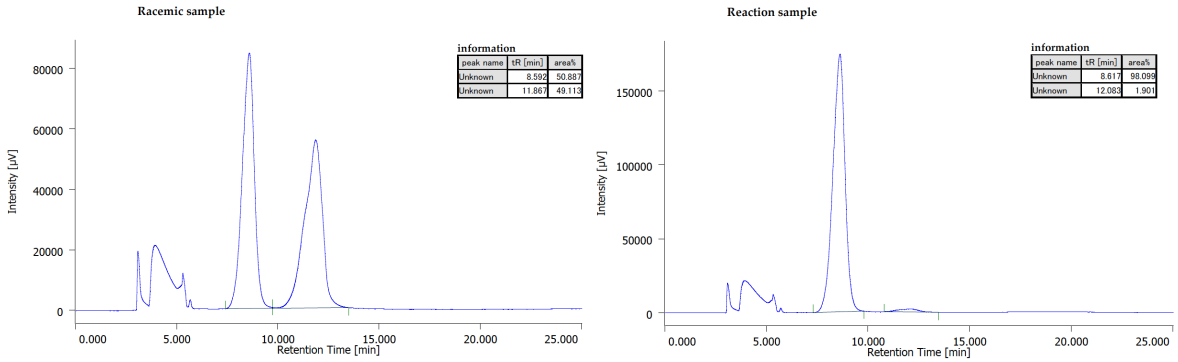

(*S*)-2-((*S*)-(3,5-Di-*tert*-butyl-4-hydroxyphenyl)(2-methoxyphenyl)methyl)-1-(2,3-dihydro-1*H*-pyrrolo[2,3-*b*]pyridin-1-yl)-3,3,3-trifluoropropan-1-one (20q):

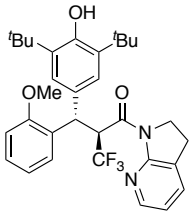

Obtained in 97% yield (107.6 mg); viscous foam; ^{1}H NMR (400 MHz, 300 K, $CDCl_3$): δ 8.29–8.26 (m, 1H), 7.54 (br, 1H), 7.42–7.39 (m, 1H), 7.20–7.10 (m, 4H), 6.97–6.92 (m, 2H), 6.85–6.82 (m, 1H), 5.02 (br, 1H), 4.89 (s, 1H), 3.95–3.86 (m, 4H), 3.59–3.52 (m, 1H), 2.89–2.80 (m, 1H), 2.68–2.58 (m, 1H), 1.17 (s, 18H); ^{13}C NMR (100 MHz, 300 K, $CDCl_3$): δ 166.27 (br), 157.14, 155.33, 152.16, 145.90, 134.93, 133.97, 131.35, 129.71, 127.75, 126.44, 125.52 (q, J = 281.9 Hz), 125.37, 120.45, 118.58, 111.17, 55.39, 49.83 (br), 45.84, 34.09, 30.09, 23.69; ^{19}F NMR (376 MHz, 300 K, $CDCl_3$): δ –63.51 (br); IR ($CHCl_3$ film): $\tilde{\nu}$ 3639, 1663, 1592, 1425, 758 cm^{-1}; HRMS (ESI): *m/z* calculated for $C_{32}H_{38}F_3N_2O_3$ $[M+H]^+$: 555.2829, found: 555.2822; $[\alpha]_D^{26}$ –97.9 (*c* 1.0, $CHCl_3$, 98% ee sample). Enantiomeric excess of the product was determined to be 98% ee by chiral stationary phase HPLC analysis (CHIRALCEL OD-H (ø 0.46 cm x 25 cm), hexane/2-propanol = 49/1, flow rate 1.0 mL/min, detection at 254 nm, t_R = 10.3 min (major), 15.7 min (minor)).

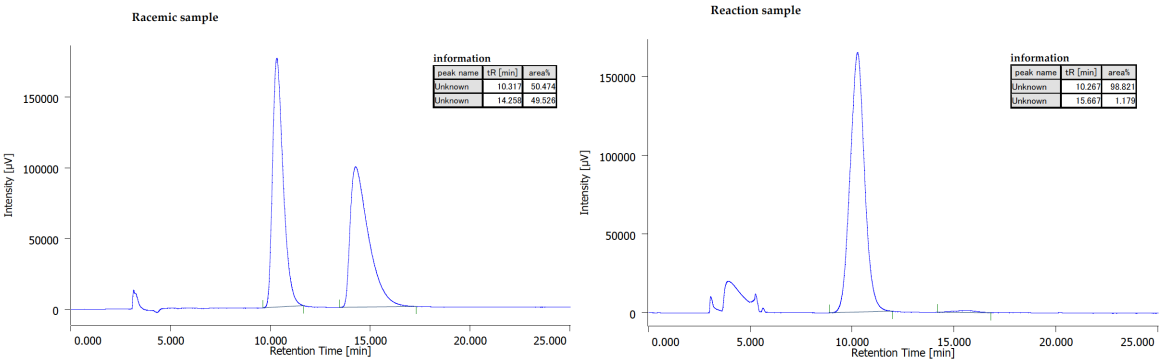

(*S*)-2-((*S*)-(3,5-Di-*tert*-butyl-4-hydroxyphenyl)(3-methoxyphenyl)methyl)-1-(2,3-dihydro-1*H*-pyrrolo[2,3-*b*]pyridin-1-yl)-3,3,3-trifluoropropan-1-one (20r):

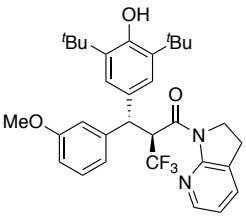

Obtained in 95% yield (115.6 mg); viscous foam; ^{1}H NMR (400 MHz, 300 K, $CDCl_3$): δ 8.28–8.26 (m, 1H), 7.44–7.40 (m, 1H), 7.25 (t, J = 7.9 Hz, 1H), 7.14–7.11 (m, 1H), 7.07 (t, J = 2.1 Hz, 1H), 7.01–6.92 (m, 4H), 6.77–6.74 (m, 1H), 4.94 (s, 1H), 4.59 (d, J = 11.7 Hz, 1H), 4.00–3.84 (m, 1H), 3.82 (s, 3H), 3.56–3.49 (m, 1H), 2.91–2.82 (m, 1H), 2.69–2.60 (m, 1H), 1.17 (s, 18H); ^{13}C NMR (100 MHz, 300 K, $CDCl_3$): δ 165.74 (br), 159.53, 155.19, 152.36, 145.97, 142.96, 135.27, 134.09, 131.18, 129.35, 126.41, 125.28 (q, J = 281.9 Hz), 124.87, 120.69, 118.66, 114.32, 111.93, 55.11, 51.49 (q, J = 24.4 Hz), 51.03 (br), 45.76, 34.12, 30.03, 23.61; ^{19}F NMR (376 MHz, 300 K, $CDCl_3$): δ –62.81 (d, J = 7.7 Hz); IR ($CHCl_3$ film): $\tilde{\nu}$ 3639, 1664, 1594, 1426, 757 cm^{-1}; HRMS (ESI): *m/z* calculated for $C_{32}H_{38}F_3N_2O_3$ $[M+H]^+$: 555.2829, found: 555.2829; $[\alpha]_D^{26}$ –96.3 (*c* 1.0, $CHCl_3$, 96% ee sample). Enantiomeric excess of the product was determined to be 96% ee by chiral stationary phase HPLC analysis (CHIRALCEL OD-H (ø 0.46 cm x 25 cm), hexane/2-propanol = 49/1, flow rate 1.0 mL/min, detection at 254 nm, t_R = 10.6 min (major), 18.6 min (minor)).

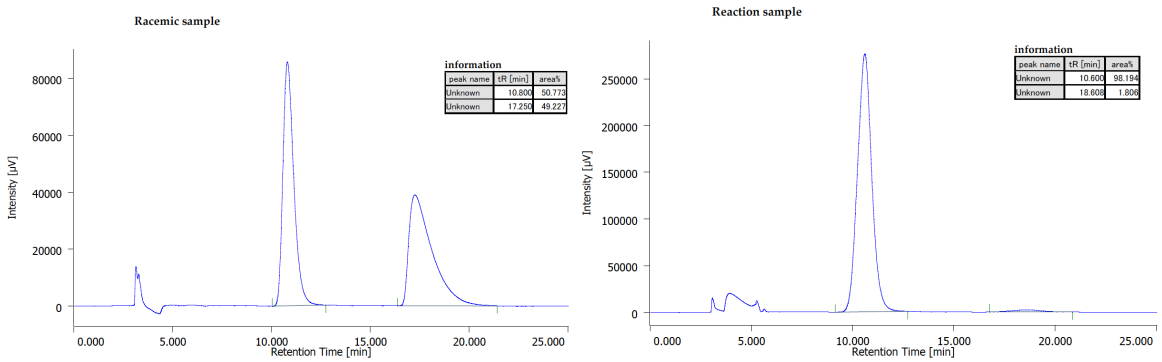

(*S*)-2-((*R*)-(3,5-Di-*tert*-butyl-4-hydroxyphenyl)(4-methoxyphenyl)methyl)-1-(2,3-dihydro-1*H*-pyrrolo[2,3-*b*]pyridin-1-yl)-3,3,3-trifluoropropan-1-one (20s):

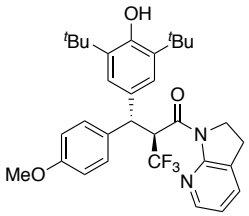

Obtained in 91% yield (101.3 mg); viscous foam; ^{1}H NMR (400 MHz, 300 K, $CDCl_3$): δ 8.29–8.26 (m, 1H), 7.44–7.39 (m, 3H), 6.98–6.85 (m, 6H), 4.92 (s, 1H), 4.59 (d, J = 11.8 Hz, 1H), 3.96–3.88 (m, 1H), 3.78 (s, 3H), 3.57–3.50 (m, 1H), 2.90–2.81 (m, 1H), 2.68–2.58 (m, 1H), 1.17 (s, 18H); ^{13}C NMR (100 MHz, 300 K, $CDCl_3$): δ 165.90 (q, J = 2.8 Hz), 158.31, 155.18, 152.23, 145.95, 135.23, 134.02, 133.56, 131.65, 129.22, 126.37, 125.31 (q, J = 281.8 Hz), 124.73, 118.60, 113.84, 55.16, 51.67 (q, J = 24.1 Hz), 50.23 (br), 45.75, 34.09, 30.01, 23.60; ^{19}F NMR (376 MHz, 300 K, $CDCl_3$): δ –62.66 (d, J = 7.7 Hz); IR ($CHCl_3$ film): $\tilde{\nu}$ 3639, 1663, 1593, 1426 cm^{-1}; HRMS (ESI): *m/z* calculated for $C_{32}H_{38}F_3N_2O_3$ $[M+H]^+$: 555.2829, found: 555.2825; $[\alpha]_D^{26}$ –91.1 (*c* 1.0, $CHCl_3$, 96% ee sample). Enantiomeric excess of the product was determined to be 96% ee by chiral stationary phase HPLC analysis (CHIRALCEL OD-H (ø 0.46 cm x 25 cm), hexane/2-propanol = 49/1, flow rate 1.0 mL/min, detection at 254 nm, t_R = 10.7 min (major), 19.5 min (minor)).

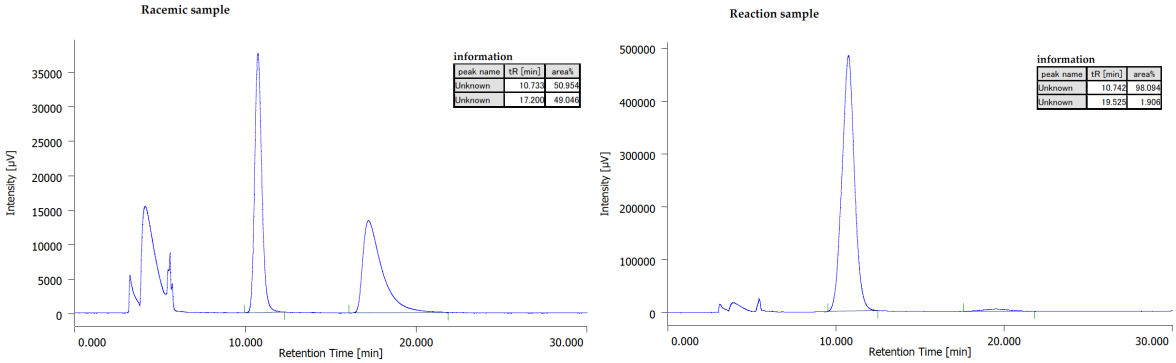

(*S*)-2-((*S*)-(3,5-Di-*tert*-butyl-4-hydroxyphenyl)(*o*-tolyl)methyl)-1-(2,3-dihydro-1*H*-pyrrolo[2,3-*b*]pyridin-1-yl)-3,3,3-trifluoropropan-1-one (20t):

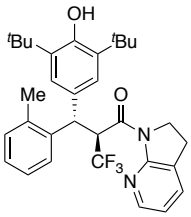

Obtained in 96% yield (103.3 mg); white solid; m.p. : 203–205 °C; ^{1}H NMR (400 MHz, 300 K, $CDCl_3$): δ 8.30–8.27 (m, 1H), 7.75 (d, *J* = 7.8 Hz, 1H), 7.41–7.37 (m, 1H), 7.29–7.25 (m, 1H), 7.12–7.01 (m, 3H), 6.99 (s, 2H), 6.94 (dd, *J* = 7.4, 5.1 Hz, 1H), 4.91 (s, 1H), 4.89 (d, *J* = 11.7 Hz, 1H), 3.94–3.85 (m, 1H), 3.52–3.45 (m, 1H), 2.87–2.79 (m, 1H), 2.62–2.53 (m, 1H), 2.41 (s, 3H), 1.16 (s, 18H); ^{13}C NMR (100 MHz, 300 K, $CDCl_3$): δ 166.04 (br), 155.19, 152.26, 145.92, 139.15, 135.90, 135.07, 134.03, 130.72, 130.06, 127.35, 126.39, 126.36, 125.71, 125.53, 125.38 (q, *J* = 282.0 Hz), 118.58, 51.12 (q, *J* = 23.6), 45.76 (br), 34.07, 30.01, 23.59, 20.12; ^{19}F NMR (376 MHz, 300 K, $CDCl_3$): δ –62.72 (d, *J* = 7.5 Hz); IR ($CHCl_3$ film): $\tilde{\nu}$ 3639, 1664, 1592, 1426, 759 cm^{-1}; HRMS (ESI): *m/z* calculated for $C_{32}H_{38}F_3N_2O_2$ $[M+H]^+$: 539.2880, found: 539.2873; $[\alpha]_D^{26}$ –45.2 (*c* 1.0, $CHCl_3$, 94% ee sample). Enantiomeric excess of the product was determined to be 94% ee by chiral stationary phase HPLC analysis (CHIRALCEL OD-H (ø 0.46 cm x 25 cm), hexane/2-propanol = 49/1, flow rate 0.5 mL/min, detection at 254 nm, t_R = 14.6 min (major), 16.8 min (minor)).

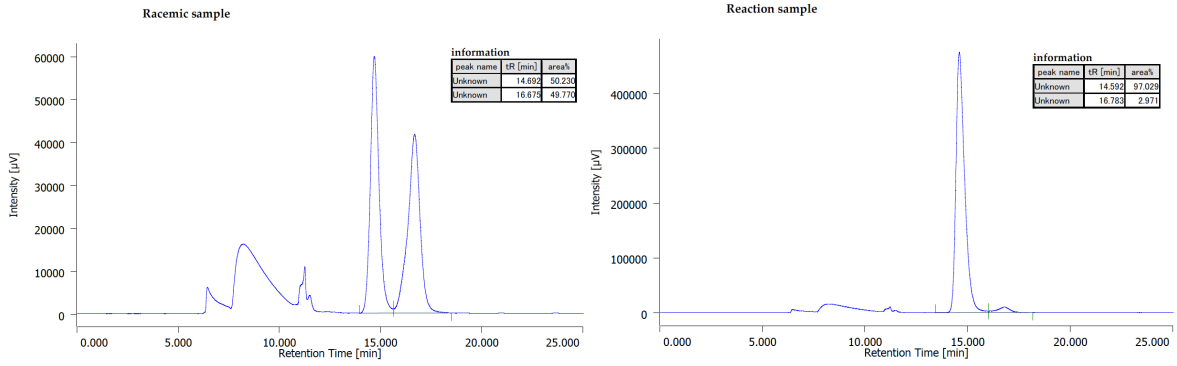

(*S*)-2-((*S*)-(3,5-Di-*tert*-butyl-4-hydroxyphenyl)(furan-2-yl)methyl)-1-(2,3-dihydro-1*H*-pyrrolo[2,3-*b*]pyridin-1-yl)-3,3,3-trifluoropropan-1-one (20u):

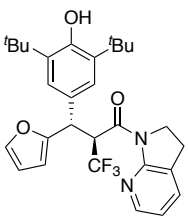

Obtained in 80% yield (83.0 mg); light brown solid; m.p. : 198–200 °C; ^{1}H NMR (400 MHz, 300 K, $CDCl_3$): δ 8.25–8.22 (m, 1H), 7.42–7.41 (m, 1H), 7.39–7.35 (m, 1H), 7.10 (s, 2H), 6.91 (dd, *J* = 7.4, 5.1 Hz, 1H), 6.81–6.72 (m, 1H), 6.31–6.27 (m, 2H), 4.97 (s, 1H), 4.67 (d, *J* = 11.7 Hz, 1H), 3.90–3.82 (m, 1H), 3.54–3.47 (m, 1H), 2.85–2.76 (m, 1H), 2.60–2.50 (m, 1H), 1.20 (s, 18H); ^{13}C NMR (100 MHz, 300 K, $CDCl_3$): δ 165.33 (q, *J* = 3.2 Hz), 154.92, 153.34, 152.65, 146.02, 141.98, 135.27, 133.84, 128.66, 126.08, 125.28, 124.94 (q, *J* = 281.5 Hz), 118.59, 110.25, 107.00, 51.40 (q, *J* = 24.8 Hz), 45.88, 44.07 (br), 34.07, 30.00, 23.65; ^{19}F NMR (376 MHz, 300 K, $CDCl_3$): δ –64.64 (d, *J* = 7.8 Hz); IR ($CHCl_3$ film): $\tilde{\nu}$ 3639, 1663, 1593, 1427, 759 cm^{-1}; HRMS (ESI): *m/z* calculated for $C_{29}H_{34}F_3N_2O_3$ $[M+H]^+$: 515.2516, found: 515.2521; $[\alpha]_D^{26}$ –59.8 (*c* 1.0, $CHCl_3$, 96% ee sample). Enantiomeric excess of the product was determined to be 96% ee by chiral stationary phase HPLC analysis (CHIRALCEL OD-H (ø 0.46 cm x 25 cm), hexane/2-propanol = 49/1, flow rate 1.0 mL/min, detection at 254 nm, t_R = 7.7 min (major), 10.2 min (minor)).

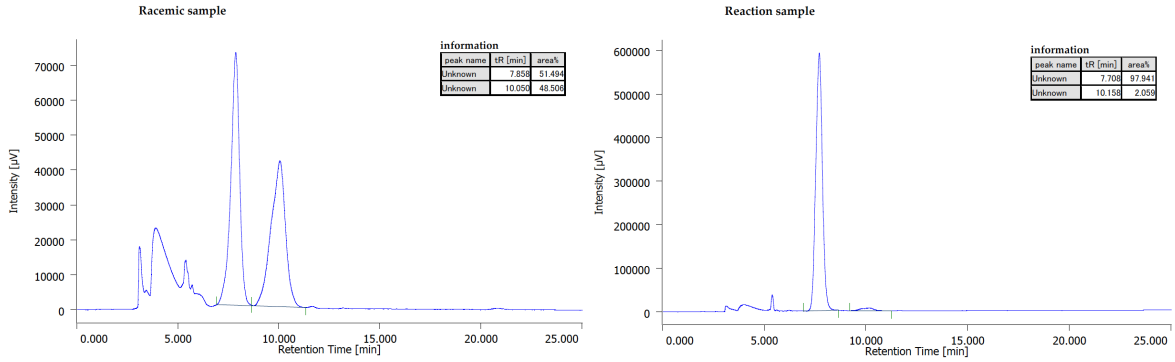

(2*S*,3*R*)-3-(3,5-Di-*tert*-butyl-4-hydroxyphenyl)-1-(2,3-dihydro-1*H*-pyrrolo[2,3-*b*]pyridin-1-yl)-2-methyl-3-phenylpropan-1-one (21):

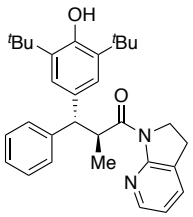

Obtained in 72% yield (67.9 mg); white solid; m.p. : 163–165 °C; ^{1}H NMR (400 MHz, 300 K, $CDCl_3$): δ 8.21 (dd, *J* = 5.2, 1.6 Hz, 1H), 7.42–7.28 (m, 5H), 7.19–7.14 (m, 1H), 6.97 (s, 2H), 6.85 (dd, *J* = 7.3, 5.1 Hz, 1H), 5.64–5.56 (m, 1H), 4.86 (s, 1H), 4.12 (d, *J* = 11.5 Hz, 1H), 3.89–3.81 (m, 1H), 3.71–3.64 (m, 1H), 2.85–2.76 (m, 1H), 2.68–2.58 (m, 1H), 1.19 (s, 18H), 1.15 (d, *J* = 6.6 Hz, 3H); ^{13}C NMR (100 MHz, 300 K, $CDCl_3$): δ 176.21, 156.08, 151.73, 146.04, 143.70, 134.89, 134.15, 133.36, 128.54, 128.40, 126.27, 126.00, 124.43, 117.75, 56.60, 45.84, 41.91, 34.07, 30.09, 23.95, 16.51; IR ($CHCl_3$ film): $\tilde{\nu}$ 3640, 1650, 1589, 1421, 751 cm^{-1}; HRMS (ESI): *m/z* calculated for $C_{31}H_{39}N_2O_2$ $[M+H]^+$: 471.3006, found: 471.3003; $[\alpha]_D^{26}$ –53.7 (*c* 1.0, $CHCl_3$, 87% ee sample). Enantiomeric excess of the product was determined to be 87% ee by chiral stationary phase HPLC analysis (CHIRALPAK IE (ø 0.46 cm x 25 cm), hexane/2-propanol = 20/1, flow rate 1.0 mL/min, detection at 254 nm, t_R = 10.7 min (major), 11.8 min (minor)).

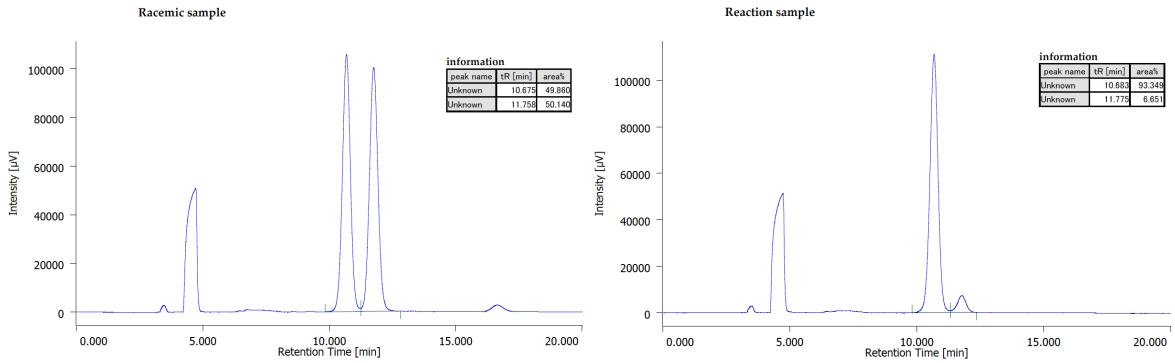

(2*S*,3*R*)-2-Azido-3-(3,5-di-*tert*-butyl-4-hydroxyphenyl)-1-(2,3-dihydro-1*H*-pyrrolo[2,3-*b*]pyridin-1-yl)-3-phenylpropan-1-one (22):

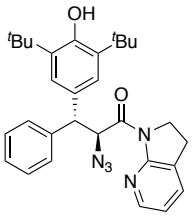

Obtained in 83% yield (82.8 mg); white solid; m.p. : 165–167 °C; ^{1}H NMR (400 MHz, 300 K, $CDCl_3$): δ 8.19–8.17 (m, 1H), 7.53–7.50 (m, 2H), 7.37 (dd, J = 8.4, 7.0 Hz, 3H), 7.27–7.23 (m, 1H), 6.97 (s, 2H), 6.90–6.84 (m, 2H), 4.93 (s, 1H), 4.53 (d, J = 11.2 Hz, 1H), 3.96–3.88 (m, 1H), 3.70–3.62 (m, 1H), 2.89–2.81 (m, 1H), 2.69–2.59 (m, 1H), 1.19 (s, 18H); ^{13}C NMR (100 MHz, 300 K, $CDCl_3$): δ 169.55, 155.08, 152.44, 145.95, 140.94, 135.27, 133.82, 130.15, 128.65, 128.43, 126.85, 126.07, 125.05, 118.56, 61.69, 54.02, 45.71, 34.08, 30.03, 23.86; IR ($CHCl_3$ film): $\tilde{\nu}$ 3637, 2102, 1656, 1591, 1426 cm^{-1}; HRMS (ESI): *m/z* calculated for $C_{30}H_{36}N_5O_2$ $[M+H]^+$: 498.2864, found: 498.2862; $[\alpha]_D^{26}$ 119.3 (*c* 1.0, $CHCl_3$, 90% ee sample). Enantiomeric excess of the product was determined to be 90% ee by chiral stationary phase HPLC analysis (CHIRALPAK IA (ø 0.46 cm x 25 cm), hexane/2-propanol = 9/1, flow rate 1.0 mL/min, detection at 254 nm, t_R = 7.3 min (major), 10.5 min (minor)).

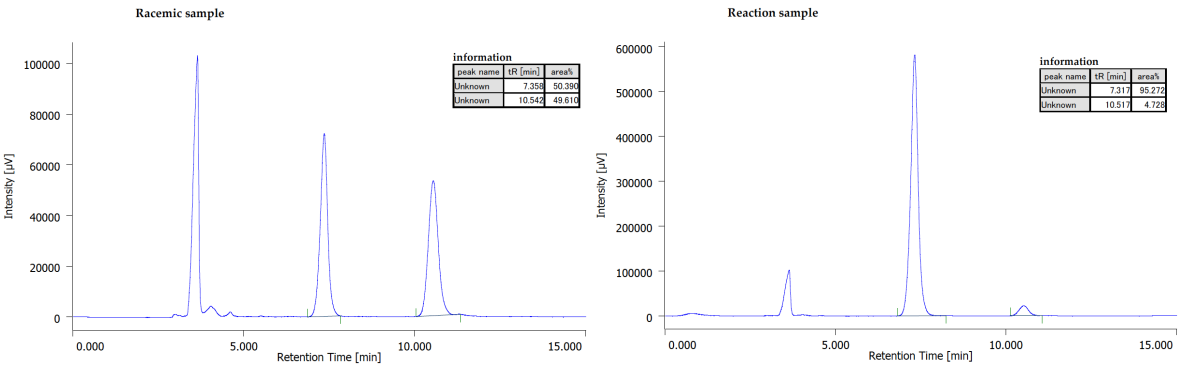

(2*S*,3*R*)-2-(Benzyloxy)-3-(3,5-di-*tert*-butyl-4-hydroxyphenyl)-1-(2,3-dihydro-1*H*-pyrrolo[2,3-*b*]pyridin-1-yl)-3-phenylpropan-1-one (23):

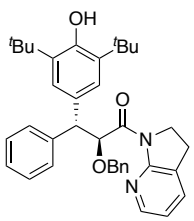

Obtained in 81% yield (91.0 mg); white solid; m.p. : 173–175 °C; ^{1}H NMR (400 MHz, 300 K, $CDCl_3$): δ 8.13–8.11 (m, 1H), 7.48–7.42 (m, 2H), 7.32–7.29 (m, 3H), 7.21–7.07 (m, 6H), 6.96–6.93 (m, 3H), 6.84 (dd, *J* = 7.3, 5.1 Hz, 1H), 4.88 (s, 1H), 4.63 (d, *J* = 12.0 Hz, 1H), 4.53 (d, *J* = 12.0 Hz, 1H), 4.43 (d, *J* = 9.5 Hz, 1H), 3.86–3.77 (m, 1H), 3.56–3.49 (m, 1H), 2.79–2.71 (m, 1H), 2.57–2.47 (m, 1H), 1.18 (s, 18H); ^{13}C NMR (100 MHz, 300 K, $CDCl_3$): δ 172.41, 155.57, 152.11, 145.64, 141.99, 138.31, 134.83, 133.50, 130.53, 128.82, 128.14, 128.07, 127.74, 127.17, 126.08, 126.03, 125.54, 118.00, 79.53, 72.14, 55.81, 45.72, 34.03, 30.03, 23.94; IR ($CHCl_3$ film): $\tilde{\nu}$ 3638, 1660, 1590, 1424, 1236 cm^{-1}; HRMS (ESI): *m/z* calculated for $C_{37}H_{43}N_2O_3$ $[M+H]^+$: 563.3268, found: 563.3268; $[\alpha]_D^{26}$ 46.7 (*c* 1.0, $CHCl_3$, 90% ee sample). Enantiomeric excess of the product was determined to be 90% ee by chiral stationary phase HPLC analysis (CHIRALPAK IA (ø 0.46 cm x 25 cm), hexane/2-propanol = 9/1, flow rate 1.0 mL/min, detection at 254 nm, t_R = 8.4 min (major), 12.2 min (minor)).

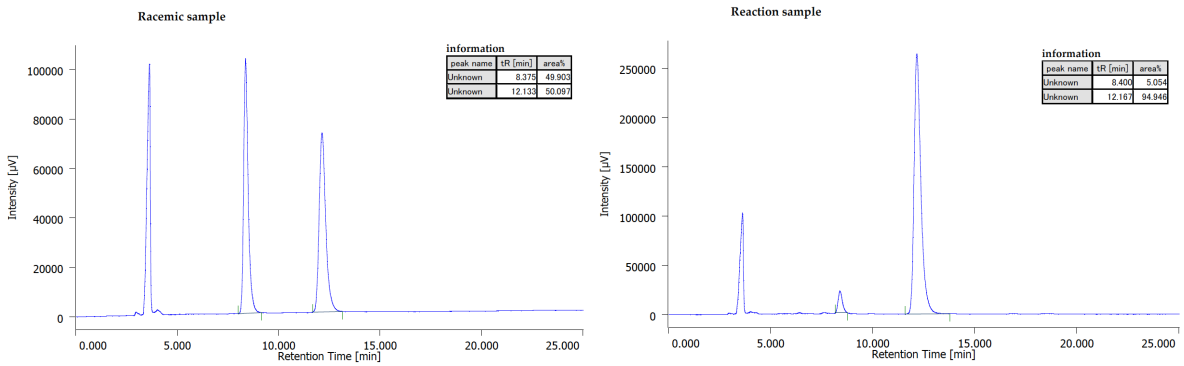

(*S*)-1-(2,3-Dihydro-1*H*-pyrrolo[2,3-*b*]pyridin-1-yl)-3,3,3-trifluoro-2-((*R*)-(4-hydroxyphenyl)(phenyl)methyl)propan-1-one (24):

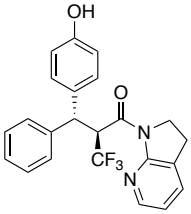

A 50 mL flask equipped with a magnetic stirring bar and a 3-way glass stopcock was charged with **20a** (157.4 mg, 0.3 mmol) and $AlCl_3$ (240.0 mg, 1.8 mmol). To the above mixture was added anhydrous benzene (12 mL) under argon. The resulting mixture was vigorously stirred at 60 °C for 4 h. The reaction mixture was quenched with water and the biphasic mixture was extracted with EtOAc. The combined organic layers were dried over anhydrous Na_2SO_4. After evaporation of the solvent under reduced pressure, the residue was purified by automated flash column chromatography (Biotage Isolera One) with pre-packed silica gel column to afford compound **24**, 87.0 mg (70%). White solid; m.p. : 223–225 °C; ^{1}H NMR (400 MHz, 300 K, $CDCl_3$): δ 8.31–8.28 (m, 1H), 7.47–7.44 (m, 3H), 7.33–7.28 (m, 2H), 7.22–7.18 (m, 1H), 7.11–6.96 (m, 4H), 6.48–6.44 (m, 2H), 5.61 (s, 1H), 4.68 (d, *J* = 11.8 Hz, 1H), 4.01–3.93 (m, 1H), 3.67–3.59 (m, 1H), 2.93–2.84 (m, 1H), 2.79–2.70 (m, 1H); ^{13}C NMR (100 MHz, 300 K, $CDCl_3$): δ 165.99 (q, *J* = 2.9 Hz), 155.01, 154.51, 145.94, 141.23, 134.18, 133.24, 129.11, 128.54, 128.13, 126.83, 126.62, 125.15 (q, *J* = 282.3 Hz), 119.03, 115.09, 50.98 (q, *J* = 24.5 Hz), 50.08 (br), 45.89, 23.69; ^{19}F NMR (376 MHz, 300 K, $CDCl_3$): δ –62.82 (d, *J* = 7.7 Hz); IR ($CHCl_3$ film): $\tilde{\nu}$ 3382, 1638, 1593, 1427, 1216, 759 cm^{-1}; HRMS (ESI): *m/z* calculated for $C_{23}H_{20}F_3N_2O_2$ $[M+H]^+$: 413.1471, found: 413.1471; $[\alpha]_D^{26}$ –141.1 (*c* 1.0, $CHCl_3$, 97% ee sample). Enantiomeric excess of the product was determined to be 97% ee by chiral stationary phase HPLC analysis (CHIRALPAK IC (ø 0.46 cm x 25 cm), hexane/2-propanol = 9/1, flow rate 1.0 mL/min, detection at 254 nm, t_R = 10.8 min (major), 17.9 min (minor)).

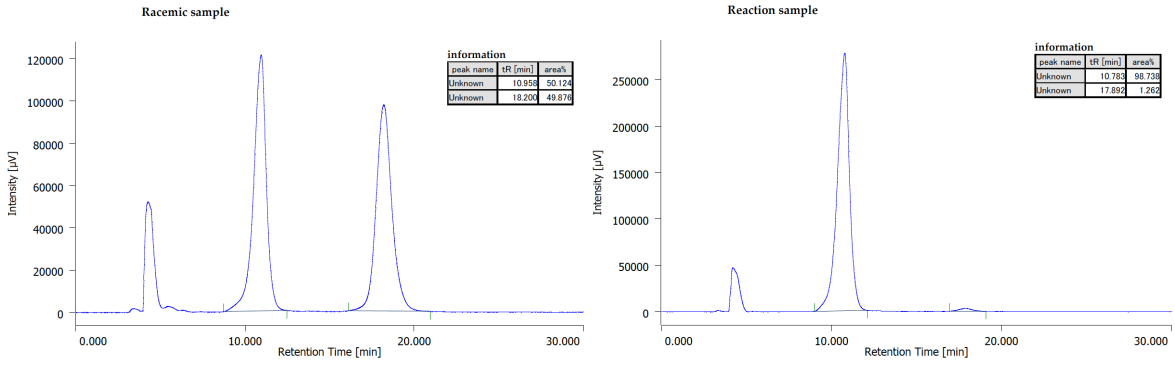

Methyl (*S*)-3,3,3-trifluoro-2-((*R*)-(4-hydroxyphenyl)(phenyl)methyl)propanoate (27):

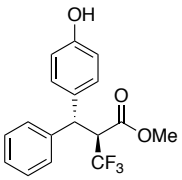

A 20 mL test tube equipped with a magnetic stirring bar and a 3-way glass stopcock was charged with **24** (41.2 mg, 0.1 mmol). The test tube was placed in a cooling bath at –20 °C and anhydrous THF (1.0 mL) was added under argon. A solution of $LiAlH_4$ (1.0 M in Et_2O, 0.4 mL, 0.4 mmol) was added dropwise. The resulting mixture was vigorously stirred at –20 °C for 8 h. The reaction mixture was diluted with 5 mL EtOAc and quenched with citric acid (1.0 M in THF, 1 mL). The biphasic mixture was extracted with EtOAc. The combined organic layers were dried over anhydrous Na_2SO_4. After evaporation of the solvent under reduced pressure, the crude aldehyde was directly used in the following step. ^{1}H NMR analysis of the crude aldehyde indicated that no epimerization occoured during the reduction step. The crude aldehyde was dissolved in water (1.0 mL) and *tert*-butanol (1.0 mL). NaH_2PO_4 (36.0 mg, 0.3 mmol), 2-methylbut-2-ene (0.2 mL, 1.9 mmol) and $NaClO_2$ (31.7 mg, 0.35 mmol) were subsequently added to the solution at 0 °C. The reaction was placed at room temperature and stirred for 1 h. The reaction was quenched by adding Na_2SO_3 and 1N HCl aq., and the biphasic mixture was extracted with EtOAc. The combined organic layers were dried over anhydrous Na_2SO_4 and concentrated to give the crude acid. To the crude acid was added dropwise fresh prepared CH_2N_2 in Et_2O solution. After stiring 5 min at room temperature, the mixture was concentrated and purified by PTLC (20% EtOAc/hexane) to afford compound **27**, 29.6 mg (91%) over 3 steps. Colorless oil; ^{1}H NMR (400 MHz, 300 K, $CDCl_3$): δ 7.33–7.26 (m, 4H), 7.22–7.14 (m, 3H), 6.71–6.67 (m, 2H), 5.06 (s, 1H), 4.51 (d, J = 11.9 Hz, 1H), 4.14–4.05 (m, 1H), 3.52 (s, 3H); ^{13}C NMR (100 MHz, 300 K, $CDCl_3$): δ 167.31 (q, J = 3.3 Hz), 154.72, 140.23, 132.49, 128.91, 128.73, 127.72, 127.21, 124.12 (q, J = 281.9 Hz), 115.63, 55.43 (q, J = 25.9 Hz), 52.70, 48.98 (q, J = 1.8 Hz); ^{19}F NMR (376 MHz, 300 K, $CDCl_3$): δ –64.07 (d, J = 7.2 Hz); IR ($CHCl_3$ film): $\tilde{\nu}$ 3446, 1748, 1514, 1438, 804, 698 cm^{-1}; HRMS (ESI): *m/z* calculated for $C_{17}H_{15}F_3O_3Na$ [M+Na]$^+$: 347.0866, found: 347.0861; $[\alpha]_D^{26}$ –18.7 (*c* 1.0, $CHCl_3$, 97% ee sample). Enantiomeric excess of the product was determined to be 97% ee by chiral stationary phase HPLC analysis (CHIRALPAK IA (ø 0.46 cm x 25 cm), hexane/2-propanol = 20/1, flow rate 1.0 mL/min, detection at 254 nm, t_R = 17.8 min (minor), 19.9 min (major)).

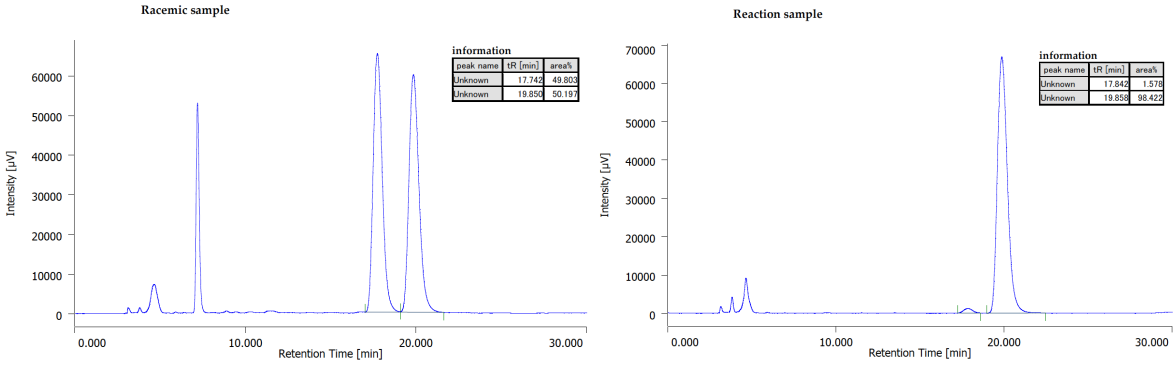

Methyl (2*S*,3*R*)-2-azido-3-(3,5-di-*tert*-butyl-4-hydroxyphenyl)-3-phenylpropanoate (28):

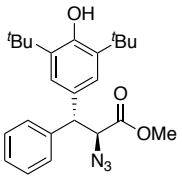

A 20 mL screw-capped test tube equipped with a magnetic stirring bar was charged with compound **22** (99.5 mg, 0.2 mmol) and 2 M HCl in MeOH (4 mL). Then the test tube was sealed and heated at 100 °C. After stirring 24 h, the reaction mixture was concentrated and purified by by silica gel chromatography using a gradient of 5 to 40% EtOAc/hexane to afford compound **28**, 73.9 mg (90%). White solid; m.p. : 75–77 °C; ^{1}H NMR (400 MHz, 300 K, $CDCl_3$): δ 7.38–7.30 (m, 4H), 7.27–7.22 (m, 1H), 7.04 (s, 2H), 5.11 (s, 1H), 4.40 (s, 2H), 3.55 (s, 3H), 1.39 (s, 18H); ^{13}C NMR (100 MHz, 300 K, $CDCl_3$): δ 170.19, 152.91, 139.89, 135.94, 130.04, 128.68, 128.36, 127.18, 124.81, 65.90, 52.85, 52.30, 34.38, 30.29; IR ($CHCl_3$ film): $\tilde{\nu}$ 3637, 2106, 1744, 1236, 807, 700 cm^{-1}; HRMS (ESI): *m/z* calculated for $C_{24}H_{31}N_3O_3Na$ $[M+Na]^+$: 432.2258, found: 432.2252; $[\alpha]_D^{26}$ 76.7 (*c* 1.0, $CHCl_3$, 90% ee sample). Enantiomeric excess of the product was determined to be 90% ee by chiral stationary phase HPLC analysis (two CHIRALPAK IA-3 (ø 0.46 cm x 25 cm) in tandem, hexane/2-propanol = 49/1, flow rate 0.5 mL/min, detection at 254 nm, t_R = 17.9 min (minor), 20.2 min (major)).

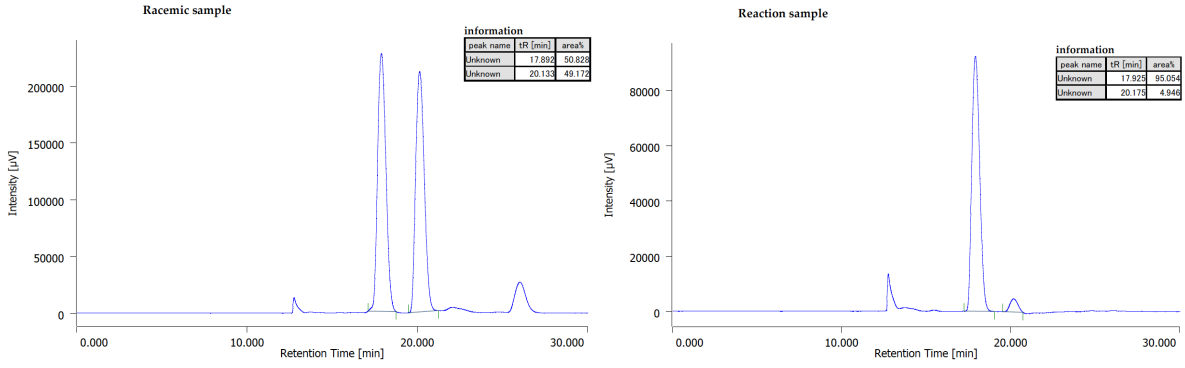

3.6 Synthetic procedures for photocatalytic acylation of α-oxy C(sp^3)–H bond

A oven-dried 20 mL test tube equipped with a magnetic stirring bar and 3-way glass stopcock was charged with $NiCl_2$·dtbbpy (15.9 mg, 0.04 mmol, 10 mol% catalyst loading), $Ir[dF(CF_3)ppy]_2(dtbbpy)PF_6$ (9.0 mg, 0.008 mmol, 2 mol%), K_3PO_4 (127.4 mg, 0.60 mmol, 1.5 equiv.) and acyl chloride (0.4 mmol, 1.0 equiv)(if solid, otherwise liquid acyl chlorides were added after addition of solvent via syringe). The vial was sealed and underwent argon/vacuum cycle three times. Under argon, corresponding anhydrous solvent was added via a syringe. The reaction mixture was stirred 5 cm away from a 21 W blue LED light with a cooling fan for maintaining room temperature. Reaction progress was monitored by TLC. After stirred for an indicated time, the reaction mixture

was filtered through a plug of silica gel and washed with EtOAc (50 mL). The filtrate was concentrated, and the resulting residue was purified by automated flash column chromatography (Biotage Isolera One) with pre-packed silica gel column.

Phenyl(tetrahydrofuran-2-yl)methanone (30a):

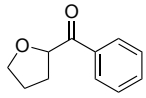

Obtained in 75% yield (52.9 mg, using 10 mol% $NiCl_2$·dtbbpy, 2 mL THF, 24 h); colorless oil; ^{1}H NMR (400 MHz, 300 K, $CDCl_3$): δ 8.01–7.98 (m, 2H), 7.59–7.55 (m, 1H), 7.49–7.44 (m, 2H), 5.26 (dd, J = 8.4, 5.8 Hz, 1H), 4.07–3.95 (m, 2H), 2.33–2.25 (m, 1H), 2.19–2.10 (m, 1H), 2.01–1.94 (m, 2H); ^{13}C NMR (100 MHz, 300 K, $CDCl_3$): δ 198.84, 135.20, 133.37, 128.83, 128.70, 80.11, 69.49, 29.37, 25.73. Characterization data are consistent with data reported in the literature.[2]

(4-Methoxyphenyl)(tetrahydrofuran-2-yl)methanone (30b):

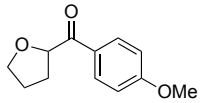

Obtained in 81% yield (66.9 mg, using 10 mol% $NiCl_2$·dtbbpy, 2 mL THF, 24 h); colorless oil; ^{1}H NMR (400 MHz, 300 K, $CDCl_3$): δ 7.99 (d, J = 8.9 Hz, 2H), 6.94 (d, J = 8.9 Hz, 2H), 5.21 (dd, J = 8.3, 5.8 Hz, 1H), 4.06–3.93 (m, 2H), 3.87 (s, 3H), 2.26 (dq, J = 12.5, 7.7 Hz, 1H), 2.18–2.10 (m, 1H), 2.00–1.93 (m, 2H); ^{13}C NMR (100 MHz, 300 K, $CDCl_3$): δ 197.32, 163.69, 131.13, 128.19, 113.87, 79.91, 69.42, 55.57, 29.42, 25.75; IR ($CHCl_3$ film): $\tilde{\nu}$ 3018, 1684, 1600, 1509, 1461, 1262, 1217, 776, 741 cm^{-1}; HRMS (ESI): *m/z* calculated for $C_{12}H_{15}O_3$ $[M+H]^+$: 207.1016, found: 207.1015.

Benzo[*d*][1,3]dioxol-5-yl(tetrahydrofuran-2-yl)methanone (30c):

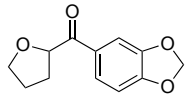

Obtained in 52% yield (45.8 mg, using 10 mol% $NiCl_2$·dtbbpy, 2 mL THF, 24 h); colorless oil; ^{1}H NMR (400 MHz, 300 K, $CDCl_3$): δ 7.62 (dd, J = 8.2, 1.7 Hz, 1H), 7.48 (d, J = 1.7 Hz, 1H), 6.86 (d, J = 8.2 Hz, 1H), 6.04 (s, 2H), 5.16 (dd, J = 8.3, 5.8 Hz, 1H), 4.05–3.92 (m, 2H), 2.30–2.09 (m, 2H), 2.00–1.93 (m, 2H); ^{13}C NMR (100 MHz, 300 K, $CDCl_3$): δ 196.72, 151.88, 148.12, 129.81, 125.08, 108.54, 107.96, 101.84, 79.83, 69.35, 29.32, 25.63; IR ($CHCl_3$ film): $\tilde{\nu}$ 2979, 1722, 1683, 1604, 1488, 1443, 1253, 1038, 931, 881 cm^{-1}; HRMS (ESI): *m/z* calculated for $C_{12}H_{12}O_4Na$ $[M+Na]^+$: 243.0628, found: 243.0628.

Methyl 4-(tetrahydrofuran-2-carbonyl)benzoate (30d):

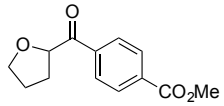

Obtained in 48% yield (45.3 mg, using 10 mol% $NiCl_2$·dtbbpy, 2 mL THF, 24 h); colorless oil; ^{1}H NMR (400 MHz, 300 K, $CDCl_3$): δ 8.14–8.11 (m, 2H), 8.07–8.04 (m, 2H), 5.23 (dd, J = 8.4, 5.7 Hz, 1H), 4.03–3.95 (m,54H), 2.33–2.13 (m, 2H), 2.04–1.93 (m, 2H); ^{13}C NMR (100 MHz, 300 K, $CDCl_3$): δ 198.36, 166.18, 138.44, 133.95, 129.74, 128.71, 80.28, 69.41, 52.46, 28.90, 25.61; IR ($CHCl_3$ film): $\tilde{\nu}$ 3019, 1722, 1698, 1437, 1407, 1282, 1215, 771, 669 cm^{-1}; HRMS (ESI): *m/z* calculated for $C_{13}H_{14}O_4Na$ $[M+Na]^+$: 257.0784, found: 257.0782.

(3-Fluorophenyl)(tetrahydrofuran-2-yl)methanone (30e):

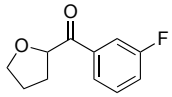

Obtained in 51% yield (39.5 mg, using 10 mol% $NiCl_2$·dtbbpy, 2 mL THF, 24 h); colorless oil; ^{1}H NMR (400 MHz, 300 K, $CDCl_3$): δ 7.79 (dt, *J* = 7.8, 1.3 Hz, 1H), 7.72–7.68 (m, 1H), 7.45 (td, *J* = 8.0, 5.5 Hz, 1H), 7.30–7.25 (m, 1H), 5.18 (dd, *J* = 8.4, 5.8 Hz, 1H), 4.05–3.94 (m, 2H), 2.32–2.12 (m, 2H), 2.03–1.93 (m, 2H); ^{13}C NMR (100 MHz, 300 K, $CDCl_3$): δ 197.65 (d, *J* = 2.0 Hz), 162.87 (d, *J* = 247.9 Hz), 137.28 (d, *J* = 6.3 Hz), 130.36 (d, *J* = 7.6 Hz), 124.67 (d, *J* = 3.1 Hz), 120.40 (d, *J* = 21.6 Hz), 115.69 (d, *J* = 22.5 Hz), 80.30, 69.53, 29.11, 25.71; ^{19}F NMR (376 MHz, 300 K, $CDCl_3$): δ –111.71; IR ($CHCl_3$ film): $\tilde{\nu}$ 3010, 1698, 1588, 1484, 1444, 1255, 798, 723 cm^{-1}; HRMS (ESI): *m/z* calculated for $C_{11}H_{12}O_2F$ $[M+H]^+$: 195.0816, found: 195.0816.

(3-Chlorophenyl)(tetrahydrofuran-2-yl)methanone (30f):

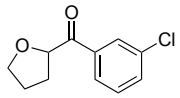

Obtained in 49% yield (41.6 mg, using 10 mol% $NiCl_2$·dtbbpy, 2 mL THF, 24 h); colorless oil; ^{1}H NMR (400 MHz, 300 K, $CDCl_3$): δ 7.98 (t, *J* = 1.9 Hz, 1H), 7.89–7.87 (m, 1H), 7.56–7.53 (m, 1H), 7.41 (t, *J* = 7.9 Hz, 1H), 5.18 (dd, *J* = 8.3, 5.8 Hz, 1H), 4.04–3.94 (m, 2H), 2.32–2.12 (m, 2H), 2.03–1.92 (m, 2H); ^{13}C NMR (100 MHz, 300 K, $CDCl_3$): δ 197.54, 136.66, 134.91, 133.19, 129.90, 128.89, 126.90, 80.13, 69.41, 28.95, 25.59; IR ($CHCl_3$ film): $\tilde{\nu}$ 3015, 1697, 1571, 1424, 1279, 1223, 1181, 667 cm^{-1}; HRMS (ESI): *m/z* calculated for $C_{11}H_{11}O_2ClNa$ $[M+Na]^+$: 233.0340, found: 233.0340.

(4-Fluorophenyl)(tetrahydrofuran-2-yl)methanone (30g):

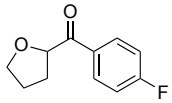

Obtained in 52% yield (40.4 mg, using 10 mol% $NiCl_2$·dtbbpy, 2 mL THF, 24 h); colorless oil; ^{1}H NMR (400 MHz, 300 K, $CDCl_3$): δ 8.08–8.02 (m, 2H), 7.17–7.11 (m, 2H), 5.19 (dd, *J* = 8.2, 5.8 Hz, 1H), 4.04–3.94 (m, 2H), 2.31–2.13 (m, 2H), 2.01–1.94 (m, 2H); ^{13}C NMR (100 MHz, 300 K, $CDCl_3$): δ 197.13, 165.78 (d, *J* = 253.5 Hz), 131.53 (d, *J* = 3.2 Hz), 131.52 (d, *J* = 9.2 Hz), 115.71 (d, *J* = 21.8 Hz), 80.05, 69.37, 28.94, 25.61; ^{19}F NMR (376 MHz, 300 K, $CDCl_3$): δ –104.70; IR ($CHCl_3$ film): $\tilde{\nu}$ 3018, 1693, 1599, 1507, 1232, 1216, 755, 668 cm^{-1}; HRMS (ESI): *m/z* calculated for $C_{11}H_{11}O_2FNa$ $[M+Na]^+$: 217.0635, found: 217.0634.

(4-Chlorophenyl)(tetrahydrofuran-2-yl)methanone (30h):

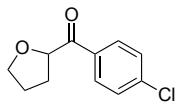

Obtained in 61% yield (51.4 mg, using 10 mol% $NiCl_2$·dtbbpy, 2 mL THF, 24 h); colorless oil; ^{1}H NMR (400 MHz, 300 K, $CDCl_3$): δ 7.97–7.93 (m, 2H), 7.46–7.42 (m, 2H), 5.18 (dd, *J* = 8.3, 5.8 Hz, 1H), 4.03–3.93 (m, 2H), 2.31–2.12 (m, 2H), 2.01–1.93 (m, 2H); ^{13}C NMR (100 MHz, 300 K, $CDCl_3$): δ 197.57, 139.70, 133.42, 130.26, 128.89, 80.09, 69.38, 28.91, 25.61; IR ($CHCl_3$ film): $\tilde{\nu}$ 3018, 1730, 1694, 1589, 1487, 1402, 1218, 763 cm^{-1}; HRMS (ESI): *m/z* calculated for $C_{11}H_{11}O_2ClNa$ $[M+Na]^+$: 233.0340, found: 233.0343.

(3,5-Dimethylphenyl)(tetrahydrofuran-2-yl)methanone (30i):

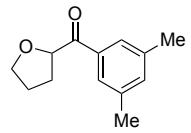

Obtained in 73% yield (59.8 mg, using 10 mol% $NiCl_2$·dtbbpy, 2 mL THF, 24 h); colorless oil; ^{1}H NMR (400 MHz, 300 K, $CDCl_3$): δ 7.58 (s, 2H), 7.20 (s, 1H), 5.25 (dd, J = 8.4, 5.8 Hz, 1H), 4.07–3.94 (m, 2H), 2.368 (s, 3H), 2.367 (s, 3H), 2.32–2.23 (m, 1H), 2.14–2.06 (m, 1H), 2.00–1.93 (m, 2H); ^{13}C NMR (100 MHz, 300 K, $CDCl_3$): δ 199.18, 138.32, 135.31, 135.04, 126.48, 79.97, 69.43, 29.53, 25.71, 21.34; IR ($CHCl_3$ film): $\tilde{\nu}$ 3010, 1690, 1604, 1445, 1381, 1294, 1052, 929, 859 cm^{-1}; HRMS (ESI): *m/z* calculated for $C_{13}H_{17}O_2$ $[M+H]^+$: 205.1223, found: 205.1221.

(Tetrahydrofuran-2-yl)(*o*-tolyl)methanone (30j):

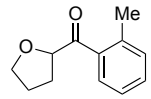

Obtained in 43% yield (32.7 mg, using 10 mol% $NiCl_2$·dtbbpy, 2 mL THF, 24 h); colorless oil; ^{1}H NMR (400 MHz, 300 K, $CDCl_3$): δ 7.62 (dd, J = 8.0, 1.5 Hz, 1H), 7.37 (dd, J = 7.5, 1.4 Hz, 1H), 7.27–7.23 (m, 2H), 5.11 (dd, J = 8.3, 5.8 Hz, 1H), 4.04–3.92 (m, 2H), 2.48 (s, 3H), 2.25–2.16 (m, 1H), 2.10–2.02 (m, 1H), 1.98–1.91 (m, 2H); ^{13}C NMR (100 MHz, 300 K, $CDCl_3$): δ 203.66, 138.54, 136.33, 131.93, 131.42, 128.64, 125.63, 81.64, 69.54, 29.28, 25.67, 21.10; IR ($CHCl_3$ film): $\tilde{\nu}$ 3010, 1680, 1456, 1265, 1200, 1089, 792, 663 cm^{-1}; HRMS (ESI): *m/z* calculated for $C_{12}H_{15}O_2$ $[M+H]^+$: 191.1067, found: 191.1067.

2-Phenyl-1-(tetrahydrofuran-2-yl)ethan-1-one (30k):

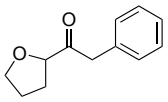

Obtained in 46% yield (35.2 mg, using 10 mol% $NiCl_2$·dtbbpy, 2 mL THF, 24 h); colorless oil; ^{1}H NMR (400 MHz, 300 K, $CDCl_3$): δ 7.33–7.29 (m, 2H), 7.26–7.19 (m, 3H), 4.39 (dd, J = 8.2, 6.3 Hz, 1H), 3.95–3.81 (m, 4H), 2.18–2.09 (m, 1H), 1.96–1.77 (m, 3H); ^{13}C NMR (100 MHz, 300 K, $CDCl_3$): δ 209.74, 133.87, 129.76, 128.65, 126.98, 83.16, 69.46, 45.56, 29.25, 25.70; IR ($CHCl_3$ film): $\tilde{\nu}$ 2959, 2871, 1706, 1452, 1232, 1197, 796, 736 cm^{-1}; HRMS (ESI): *m/z* calculated for $C_{12}H_{14}O_2Na$ $[M+Na]^+$: 213.0886, found: 213.0884.

3-Phenyl-1-(tetrahydrofuran-2-yl)propan-1-one (30l):

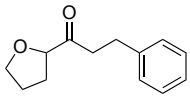

Obtained in 66% yield (54.0 mg, using 10 mol% $NiCl_2$·dtbbpy, 2 mL THF, 24 h); colorless oil; ^{1}H NMR (400 MHz, 300 K, $CDCl_3$): δ 7.29–7.25 (m, 2H), 7.20–7.16 (m, 3H), 4.31–4.28 (m, 1H), 3.94–3.85 (m, 2H), 2.96–2.76 (m, 4H), 2.19–2.10 (m, 1H), 1.91–1.79 (m, 3H); ^{13}C NMR (100 MHz, 300 K, $CDCl_3$): δ 211.68, 141.29, 128.56, 128.47, 126.19, 83.59, 69.46, 40.04, 29.35, 29.07, 25.72. Characterization data are consistent with data reported in the literature.[3]

((±)-*trans*-2-Phenylcyclopropyl)(tetrahydrofuran-2-yl)methanone (30m):

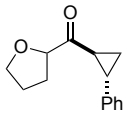

Obtained in 85% yield as a mixture of two diastereoisomers with 1:1 ratio (73.7 mg, using 10 mol% $NiCl_2$·dtbbpy, 2 mL THF, 24 h); colorless oil. Two diastereoisomers were separated by preparative HPLC (CHIRALPAK IC (ø 20 mm x 250 mm), hexane/2-propanol = 5/1, flow rate 20.0 mL/min) and characterized respectively. Isomer 1: ^{1}H NMR (400 MHz, 300 K, $CDCl_3$): δ 7.31–7.26 (m, 2H), 7.23–7.19 (m, 1H),), 7.12–7.09 (m, 2H), 4.46 (dd, *J* = 8.2, 6.3 Hz, 1H), 3.93 (t, *J* = 6.7 Hz, 2H), 2.57–2.49 (m, 2H), 2.28–2.19 (m, 1H), 2.03–1.84 (m, 3H), 1.71 (ddd, *J* = 9.0, 5.5, 4.1 Hz, 1H), 1.43 (ddd, *J* = 8.1, 6.7, 4.1 Hz, 1H); ^{13}C NMR (100 MHz, 300 K, $CDCl_3$): δ 210.26, 140.25, 128.51, 126.56, 126.09, 83.75, 69.42, 29.80, 29.57, 28.03, 25.55, 19.31; Isomer 2: ^{1}H NMR (400 MHz, 300 K, $CDCl_3$): δ 7.30–7.26 (m, 2H), 7.22–7.18 (m, 1H),), 7.13–7.10 (m, 2H), 4.48 (dd, *J* = 8.3, 6.2 Hz, 1H), 4.02–3.91 (m, 2H), 2.58–2.51 (m, 2H), 2.26–2.17 (m, 1H), 2.05–1.88 (m, 3H), 1.68 (ddd, *J* = 8.7, 5.6, 4.0 Hz, 1H), 1.42 (ddd, *J* = 8.2, 6.7, 4.0 Hz, 1H); ^{13}C NMR (100 MHz, 300 K, $CDCl_3$): δ 209.97, 140.19, 128.48, 126.55, 126.25, 83.67, 69.39, 29.57, 29.16, 28.07, 25.52, 19.50; IR ($CHCl_3$ film): $\tilde{\nu}$ 3010, 2875, 1696, 1400, 1229, 1181, 1061, 797, 738 cm^{-1}; HRMS (ESI): *m/z* calculated for $C_{14}H_{17}O_2$ $[M+H]^+$: 217.1223, found: 217.1220.

Cyclopentyl(tetrahydrofuran-2-yl)methanone (30n):

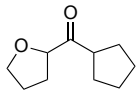

Obtained in 52% yield (35.2 mg, using 10 mol% $NiCl_2$·dtbbpy, 2 mL THF, 24 h); colorless oil; ^{1}H NMR (400 MHz, 300 K, $CDCl_3$): δ 4.43–4.40 (m, 1H), 3.98–3.86 (m, 2H), 3.19–3.11 (m, 1H), 2.23–2.13 (m, 1H), 1.97–1.53 (m, 11H); ^{13}C NMR (100 MHz, 300 K, $CDCl_3$): δ 214.61, 82.92, 69.29, 47.00, 29.37, 29.21, 29.03, 26.13, 26.05, 25.59; IR ($CHCl_3$ film): $\tilde{\nu}$ 2959, 2871, 1706, 1452, 1232, 1197, 794, 727 cm^{-1}; HRMS (ESI): *m/z* calculated for $C_{10}H_{17}O_2$ $[M+H]^+$: 169.1223, found: 169.1220.

(Adamantan-1-yl)(tetrahydrofuran-2-yl)methanone (30o):

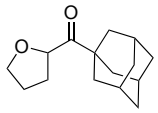

Obtained in 65% yield (60.8 mg, using 10 mol% $NiCl_2$·dtbbpy, 2 mL THF, 24 h); colorless oil; ^{1}H NMR (400 MHz, 300 K, $CDCl_3$): δ 4.78 (dd, *J* = 7.9, 6.2 Hz, 1H), 3.99 (q, *J* = 7.2 Hz, 1H), 3.88 (td, *J* = 7.5, 5.6 Hz, 1H), 2.15–1.68 (m, 19H); ^{13}C NMR (100 MHz, 300 K, $CDCl_3$): δ 214.53, 77.78, 69.38, 45.76, 38.09, 36.65, 29.72, 27.96, 25.99; IR ($CHCl_3$ film): $\tilde{\nu}$ 2908, 2853, 1703, 1452, 1014, 794, 741 cm^{-1}; HRMS (ESI): *m/z* calculated for $C_{15}H_{23}O_2$ $[M+H]^+$: 235.1693, found: 235.1692.

(4*S*)-4,7,7-Trimethyl-1-(tetrahydrofuran-2-carbonyl)-2-oxabicyclo[2.2.1]heptan-3-one (30p):

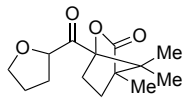

Obtained in 45% yield as a mixture of two diastereoisomers with 1:1 ratio (45.7 mg, using 10 mol% $NiCl_2$·dtbbpy, 2 mL THF, 24 h); brown oil; ^{1}H NMR (400 MHz, 300 K, $CDCl_3$): δ 4.87–4.81 (m, 2H), 4.06–3.91 (m, 4H), 2.49–2.38 (m, 2H), 2.33–2.25 (m, 2H), 2.07–1.83 (m, 10H), 1.74–1.65 (m, 2H), 1.41 (s, 3H), 1.11 (s, 3H), 1.10 (s, 3H), 1.04 (s, 3H), 0.97 (s, 3H), 0.93 (s, 3H); ^{13}C NMR (100 MHz, 300 K, $CDCl_3$): δ 206.77, 206.64, 178.67, 178.39, 95.57, 95.33, 81.39, 80.64, 69.71, 69.56, 55.50, 55.27, 55.22, 54.77, 32.54, 31.48, 29.29, 29.00, 28.19, 25.67, 25.37, 17.11, 16.75, 16.44, 9.63, 9.51; IR ($CHCl_3$ film): $\tilde{\nu}$ 2973, 2878, 1785, 1720, 1396, 1231, 1199, 1078, 793, 735 cm^{-1}; HRMS (ESI): *m/z* calculated for $C_{14}H_{21}O_4$ $[M+H]^+$: 253.1434, found: 253.1430.

Phenyl(tetrahydro-2*H*-pyran-2-yl)methanone (30q):

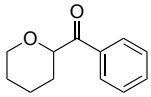

Obtained in 47% yield (35.8 mg, using 10 mol% $NiCl_2$·dtbbpy, 2 mL THP, 24 h); colorless oil; ^{1}H NMR (400 MHz, 300 K, $CDCl_3$): δ 7.99–7.96 (m, 2H), 7.58–7.53 (m, 1H), 7.47–7.43 (m, 2H), 4.73–4.69 (m, 1H), 4.18–4.13 (m, 1H), 3.65–3.59 (m, 1H), 1.97–1.91 (m, 2H), 1.74–1.56 (m, 4H); ^{13}C NMR (100 MHz, 300 K, $CDCl_3$): δ 198.40, 135.09, 133.17, 128.84, 128.50, 79.88, 68.65, 28.88, 25.55, 23.16; IR ($CHCl_3$ film): $\tilde{\nu}$ 3010, 2942, 2853, 1692, 1597, 1449, 1227, 1205, 1091, 970, 747, 695 cm^{-1}; HRMS (ESI): *m/z* calculated for $C_{12}H_{14}O_2Na$ $[M+Na]^+$: 213.0886, found: 213.0887.

(1,4-Dioxan-2-yl)(phenyl)methanone (30r):

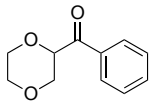

Obtained in 45% yield (34.8 mg, using 10 mol% $NiCl_2$·dtbbpy, 2 mL 1,4-dioxane, 24 h); colorless oil; ^{1}H NMR (400 MHz, 300 K, $CDCl_3$): δ 8.00–7.97 (m, 2H), 7.62–7.57 (m, 1H), 7.50–7.46 (m, 2H), 4.98 (dd, *J* = 9.4, 2.9 Hz, 1H), 4.10 (dd, *J* = 11.8, 2.9 Hz, 1H), 3.98 (dt, *J* = 11.8, 2.6 Hz, 1H), 3.93–3.87 (m, 1H), 3.79 (dt, *J* = 11.9, 2.5 Hz, 1H), 3.75–3.68 (m, 2H); ^{13}C NMR (100 MHz, 300 K, $CDCl_3$): δ 195.85, 134.82, 133.72, 128.84, 128.69, 77.51, 68.18, 66.80, 66.37; IR ($CHCl_3$ film): $\tilde{\nu}$ 3017, 2971, 2860, 1692, 1598, 1449, 1270, 1215, 1130, 1112, 751, 693 cm^{-1}; HRMS (ESI): *m/z* calculated for $C_{11}H_{12}O_3Na$ $[M+Na]^+$: 215.0679, found: 215.0679.

2,3-Dimethoxy-1-phenylpropan-1-one (30s):

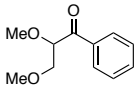

Obtained in 56% yield (43.7 mg, using 10 mol% $NiCl_2$·dtbbpy, 2 mL DME, 24 h); colorless oil; ^{1}H NMR (400 MHz, 300 K, $CDCl_3$): δ 8.06–8.04 (m, 2H), 7.61–7.57 (m, 1H), 7.50–7.46 (m, 2H), 4.71 (t, *J* = 5.0 Hz, 1H), 3.75 (d, *J* = 5.0 Hz, 2H), 3.44 (s, 3H), 3.38 (s, 3H); ^{13}C NMR (100 MHz, 300 K, $CDCl_3$): δ 198.58, 135.59, 133.61, 128.82, 128.74, 84.36, 73.32, 59.54, 58.25; IR ($CHCl_3$ film): $\tilde{\nu}$ 3063, 2988, 2827, 1735, 1693, 1448, 1228, 1193, 1112 cm^{-1}; HRMS (ESI): *m/z* calculated for $C_{11}H_{15}O_3$ $[M+H]^+$: 195.1016, found: 195.1013.

2-(2-Methoxyethoxy)-1-phenylethan-1-one (30s'):

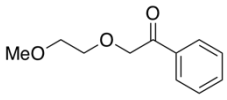

Obtained in 21% yield (16.3 mg, using 10 mol% $NiCl_2$·dtbbpy, 2 mL DME, 24 h); colorless oil; ^{1}H NMR (400 MHz, 300 K, $CDCl_3$): δ 7.95–7.92 (m, 2H), 7.60–7.56 (m, 1H), 7.49–7.44 (m, 2H), 4.84 (s, 2H), 3.79–3.76 (m, 2H), 3.64–3.61 (m, 2H), 3.39 (s, 3H); ^{13}C NMR (100 MHz, 300 K, $CDCl_3$): δ 196.52, 135.04, 133.62, 128.82, 127.99, 74.30, 72.22, 70.96, 58.25. Characterization data are consistent with data reported in the literature.[4]

2-Ethoxy-1-phenylpropan-1-one (30t):

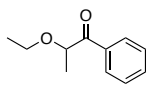

Obtained in 44% yield (31.6 mg, using 10 mol% $NiCl_2$·dtbbpy, 2 mL Et_2O, 24 h); colorless oil; ^{1}H NMR (400 MHz, 300 K, $CDCl_3$): δ 8.09–8.07 (m, 2H), 7.60–7.55 (m, 1H), 7.49–7.44 (m, 2H), 4.67 (q, *J* = 6.9 Hz, 1H), 3.59–

3.45 (m, 2H), 1.50 (d, J = 6.9 Hz, 3H), 1.22 (t, J = 7.0 Hz, 3H) ^{13}C NMR (100 MHz, 300 K, $CDCl_3$): δ 201.11, 134.85, 133.27, 128.80, 128.55, 79.13, 65.23, 18.88, 15.37. Characterization data are consistent with data reported in the literature.[5]

Large Scale Reaction Using Benzoyl Chloride

A oven-dried 20 mL test tube equipped with a magnetic stirring bar and 3-way glass stopcock was charged with $NiCl_2$·dtbbpy (39.8 mg, 0.1 mmol, 10 mol% catalyst loading), $Ir[dF(CF_3)ppy]_2(dtbbpy)PF_6$ (22.4 mg, 0.02 mmol, 2 mol%), K_3PO_4 (318.4 mg, 1.5 mmol, 1.5 equiv.). The vial was sealed and underwent argon/vacuum cycle three times. Under argon, anhydrous THF (5.0 mL) and benzoyl chloride (116.0 µL, 1.0 mmol, 1.0 equiv) were added via syringe. The reaction mixture was stirred 5 cm away from a 21 W blue LED light with a cooling fan for maintaining room temperature. After stirred for 24 h, the reaction mixture was filtered through a plug of silica gel and washed with EtOAc. The filtrate was concentrated, and the resulting residue was purified by automated flash column chromatography (Biotage Isolera One) with pre-packed silica gel column. **30a** was obtained in 69% yield (121.3 mg).

Kinetic Isotope Effect Experiment

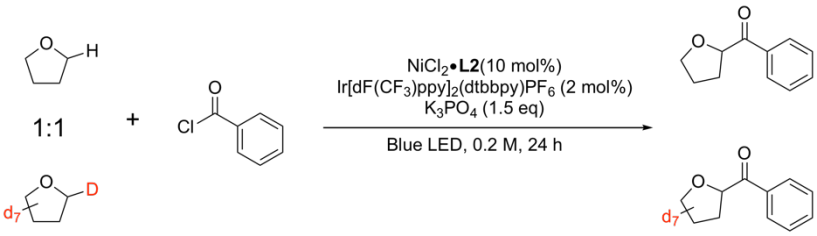

k_H/k_D = 2.4:1

A oven-dried 20 mL test tube equipped with a magnetic stirring bar and 3-way glass stopcock was charged with $NiCl_2$·dtbbpy (8.0 mg, 0.02 mmol, 10 mol% catalyst loading), $Ir[dF(CF_3)ppy]_2(dtbbpy)PF_6$ (4.4 mg, 0.004 mmol, 2 mol%), K_3PO_4 (64.0 mg, 0.30 mmol, 1.5 equiv.) The vial was sealed and underwent argon/vacuum cycle three times. Under argon, anhydrous THF (0.5 mL) and THF-d_8 (0.5 mL) were added separately via syringe. Benzoyl chloride (0.2 mmol, 48.0 µL) was added to the mixture. The reaction mixture was stirred 5 cm away from a 21 W blue LED light with a cooling fan for 24 h. After standard work-up, yield was measured by ^{1}H and ^{2}H NMR. 1,3,5-trimethoxybenzene was used as internal standard for non-deuterated product, and DMF-d_7 was used for deuterated product.

Synthesis of Ni(II) Complex 31

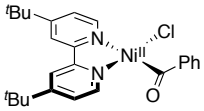

A flame-dried 20 mL test tube equipped with a magnetic stirring bar and 3-way glass stopcock was charged with $Ni(COD)_2$ (440.0 mg, 1.6 mmol) and 4,4´-di-*tert*-butyl-2,2'-pyridine (430.0 mg, 1.6 mmol) in a glove box. To the mixture was added anhydrous diethyl ether (16.0 mL) was added. The resulting mixture was stirred for 12 h at room temperature. To the reaction tube was added benzoyl chloride (186.0 µL, 1.6 mmol) and stirred for 30 min. The resulting dark red suspension was filtered under argon. The red filter cake was collected, dried under vacuum and stored at –20 °C in glove box. Obtained in 75% yield (560.0 mg, 1.20 mmol); red powder; ^{1}H NMR (500 MHz, 300 K, CD_2Cl_2): δ 8.88 (d, J = 5.5 Hz, 1H), 8.59 (d, J = 7.2 Hz, 2H), 7.88 (d, J = 9.9 Hz, 2H), 7.75 (d, J = 5.9 Hz, 1H), 7.53 (d, J = 5.6 Hz, 1H), 7.50–7.42 (m, 3H), 7.21 (d, J = 5.9 Hz, 1H), 1.42 (s, 9H), 1.35 (s, 9H); ^{13}C NMR (125 MHz, 300 K, CD_2Cl_2): δ 238.49, 153.85, 153.03, 145.54, 141.94, 140.35, 138.76, 121.33, 118.87, 118.02, 114.29, 113.38, 108.07, 106.91, 25.45, 20.16, 19.88.

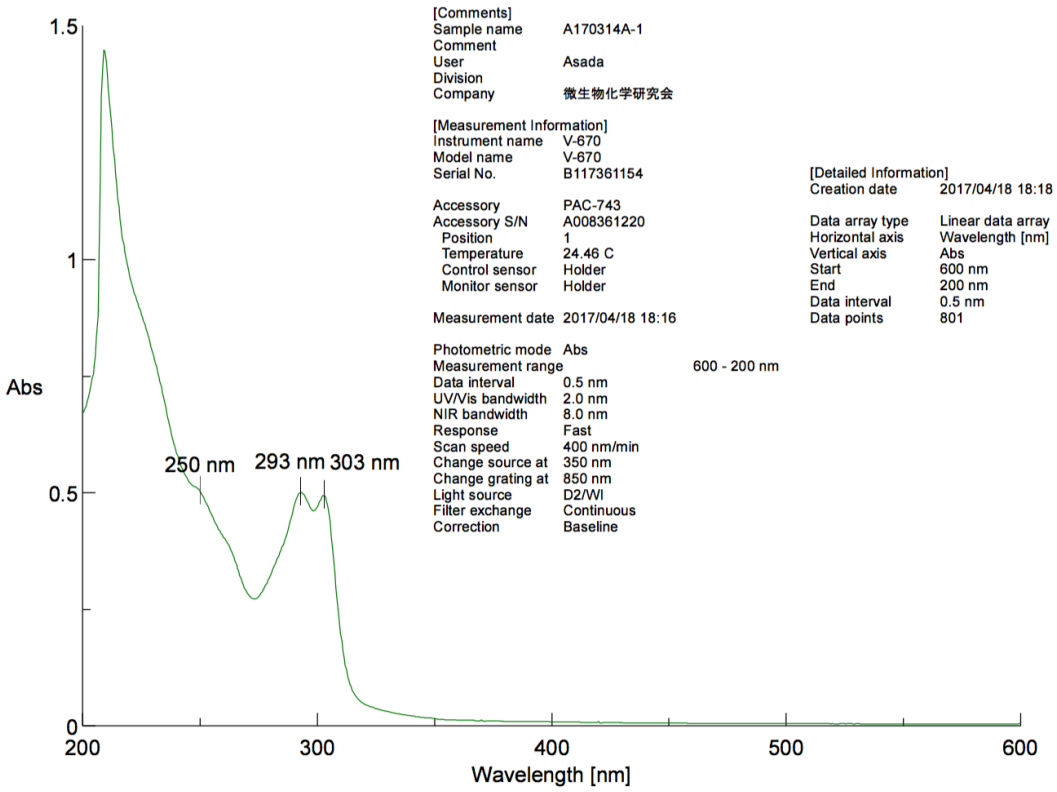

Asymmetric photocatalytic α-benzoylation of THF

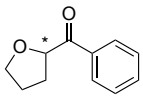

A flame-dried 20 mL test tube equipped with a magnetic stirring bar and 3-way glass stopcock was charged with Ir[dF(CF3)ppy]$_2$(dtbbpy)PF_6 (4.5 mg, 0.004 mmol, 2 mol%), $KHCO_3$ (30.0 mg, 0.30 mmol, 1.5 equiv.) The vial was sealed and underwent argon/vacuum cycle three times. Benzoyl chloride (23 μL, 0.2 mmol) was subsequently added. To the reaction test tube was added the catalyst solution prepared as follows at room temperature: A flame-dried 20 mL test tube equipped with a magnetic stirring bar and 3-way glass stopcock was charged with NiCl2·DME (4.4 mg, 0.02 mmol, 10 mol% catalyst loading) and (*S*)-^{i}Pr-BOX (5.3 mg, 0.02 mmol). The vial was sealed and underwent argon/vacuum cycle three times. To the mixture was added anhydrous THF (1.0 mL) was added via syringe. The mixture was stirred at room temperature for 1 h. The reaction mixture was stirred 5 cm away from a 21 W blue LED light with a cooling fan for maintaining room temperature. Reaction progress was monitored by TLC. After stirred for 24 h, the reaction mixture was filtered through a plug of silica gel and washed with EtOAc (50 mL). The filtrate was concentrated, and the resulting residue was submitted to ^{1}H NMR analysis to determine the yield, 73%. Enantiomeric excess of the product was determined to be 64% ee by chiral stationary phase HPLC analysis (CHIRALPAK IC (ø 0.46 cm x 25 cm), hexane/2-propanol = 3/1, flow rate 1.0 mL/min, detection at 254 nm, t_R = 10.1 min (minor), 11.4 min (major)).

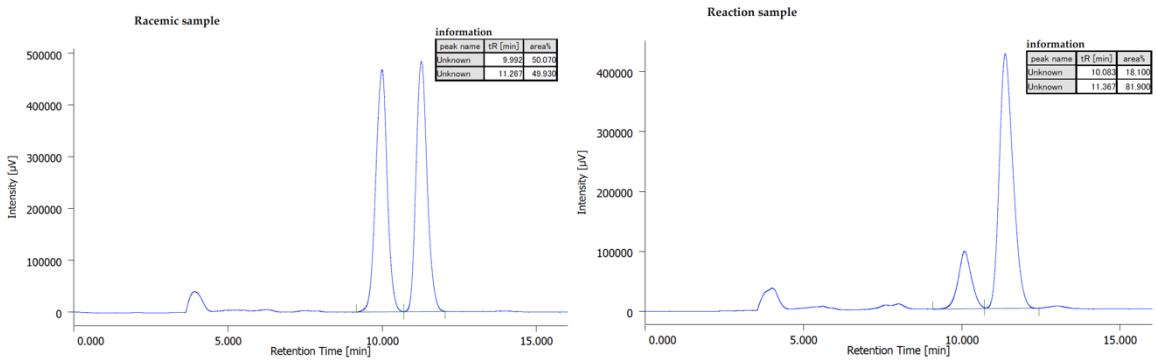

3.7 Synthetic procedures for photocatalytic arylation of α-oxy C(sp^3)–H bond

A oven-dried 20 mL test tube equipped with a magnetic stirring bar and 3-way glass stopcock was charged with $NiCl_2$·bpy (5.7 mg, 0.02 mmol for 5 mol% catalyst loading or 11.4 mg, 0.04 mmol for 10 mol% catalyst loading), $Ir[dF(CF_3)ppy]_2(dtbbpy)PF_6$ (9.0 mg, 0.008 mmol, 2 mol%), Cs_2CO_3 (156.4 mg, 0.48 mmol, 1.2 equiv.) and aryl bromide (0.4 mmol, 1.0 equiv))(if solid, otherwise liquid aryl bromides were added after addition of solvent via syringe). The vial was sealed and underwent argon/vacuum cycle three times. Under argon, corresponding anhydrous solvent was added via a syringe. The reaction mixture was stirred 5 cm away from a 21 W blue LED light with a cooling fan for maintaining room temperature. Reaction progress was monitored by TLC. After stirred for an indicated time, the reaction mixture was filtered through a plug of silica gel and washed with EtOAc (50 mL). The filtrate was concentrated, and the resulting residue was purified by automated silica gel column chromatography (Biotage Isolera One).

1-(4-(Tetrahydrofuran-2-yl)phenyl)ethan-1-one)(40a):

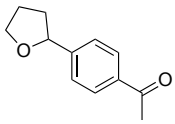

Obtained in 72% yield (54.9 mg, using 5 mol% $NiCl_2$·bpy, 8 mL THF, 12 h); colorless oil; ^1H NMR (400 MHz, 300 K, $CDCl_3$): δ 7.93 (d, J = 8.3 Hz, 2H), 7.42 (d, J = 8.0 Hz, 2H), 4.95 (t, J = 7.2 Hz, 1H), 4.11 (dt, J = 8.3, 6.8 Hz, 1H), 3.96 (dt, J = 8.3, 6.9 Hz, 1H), 2.59 (s, 3H), 2.37 (dq, J = 12.4, 6.7 Hz, 1H), 2.05-1.98 (m, 2H), 1.82-1.73 (m, 1H); ^{13}C NMR (100 MHz, 300 K, $CDCl_3$): δ 197.93, 149.31, 136.18, 128.57, 125.71, 80.25, 68.98, 34.81, 26.72, 26.08. Characterization data are consistent with data reported in the literature.[31,32]

4-(Tetrahydrofuran-2-yl)benzonitrile(40b):

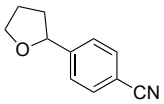

Obtained in 72% yield (50.1 mg, using 5 mol% $NiCl_2$·bpy, 8 mL THF, 12 h); colorless oil; ^1H NMR (400 MHz, 300 K, $CDCl_3$): δ 7.62 (d, J = 8.3 Hz, 2H), 7.44 (d, J = 8.2 Hz, 2H), 4.93 (t, J = 7.2 Hz, 1H), 4.10 (dt, J = 8.3, 6.8 Hz, 1H), 3.96 (dt, J = 8.3, 7.0 Hz, 1H), 2.42-2.34 (m, 1H), 2.05-1.97 (m, 2H), 1.74 (dq, J = 12.2, 7.8 Hz, 1H); ^{13}C NMR (100 MHz, 300 K, $CDCl_3$): δ 149.33, 132.25, 126.25, 119.05, 110.88, 79.91, 69.04, 34.79, 26.02. Characterization data are consistent with data reported in the literature.[31,32]

Methyl 4-(tetrahydrofuran-2-yl)benzoate(40c):

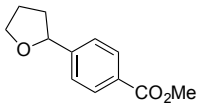

Obtained in 70% yield (58.1 mg, using 5 mol% $NiCl_2$·bpy, 8 mL THF, 12 h); colorless oil; ^1H NMR (400 MHz, 300 K, $CDCl_3$): δ 8.00 (d, *J* = 8.4 Hz, 2H), 7.40 (d, *J* = 8.1 Hz, 2H), 4.94 (t, *J* = 7.2 Hz, 1H), 4.11 (dt, *J* = 8.3, 6.8 Hz, 1H), 3.98-3.92 (m, 1H), 3.90 (s, 3H), 2.36 (dq, *J* = 12.6, 6.7 Hz, 1H), 2.07-1.94 (m, 1H), 2.04-1.97 (m, 2H), 1.81-1.72 (m, 2H); ^{13}C NMR (100 MHz, 300 K, $CDCl_3$): δ 167.11, 149.06, 129.77, 129.04, 125.53, 80.29, 68.96, 52.13, 34.81, 26.08. Characterization data are consistent with data reported in the literature.[31]

5-(Tetrahydrofuran-2-yl)isobenzofuran-1(3*H*)-one(40d):

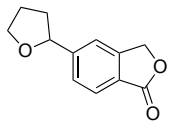

Obtained in 73% yield (59.6 mg, using 5 mol% $NiCl_2$·bpy, 8 mL THF, 12 h); white solid, m. p.: 98–100 °C; ^1H NMR (400 MHz, 300 K, $CDCl_3$): δ 7.86 (d, *J* = 8.0 Hz, 2H), 7.51-7.45 (m, 2H), 5.30 (s, 3H), 5.01 (t, *J* = 7.3 Hz, 1H), 4.13 (dt, *J* = 8.4, 6.8 Hz, 1H), 3.99 (dt, *J* = 8.3, 6.9 Hz, 1H), 2.47-2.38 (m, 1H), 2.08-2.00 (m, 2H), 1.78 (dq, *J* = 12.2, 7.8 Hz, 1H); ^{13}C NMR (100 MHz, 300 K, $CDCl_3$): δ 171.07, 151.07, 147.12, 126.71, 125.69, 124.66, 118.92, 80.21, 69.71, 69.09, 35.05, 26.08; IR ($CHCl_3$ film): $\tilde{\nu}$ 2876, 2348, 1766, 1620, 1455, 1366, 1345, 1203, 744, 692, 666 cm^{-1}; HRMS (ESI): *m/z* calculated for $C_{12}H_{13}O_3$ $[M+H]^+$: 205.0859, found: 205.0858.

2-(4-Chlorophenyl)tetrahydrofuran(40e):

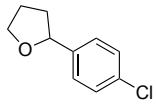

Obtained in 63% yield (46.4 mg, using 10 mol% $NiCl_2$·bpy, 6 mL THF with 2 mL acetone, 24 h); colorless oil; ^1H NMR (400 MHz, 300 K, $CDCl_3$): δ 7.30-7.24 (m, 4H), 4.85 (t, *J* = 7.2 Hz, 1H), 4.08 (dt, *J* = 8.2, 6.8 Hz, 1H), 3.92 (dt, *J* = 8.2, 6.9 Hz, 1H), 2.35-2.27 (m, 1H), 2.03-1.96 (m, 1H), 1.79-1.70 (m, 1H); ^{13}C NMR (100 MHz, 300 K, $CDCl_3$): δ 142.16, 132.84, 128.51, 127.11, 80.12, 68.83, 34.80, 26.09. Characterization data are consistent with data reported in the literature.[31]

2-([1,1'-Biphenyl]-4-yl)tetrahydrofuran(40f):

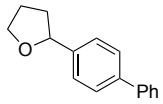

Obtained in 60% yield (53.7 mg, using 5 mol% $NiCl_2$·bpy, 6 mL THF with 2 mL acetone, 48 h); colorless oil; ^1H NMR (400 MHz, 300 K, $CDCl_3$): δ 7.59-7.54 (m, 4H), 7.44-7.39 (m, 4H), 7.34-7.30 (m, 1H), 4.93 (t, *J* = 7.2 Hz, 1H), 4.11 (dt, *J* = 8.1, 6.8 Hz, 1H), 3.95 (dt, *J* = 7.9, 6.3 Hz, 1H), 2.38-2.30 (m, 1H), 2.06-1.97 (m, 2H), 1.88-1.76 (m, 1H); ^{13}C NMR (100 MHz, 300 K, $CDCl_3$): δ 142.65, 141.14, 140.21, 128.84, 127.27, 127.19, 127.18, 126.21, 80.57, 68.81, 34.71, 26.20. Characterization data are consistent with data reported in the literature.[32]

***N*-(4-(Tetrahydrofuran-2-yl)phenyl)acetamide(40g):**

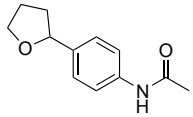

Obtained in 60% yield (49.4 mg, using 5 mol% $NiCl_2$·bpy, 6 mL THF with 2 mL acetone, 24 h); yellow solid, m. p.: 85–87 °C; ^1H NMR (400 MHz, 300 K, $CDCl_3$): δ 7.69 (br, 1H), 7.44 (d, *J* = 8.5 Hz, 2H), 7.26 (d, *J* = 9.2 Hz, 2H), 4.84 (t, *J* = 7.1 Hz, 1H), 4.08 (dt, *J* = 8.2, 6.8 Hz, 1H), 3.91 (dt, *J* = 7.8, 6.4 Hz, 1H), 2.32-2.24 (m, 1H), 2.12 (s, 3H), 2.04-1.96 (m, 2H), 1.81-1.72 (m, 1H); ^{13}C NMR (100 MHz, 300 K, $CDCl_3$): δ 168.56, 139.21, 136.99, 126.27, 119.98, 80.39, 68.60, 34.54, 26.00, 24.43; IR ($CHCl_3$ film): $\tilde{\nu}$ 3297, 2976, 2871, 1667, 1603, 1540, 1411,

1371, 1315, 1055, 721, 604 cm^{-1}; HRMS (ESI): *m/z* calculated for $C_{12}H_{16}NO_2$ $[M+H]^+$: 206.1176, found: 206.1175.

4-(Tetrahydrofuran-2-yl)benzamide(40h):

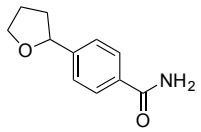

Obtained in 61% yield (47.1 mg, using 5 mol% $NiCl_2$·bpy, 6 mL THF with 2 mL acetone, 24 h); white solid, m. p.: 173–175 °C; ^1H NMR (400 MHz, 300 K, $CDCl_3$): δ 7.78 (d, *J* = 8.4 Hz, 2H), 7.41 (d, *J* = 7.9 Hz, 2H), 6.03 (br, 1H), 5.64 (br, 1H), 4.95 (t, *J* = 7.2 Hz, 1H), 4.11 (dt, *J* = 8.4, 6.8 Hz, 1H), 3.96 (dt, *J* = 8.3, 7.0 Hz, 1H), 2.37 (dq, *J* = 12.3, 6.7 Hz, 1H), 2.02 (dq, *J* = 8.4, 6.8 Hz, 1H), 1.82-1.73 (m, 1H); ^{13}C NMR (100 MHz, 300 K, $CDCl_3$): δ 169.16, 148.17, 132.17, 127.58, 125.86, 80.27, 69.00, 34.86, 26.11; IR ($CHCl_3$ film): $\tilde{\nu}$ 3374, 3168, 2975, 2859, 1649, 1616, 1566, 1415, 1394, 1215, 1071, 773, 649 cm^{-1}; HRMS (ESI): *m/z* calculated for $C_{11}H_{14}NO_2$ $[M+H]^+$: 192.1019, found: 192.1017.

2-(*o*-Tolyl)tetrahydrofuran(40i):

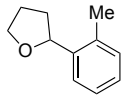

Obtained in 31% yield (20.1 mg, using 10 mol% $NiCl_2$·bpy, 6 mL THF with 2 mL acetone, 24 h); colorless oil; ^1H NMR (400 MHz, 300 K, $CDCl_3$): δ 7.44 (d, *J* = 7.5 Hz, 1H), 7.21-7.10 (m, 3H), 5.06 (t, *J* = 7.2 Hz, 1H), 4.14 (dt, *J* = 8.0, 6.5 Hz, 1H), 3.93 (dt, *J* = 8.2, 7.0 Hz, 1H), 2.39-2.33 (m, 1H), 2.30 (s, 3H), 2.04-1.97 (m, 2H), 1.72-1.64 (m, 1H); ^{13}C NMR (100 MHz, 300 K, $CDCl_3$): δ 141.96, 134.31, 130.25, 126.89, 126.12, 124.68, 78.10, 68.77, 33.29, 26.17, 19.37. Characterization data are consistent with data reported in the literature.[32]

3-(Tetrahydrofuran-2-yl)benzaldehyde(40j):

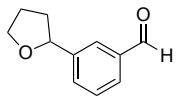

Obtained in 64% yield (45.3 mg, using 5 mol% $NiCl_2$•bpy, 6 mL THF with 2 mL acetone, 18 h); colorless oil; ^1H NMR (400 MHz, 300 K, $CDCl_3$): δ 10.02 (s, 1H), 7.87-7.85 (m, 1H), 7.77 (dt, *J* = 7.5, 1.5 Hz, 1H), 7.63-7.60 (m, 1H), 7.50 (t, *J* = 7.6 Hz, 1H), 4.96 (t, *J* = 7.2 Hz, 1H), 4.13 (dt, *J* = 8.3, 6.8 Hz, 1H), 3.97 (dt, *J* = 8.3, 6.9 Hz, 1H), 2.39 (dq, *J* = 12.6, 6.6 Hz, 1H), 2.07-2.00 (m, 2H), 1.80 (dq, *J* = 12.2, 7.7 Hz, 1H); ^{13}C NMR (100 MHz, 300 K, $CDCl_3$): δ 192.52, 144.95, 136.62, 131.88, 129.12, 128.72, 126.91, 80.11, 68.97, 34.83, 26.12; IR ($CHCl_3$ film): $\tilde{\nu}$ 2980, 2873, 2727, 1734, 1698, 1604, 1374, 1242, 798, 727 cm^{-1}.

5-(Tetrahydrofuran-2-yl)picolinonitrile(40k):

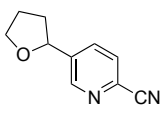

Obtained in 75% yield (52.2 mg, using 5 mol% $NiCl_2$·bpy, 6 mL THF with 2 mL acetone, 18 h); yellow oil; ^1H NMR (400 MHz, 300 K, $CDCl_3$): δ 8.68-8.67 (m, 1H), 7.82 (ddd, *J* = 8.0, 2.2, 0.8 Hz, 1H), 7.68 (dd, *J* = 7.9, 0.8 Hz, 1H), 4.99 (t, *J* = 7.3 Hz, 1H), 4.11 (dt, *J* = 8.3, 6.9 Hz, 1H), 4.01-3.95 (m, 1H), 2.49-2.41 (m, 1H), 2.13-1.98 (m, 2H), 1.77 (dq, *J* = 12.3, 7.8 Hz, 1H); ^{13}C NMR (100 MHz, 300 K, $CDCl_3$): δ 149.02, 143.36, 134.04, 132.45, 128.25, 117.42, 77.88, 69.12, 34.67, 26.03; IR ($CHCl_3$ film): $\tilde{\nu}$ 3329, 2981, 2878, 2235, 1569, 1470, 1374, 1232, 849, 558 cm^{-1}; HRMS (ESI): *m/z* calculated for $C_{10}H_{11}N_2O$ $[M+H]^+$: 175.0866, found: 175.0862.

3-Methoxy-5-(tetrahydrofuran-2-yl)pyridine(40l):

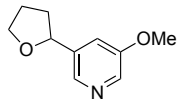

Obtained in 70% yield (50.3 mg, using 5 mol% $NiCl_2$·bpy, 6 mL THF with 2 mL acetone, 18 h); colorless oil; ^{1}H NMR (400 MHz, 300 K, $CDCl_3$): δ 8.20 (d, *J* = 2.8 Hz, 1H), 8.17 (d, *J* = 1.7 Hz, 1H), 7.68 (t, *J* = 2.3 Hz, 1H), 4.91 (t, *J* = 7.2 Hz, 1H), 4.09 (dt, *J* = 8.3, 6.9 Hz, 1H), 3.94 (dt, *J* = 8.2, 7.0 Hz, 1H), 3.86 (s, 3H), 2.37 (dq, *J* = 13.1, 6.7 Hz, 1H), 2.09-1.99 (m, 2H), 1.84-1.75 (m, 1H); ^{13}C NMR (100 MHz, 300 K, $CDCl_3$): δ 155.82, 139.87, 139.80, 136.48, 117.69, 78.28, 68.85, 55.64, 34.60, 26.05; IR ($CHCl_3$ film): $\tilde{\nu}$ 2971, 2873, 1590, 1466, 1444, 1427, 1270, 1193, 800, 711 cm^{-1}; HRMS (ESI): *m/z* calculated for $C_{10}H_{14}NO_2$ $[M+H]^+$: 180.1019, found: 180.1017.

5-(Tetrahydrofuran-2-yl)-1-tosyl-1*H*-indole(40m):

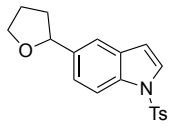

Obtained in 50% yield (68.3 mg, using 10 mol% $NiCl_2$·bpy, 6 mL THF with 2 mL acetone, 24 h); colorless oil; ^{1}H NMR (400 MHz, 300 K, $CDCl_3$): δ 7.93 (d, *J* = 8.6 Hz, 1H), 7.75-7.72 (m, 2H), 7.53 (d, *J* = 3.6 Hz, 1H), 7.50-7.49 (m, 1H), 7.28-7.26 (m, 1H), 7.21-7.18 (m, 2H), 6.61 (dd, *J* = 3.7, 0.8 Hz, 1H), 4.92 (t, *J* = 7.2 Hz, 1H), 4.10 (dt, *J* = 8.2, 6.8 Hz, 1H), 3.93 (dt, *J* = 7.9, 6.4 Hz, 1H), 2.36-2.28 (m, 4H), 2.05-1.96 (m, 2H), 1.85-1.76 (m, 1H); ^{13}C NMR (100 MHz, 300 K, $CDCl_3$): δ 144.99, 138.70, 135.44, 134.29, 130.93, 129.97, 126.91, 126.78, 122.79, 118.55, 113.57, 109.29, 80.92, 68.81, 34.91, 26.25, 21.68; IR ($CHCl_3$ film): $\tilde{\nu}$ 2975, 2870, 1595, 1459, 1372, 1271, 1226, 1187, 1173, 812, 588 cm^{-1}; HRMS (ESI): *m/z* calculated for $C_{19}H_{20}NO_3S$ $[M+H]^+$: 342.1158, found: 342.1156.

***tert*-Butyl 5-(tetrahydrofuran-2-yl)-1*H*-indazole-1-carboxylate(40n):**

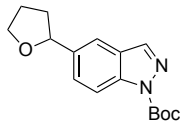

Obtained in 58% yield (66.6 mg, using 10 mol% $NiCl_2$·bpy, 6 mL THF with 2 mL acetone, 24 h); colorless oil; ^{1}H NMR (400 MHz, 300 K, $CDCl_3$): δ 8.15-8.13 (m, 2H), 7.72-7.71 (m, 1H), 7.50 (dd, *J* = 8.8, 1.6 Hz, 1H), 5.01 (t, *J* = 7.2 Hz, 1H), 4.14 (dt, *J* = 8.1, 6.8 Hz, 1H), 3.97 (dt, *J* = 8.3, 7.0 Hz, 1H), 2.42-2.34 (m, 1H), 2.07-2.00 (m, 2H), 1.88-1.77 (m, 1H), 1.73 (s, 9H); ^{13}C NMR (100 MHz, 300 K, $CDCl_3$): δ 149.32, 139.69, 139.40, 139.23, 127.24, 126.02, 117.72, 114.58, 84.89, 80.52, 68.87, 35.05, 28.29, 21.13; IR ($CHCl_3$ film): $\tilde{\nu}$ 2979, 2935, 2871, 1756, 1735, 1387, 1285, 1244, 1150, 1029, 847, 822 cm^{-1}; HRMS (ESI): *m/z* calculated for $C_{16}H_{21}N_2O_3$ $[M+H]^+$: 289.1547, found: 289.1544.

5-(Tetrahydrofuran-2-yl)quinolone(40o):

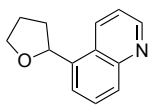

Obtained in 66% yield (52.6 mg, using 5 mol% $NiCl_2$·bpy, 6 mL THF with 2 mL acetone, 24 h); colorless oil; ^{1}H NMR (400 MHz, 300 K, $CDCl_3$): δ 8.91 (dd, *J* = 4.2, 1.6 Hz, 1H), 8.36 (ddd, *J* = 8.6, 1.7, 0.9 Hz, 1H), 8.05-8.00 (m, 1H), 7.71-7.66 (m, 2H), 7.40 (dd, *J* = 8.6, 4.2 Hz, 1H), 5.55 (t, *J* = 7.0 Hz, 1H), 4.21 (dt, *J* = 8.2, 7.2 Hz, 1H), 4.02 (dt, *J* = 8.2, 7.1 Hz, 1H), 2.55-2.46 (m, 1H), 2.14-2.00 (m, 2H), 1.91 (dq, *J* = 12.1, 7.4 Hz, 1H); ^{13}C NMR

(100 MHz, 300 K, $CDCl_3$): δ 149.95, 148.70, 139.60, 132.05, 129.13, 128.98, 125.70, 122.72, 120.71, 77.75, 68.81, 33.83, 26.03. Characterization data are consistent with data reported in the literature.[31]

1-(Tetrahydrofuran-2-yl)isoquinoline(40p):

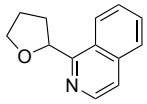

Obtained in 51% yield (52.6 mg, using 10 mol% $NiCl_2$·bpy, 6 mL THF with 2 mL acetone, 18 h); colorless oil; ^{1}H NMR (400 MHz, 300 K, $CDCl_3$): δ 8.49 (d, *J* = 5.7 Hz, 1H), 8.34 (dq, *J* = 8.4, 1.0 Hz, 1H), 7.82 (dq, *J* = 8.2, 1.0 Hz, 1H), 7.69-7.56 (m, 3H), 5.72 (t, *J* = 7.1 Hz, 1H), 4.21-4.16 (m, 1H), 4.04 (dt, *J* = 7.9, 6.1 Hz, 1H), 2.57-2.49 (m, 1H), 2.44-2.36 (m, 1H), 2.23-2.06 (m, 2H); ^{13}C NMR (100 MHz, 300 K, $CDCl_3$): δ 159.72, 141.73, 136.65, 129.91, 127.43, 127.21, 126.75, 125.41, 120.61, 79.25, 69.11, 30.85, 26.28. Characterization data are consistent with data reported in the literature.[33b]

1-(4-(1,2-Dimethoxyethyl)phenyl)ethan-1-one(40q):

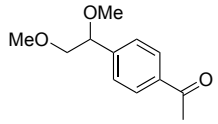

Obtained in 78% yield (65.0 mg, using 5 mol% $NiCl_2$·bpy, 8 mL DME, 12 h); colorless oil; ^{1}H NMR (400 MHz, 300 K, $CDCl_3$): δ 7.97 (d, *J* = 8.3 Hz, 2H), 7.44 (d, *J* = 8.2 Hz, 2H), 4.45 (dd, *J* = 7.6, 3.8 Hz, 1H), 3.59 (dd, *J* = 10.4, 7.6 Hz, 1H), 3.45 (dd, *J* = 10.4, 3.8 Hz, 1H), 3.39 (s, 3H), 3.31 (s, 3H), 2.61 (s, 3H); ^{13}C NMR (100 MHz, 300 K, $CDCl_3$): δ 197.71, 144.52, 136.95, 128.60, 127.19, 82.62, 76.81, 59.36, 57.30, 26.68. Characterization data are consistent with data reported in the literature.[32]

Methyl 4-(1,2-dimethoxyethyl)benzoate(40r):

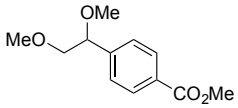

Obtained in 83% yield (74.3 mg, using 5 mol% $NiCl_2$·bpy, 8 mL DME, 12 h); colorless oil; ^{1}H NMR (400 MHz, 300 K, $CDCl_3$): δ 8.04 (d, *J* = 8.4 Hz, 2H), 7.41 (d, *J* = 7.9 Hz, 2H), 4.44 (dd, *J* = 7.7, 3.6 Hz, 1H), 3.92 (s, 3H), 3.59 (dd, *J* = 10.4, 7.7 Hz, 1H), 3.44 (dd, *J* = 10.4, 3.7 Hz, 1H), 3.39 (s, 3H), 3.31 (s, 3H); ^{13}C NMR (100 MHz, 300 K, $CDCl_3$): δ 166.92, 144.33, 130.01, 129.89, 127.04, 82.73, 76.94, 59.40, 57.34, 52.21; IR ($CHCl_3$ film): $\tilde{\nu}$ 3008, 2932, 2891, 1723, 1612, 1436, 1281, 1193, 1103, 858, 707 cm^{-1}; HRMS (ESI): *m/z* calculated for $C_{12}H_{17}O_4$ $[M+H]^+$: 225.1121, found: 225.1122.

5-(1-Ethoxyethyl)isobenzofuran-1(3*H*)-one(40s):

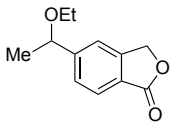

Obtained in 69% yield (56.8 mg, using 10 mol% $NiCl_2$·bpy, 3 mL Et_2O with 1mL acetone, 24 h); colorless oil; ^{1}H NMR (400 MHz, 300 K, $CDCl_3$): δ 7.89 (d, *J* = 8.2 Hz, 1H), 7.49-7.28 (m, 2H), 5.32 (s, 2H), 4.54 (q, *J* = 6.5 Hz, 1H), 3.48-3.33 (m, 2H), 1.46 (d, *J* = 6.6 Hz, 3H), 1.22 (d, *J* = 7.0 Hz, 3H); ^{13}C NMR (100 MHz, 300 K, $CDCl_3$): δ 171.00, 151.86, 147.25, 127.27, 125.93, 125.01, 119.45, 77.52, 69.73, 64.56, 24.35, 15.48; IR ($CHCl_3$ film): $\tilde{\nu}$ 2977, 2874, 1764, 1619, 1455, 1371, 1336, 1237, 845, 721 cm^{-1}; HRMS (ESI): *m/z* calculated for $C_{12}H_{15}O_3$ $[M+H]^+$: 207.1016, found: 207.1015.

Methyl 4-(1-ethoxyethyl)benzoate(40t):

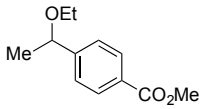

Obtained in 54% yield (45.5 mg, using 10 mol% $NiCl_2$·bpy, 3 mL Et_2O with 1mL acetone, 24 h); colorless oil; ^1H NMR (400 MHz, 300 K, $CDCl_3$): δ 8.02 (d, J = 8.3 Hz, 1H), 7.39 (d, J = 8.2 Hz, 1H), 4.46 (q, J = 6.5 Hz, 1H), 3.91 (s, 3H), 3.42-3.31 (m, 2H), 1.43 (d, J = 6.5 Hz, 3H), 1.19 (d, J = 7.0 Hz, 3H); ^{13}C NMR (100 MHz, 300 K, $CDCl_3$): δ 167.10, 149.79, 129.93, 129.34, 126.12, 77.52, 64.34, 52.17, 24.21, 15.50; IR ($CHCl_3$ film): $\tilde{\nu}$ 2976, 2869, 1725, 1611, 1436, 1277, 875, 829, 708 cm^{-1}; HRMS (ESI): *m/z* calculated for $C_{12}H_{17}O_3$ $[M+H]^+$: 209.1172, found: 209.1169.

3.8 X-ray crystallographic data

Single crystals of **5e** were obtained from 2-propanol at room temperature. Single-crystal X-ray data were collected on a Rigaku R-AXIS RAPID II imaging plate area detector with graphite-monochromated Cu-Kα radiation. Data collection was conducted at 93 K. All structures were solved by direct methods and refined by full matrix least-squares against F2 with all reflections. All non-hydrogen atoms were refined anisotropically. All hydrogen atoms were placed in standard calculated positions and were refined using the riding model. Refined structure and crystallographic parameters are summarized in Figure S1 and Table S1. CCDC 1421281 contains the supplementary crystallographic data for **5e**.

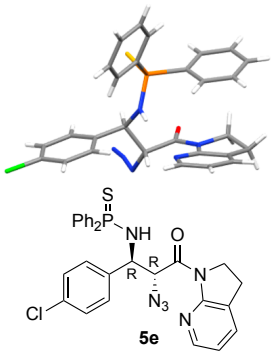

Figure S1. The structure of **5e**. White: hydrogen, gray: carbon, blue: nitrogen, red: oxygen, light green: chlorine, orange: phosphorus, yellow: sulfur.

Table S1. Selected Crystallographic Data of **5e**

	5e
molecular formula	$C_{28}H_{24}ClN_6OPS$
formula weight	559.02
crystal color, habit	colorless, prism
crystal system	orthrhombic
space group	$P2_12_12_1$
cell constants	
a (Å)	7.96937(14)
b (Å)	16.0585(3)
c (Å)	20.7942(4)
V (Å^3)	2661.17(8)
Z	4
ρ_{calcd} (g cm^{-3})	1.395
R_1	0.0401
wR_2	0.0875
F(000)	1160.00
Flack parameter	-0.007(7)

The relative and absolute configurations of other Mannich products were deduced by analogy.

Single crystals of *rac*-BINAP/Cu/**1-N$_3$** complex were obtained from 0.02 M solution of the mixture comprising of *rac*-BINAP : $[Cu(CH_3CN)_4]PF_6$: **1-N$_3$** = 1:1:1 in acetone at 5 °C. Single-crystal X-ray data were collected in a similar manner as described above (data collection was conducted at 93 K). Refined structure and crystallographic parameters are summarized in Figure S2 and Table S2. CCDC 1419458 contains the supplementary crystallographic data for the complex.

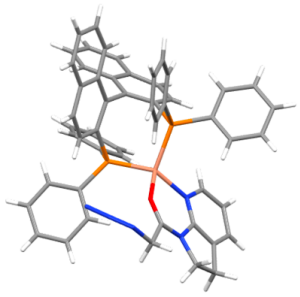

Figure S2. The structure of *rac*-BINAP/Cu/**1-N$_3$**. White: hydrogen, gray: carbon, blue: nitrogen, red: oxygen, orange: phosphorus, pink: copper.

Table S2. Selected Crystallographic Data of *rac*-BINAP/Cu/**1-N$_3$**

	rac-BINAP/Cu/**1-N$_3$**
molecular formula	$C_{58}H_{50}CuF_6N_6O_2P_3$
formula weight	1133.53
crystal color, habit	yellow, block
crystal system	monoclinic
space group	*P2$_1$*
cell constants	
a (Å)	10.00574(18)
b (Å)	17.2212(3)
c (Å)	14.8798(3)
b (deg)	90.610(6)
V (Å^3)	2563.80
Z	2
ρ_{calcd} (g cm^{-3})	1.468
R_1	0.0613
wR_2	0.1567
F(000)	1168.00

Single crystals of **8** were obtained from dichloromethane/hexane at room temperature. Single-crystal X-ray data were collected in a similar manner as described above (data collection was conducted at 93 K). Refined structure and crystallographic parameters are summarized in Figure S3 and Table S3. The absolute and relative configuration of **8** was determined to be as depicted below by Flack parameter.

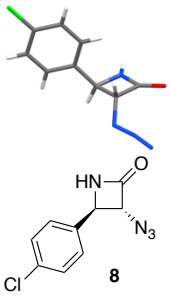

8

Figure S3. The structure of **8**. White: hydrogen, gray: carbon, blue: nitrogen, red: oxygen, light green: chlorine.

Table S3. Selected Crystallographic Data of **8**

	8
molecular formula	$C_9H_7ClN_4$
formula weight	222.63
crystal color, habit	colorless, block
crystal system	monoclinic
space group	*P2$_1$*
cell constants	
a (Å)	6.3392(11)
b (Å)	7.4556(6)
c (Å)	10.2596(9)
b (deg)	93.103(10)
V (Å^3)	484.18(10)
Z	12
ρ_{calcd} (g cm^{-3})	1.527
R_1	0.0640
wR_2	0.1813
F(000)	228.00
Flack parameter	-0.01(3)

Single crystals of **20k** were obtained from dichloromethane/hexane at –20 °C. Single-crystal X-ray data were collected in a similar manner as described above (data collection was conducted at 93 K). Refined structure and crystallographic parameters are summarized in Figure S4 and Table S4. The absolute and relative configuration of **20k** was determined to be as depicted below by Flack parameter. CCDC 1834945 contains the supplementary crystallographic data for **20k**.

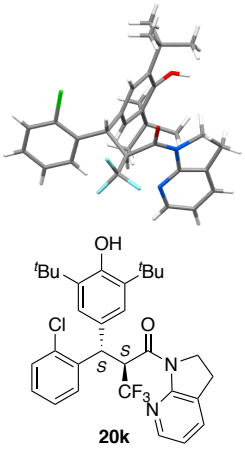

Figure S4. The structure of **20k**. White: hydrogen, gray: carbon, blue: nitrogen, red: oxygen, light green: chlorine, water blue: fluorine.

Table S4. Selected Crystallographic Data of **20k**

	20k
molecular formula	$C_{31}H_{34}ClF_3N_2O_2$
formula weight	559.07
crystal color, habit	colorless, block
crystal system	orthrhombic
space group	$P2_12_12_1$
cell constants	
a (Å)	12.8817(2)
b (Å)	16.3398(3)
c (Å)	41.6339(8)
V (Å^3)	8763.3(3)
Z	12
ρ_{calcd} (g cm^{-3})	1.271
R_1	0.0415
wR_2	0.0820
F(000)	3528.00
Flack parameter	0.050(5)

Single crystals of **24** were obtained from dichloromethane/hexane at room temperature. Single-crystal X-ray data were collected in a similar manner as described above (data collection was conducted at 93 K). Refined structure and crystallographic parameters are summarized in Figure S5 and Table S5. CCDC 1834946 contains the supplementary crystallographic data for **24**.

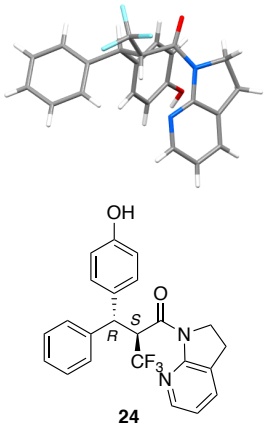

Figure S5. The structure of **24**. White: hydrogen, gray: carbon, blue: nitrogen, red: oxygen, water blue: fluorine.

Table S5. Selected Crystallographic Data of **24**

	24
molecular formula	$C_{23}H_{19}F_3N_2O_2$
formula weight	412.41
crystal color, habit	colorless, prism
crystal system	orthrhombic
space group	$P2_12_12_1$
cell constants	
a (Å)	8.38289(18)
b (Å)	15.3054(3)
c (Å)	15.5959(4)
V (Å^3)	2001.01(8)
Z	4
ρ_{calcd} (g cm^{-3})	1.369
R_1	0.0259
wR_2	0.0652
F(000)	856.00
Flack parameter	0.07(3)

The absolute configuration of the 1,6-addition product derived from **1-Me** was determined by X-ray crystallography of **21**. Single crystals of **21** were obtained from dichloromethane/hexane at room temperature. Single-crystal X-ray data were collected in a similar manner as described above (data collection was conducted

at 93 K). Refined structure and crystallographic parameters are summarized in Figure S6 and Table S6. CCDC 1834947 contains the supplementary crystallographic data for **21**.

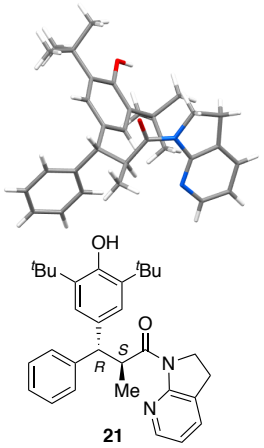

Figure S6. The structure of **21**. White: hydrogen, gray: carbon, blue: nitrogen, red: oxygen.

Table S6. Selected Crystallographic Data of **21**

	21
molecular formula	$C_{31}H_{38}N_2O_2$
formula weight	470.65
crystal color, habit	colorless, platelet
crystal system	monoclinic
space group	$P2_1$
cell constants	
a (Å)	8.6379(3)
b (Å)	15.1061(6)
c (Å)	11.0136(4)
b (deg)	93.457(7)
V (Å^3)	1434.49(10)
Z	2
ρ_{calcd} (g cm^{-3})	1.090
R_1	0.0483
wR_2	0.1336
F(000)	508.00
Flack parameter	-0.01(13)

The absolute configuration of the 1,6-addition product derived from **1-N$_3$** was determined by X-ray crystallography of **28**. Single crystals of **28** were obtained from dichloromethane/hexane at room temperature. Single-crystal X-ray data were collected in a similar manner as described above (data collection was conducted at 93 K). Refined structure and crystallographic parameters are summarized in Figure S7 and Table S7. CCDC 1834948 contains the supplementary crystallographic data for **28**.

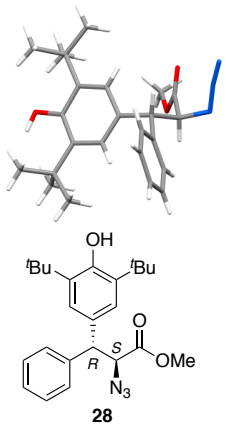

Figure S7. The structure of **28**. White: hydrogen, gray: carbon, blue: nitrogen, red: oxygen, water blue: fluorine.

Table S7. Selected Crystallographic Data of **28**

	28
molecular formula	$C_{24}H_{31}N_3O_3$
formula weight	409.53
crystal color, habit	colorless, needle
crystal system	Orthorhombic
space group	$P2_12_12_1$
cell constants	
a (Å)	5.9738(8)
b (Å)	19.278(3)
c (Å)	19.702(3)
V (Å^3)	2269.0(5)
Z	4
ρ_{calcd} (g cm^{-3})	1.199
R_1	0.0753
wR_2	0.2152
F(000)	880.00
Flack parameter	0.2(2)

The absolute configuration of the 1,6-addition product derived from **1-OBn** was determined by X-ray crystallography of **23**. Single crystals of **23** were obtained from dichloromethane/hexane at room temperature. Single-crystal X-ray data were collected in a similar manner as described above (data collection was conducted

at 93 K). Refined structure and crystallographic parameters are summarized in Figure S8 and Table S8. CCDC 1834949 contains the supplementary crystallographic data for **23**.

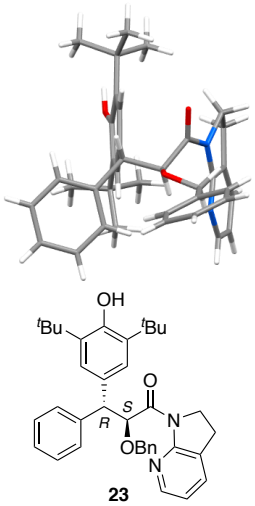

Figure S8. The structure of **23**. White: hydrogen, gray: carbon, blue: nitrogen, red: oxygen.

Table S8. Selected Crystallographic Data of **23**

	23
molecular formula	$C_{37}H_{42}N_2O_3$
formula weight	562.75
crystal color, habit	colorless, block
crystal system	monoclinic
space group	*P2₁*
cell constants	
a (Å)	9.4890(3)
b (Å)	17.1556(5)
c (Å)	9.8164(3)
b (deg)	103.700(7)
V (Å^3)	1552.55(9)
Z	2
ρ_{calcd} (g cm^{-3})	1.204
R_1	0.0340
wR_2	0.0909
F(000)	604.00
Flack parameter	0.10(8)

Single crystals of **42** were obtained from EtOAc/hexane at room temperature. Single-crystal X-ray data were collected in a similar manner as described above (data collection was conducted at 93 K). Refined structure and crystallographic parameters are summarized in Figure S9 and Table S9.

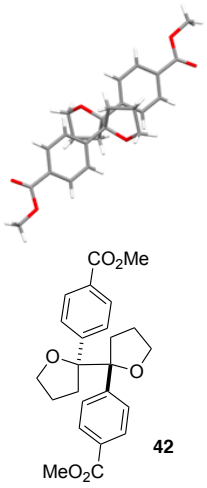

Figure S9. The structure of **42**. White: hydrogen, gray: carbon, red: oxygen.

Table S9. Selected Crystallographic Data of **42**

	42
molecular formula	$C_{24}H_{26}O_6$
formula weight	410.47
crystal color, habit	colorless, platelet
crystal system	triclinic
space group	*P2₁*
cell constants	
a (Å)	6.07469
b (Å)	8.28075
c (Å)	10.32329
a (deg)	76.21410
b (deg)	89.94130
g (deg)	81.54800
V (Å^3)	498.54314
Z	1
ρ_{calcd} (g cm^{-3})	1.367
R_1	0.0771
wR_2	0.2451
F(000)	218.00

4. References

(1) Viso, A.; Fernández de la Pradilla, R.; García, A.; Flores, A. *Chem. Rev*. **2005**, *105*, 3167.

(2) (a) Maruoka, K.; Ooi, T.; *Chem. Rev*. **2003**, *103*, 3013; b) O'Donnell, M. J. *Acc. Chem. Res*. **2004**, *37*, 506; (c) Nájera, C.; Sansano, J.M.; *Chem. Rev*. **2007**, *107*, 4584.

(3) (a) Bernardi, L. Gothelf, A. S. Hazell, R.G. Jørgensen, K. A. *J. Org. Chem.* **2003**, 68, 2583; (b) Okada, A.; Shibuguchi, T.; Ohshima, T.; Masu, H.; Yamaguchi, K.; Shibasaki, M. *Angew. Chem., Int. Ed.* **2005**, *44*, 4564; (c) Yan, X. X.; Peng, Q.; Li, Q.; Zhang, K.; Yao, J.; Hou, X. L.; Wu, Y. D. *J. Am. Chem. Soc.* **2008**, *130*, 14362; (d) Hernández-Toribio, J.; Gómez Arrayás, R.; Carretero, J. C. *J. Am. Chem. Soc.* **2008**, *130*, 16150. (e) Bandar, J. S.; Lambert, T. H. *J. Am. Chem. Soc.* **2013**, *135*, 11799; (f) Shang, D.; Liu, Y.; Zhou, X.; Liu, X.; Feng, X. *Chem. Eur. J.* **2009**, *15*, 3678; (g) Liang, G.; Tong, M.-C.; Tao, H.; Wang, C.-J.; *Adv. Synth. Catal*. **2010**, *352*, 1851; (h) Hernández-Toribio, J.; Arrayás, R. G.; Carretero, J. C. *Chem. Eur. J.* **2010**, *16*, 1153; (i) Imae, K.; Shimizu, K.; Ogata, K. Fukuzawa, S. *J. Org. Chem.* **2011**, *76*, 3604; (j) Yamashita, Y.; Yoshimoto, S.; Masuda, K.; Kobayashi, S. *Asian J. Org. Chem.* **2012**, *1*, 327; (k) Hernando, E.; Arrayás, R. G.; Carretero, J. C. *Chem. Commun*. **2012**, *48*, 9622; (l) Arai, T.; Mishiro, A.; Matsumura, E.; Awata, A.; Shirasugi, M. *Chem. Eur. J.* **2012**, *18*, 11219; (m) Cayuelas, A.; Serrano, L.; Nájera, C.; Sansano, J. M. *Tetrahedron: Asymmetry* **2014**, *25*, 1647.

(4) Weidner, K.; Kumagai, N.; Shibasaki, M. *Angew. Chem.*, *Int. Ed*. **2014**, *53*, 6150.

(5) Weidner, K.; Sun, Z.; Kumagai, N.; Shibasaki, M. *Angew. Chem.*, *Int. Ed*. **2015**, *54*, 6236.

(6) (a) Yin, L.; Brewitz, L.; Kumagai, N.; Shibasaki, M. *J. Am. Chem. Soc.* **2014**, *136*, 17958. (b) Brewitz, L.; Arteaga, F. A.; Yin, L.; Alagiri, K.; Kumagai, N.; Shibasaki, M. *J. Am. Chem. Soc.* **2015**, *137*, 15929.

(7) Recent reviews of cooperative catalysis. Lewis acid/Brønsted base: (a) Shibasaki, M.; Yoshikawa, N. *Chem. Rev.* **2002**, *102*, 2187; (b) Kumagai, N.; Shibasaki, M.; *Angew. Chem., Int. Ed.* **2011**, *50*, 4760;

(8) (a) Bräse, S.; Gil, C.; Knepper, K.; Zimmermann, V. *Angew. Chem., Int. Ed.* **2005**, *44*, 5188; (b) *Organic Azides: Syntheses and Applications* (Eds.: Bräse, S.; Banert, K.), Wiley, Chichester, 2010.

(9) Synthesis of N-diphenyl(thiophosphinoyl)imines: (a) Xu, X.; Wang, C.; Zhou, Z.; Zeng, Z.; Ma, X.; Zhao, G.; Tang, C. *Lett. Org. Chem*. **2006**, *3*, 640; (b) Xu, X.; Wang, C.; Zhou, Z.; Zeng, Z.; Ma, X.; Zhao, G.; Tang, C. *Heteroat. Chem*. **2008**, *19*, 238.

(10) (a) Köhn, M.; Breinbauer, R. *Angew. Chem., Int. Ed.* **2004**, *43*, 3106; (b) Nilsson, B. L.; Hondal, R. J.; Soellner, M. B.; Raines, R. T. *J. Am. Chem. Soc.* **2003**, *125*, 5268.; (c) Soellner, M. B.; Nilsson, B. L.; Raines, R. T. *J. Am. Chem. Soc.* **2006**, *128*, 8820; (d) Yamashita, T.; Matoba, H.; Kuranaga, T.; Inoue, M. *Tetrahedron* **2014**, *70*, 7746.

(11) For reviews on the chemistry of *para*-quinone methides, see: (a) Turner, A. B. Q. *Rev*., *Chem*. *Soc*. **1964**, *18*, 347. (b) Wagner, H.-U.; Gompper, R. *In the Chemistry of the Quinonoid Compounds*; Patai, S., Ed.; Wiley: New York, **1974**; Vol. 2, pp 1145. (c) Peter, M. G. *Angew*. *Chem*., *Int*. *Ed*. **1989**, *28*, 555. (d) Itoh, T. *Prog*. *Polym*. *Sci*. **2001**, *26*, 1019. (e) Toteva, M. M.; Richard, J. P. *Adv*. *Phys*. *Org*. *Chem*. **2011**, *45*, 39. (f) Parra, A.; Tortosa, M. *ChemCatChem* **2015**, *7*, 1524.

(12) (a) Takao, K.-i.; Sasaki, T.; Kozaki, T.; Yanagisawa, Y.; Tadano, K.-i.; Kawashima, A.; Shinonaga, H. *Org. Lett*. **2001**, *3*, 4291. (b) Martin, H. J.; Magauer, T.; Mulzer, J. *Angew*. *Chem*., *Int*. *Ed*. **2010**, *49*, 5614. (c) Jansen, R.; Gerth, K.; Steinmetz, H.; Reinecke, S.; Kessler, W.; Kirschning, A.; Müller, R. *Chem*. *Eur*. *J*. **2011**, *17*, 7739.

(13) For selected nonasymmetric reactions of *para*-quinone methides, see: (a) Hart, D. J.; Cain, P. A.; Evans, D. A. *J*. *Am*. *Chem*. *Soc*. **1978**, *100*, 1548. (b) Baik, W.; Lee, H. J.; Jang, J. M.; Koo, S.; Kim, B. H. *J. Org. Chem.* **2000**, *65*, 108. (c) Reddy, V.; Anand, R. V. *Org. Lett.* **2015**, *17*, 3390. (d) Ramanjaneyulu, B. T.; Mahesh, S.; Anand, R. V. *Org. Lett.* **2015**, *17*, 3952. (e) Gai, K.; Fang, X.; Li, X.; Xu, J.; Wu, X.; Lin, A.; Yao, H. *Chem. Commun.* **2015**, *51*, 15831. (f) Yuan, Z.; Fang, X.; Li, X.; Wu, J.; Yao, H.; Lin, A. *J. Org. Chem.* **2015**, *80*, 11123. (g) Lopez, A.; Parra, A.; Jarava-Barrera, C.; Tortosa, M. *Chem. Commun.* **2015**, *51*, 17684.

(14) For selected asymmetric 1,6-additions of *para*-quinone methides, see: (a) Chu, W.-D.; Zhang, L.-F.; Bao, X.; Zhao, X.-H.; Zeng, C.; Du, J.-Y.; Zhang, G.-B.; Wang, F.-X.; Ma, X.-Y.; Fan, C.-A. *Angew. Chem., Int. Ed.* **2013**, *52*, 9229. (b) Caruana, L.; Kniep, F.; Johansen, T. K.; Poulsen, P. H.; Jørgensen, K. A. *J. Am.*

Chem. Soc. **2014**, *136*, 15929. (c) He, F.-S.; Jin, J,-H.; Yang, Z,-T.; Yu, X.; Fossey, J. S.; Deng, W,-P. *ACS Catal.* **2016**, *6*, 652. (d) Lou, Y.; Cao, P.; Jia, T.; Zhang, Y.; Wang, M.; Liao, J. *Angew. Chem., Int. Ed.* **2015**, *54*, 12134. (e) Wang, Z.; Wong, Y. F.; Sun, J. *Angew. Chem., Int. Ed.* **2015**, *54*, 13711. (f) Dong, N.; Zhang, Z.-P.; Xue, X.-S.; Li, X.; Cheng J.-P. *Angew. Chem., Int. Ed.* **2016**, *55*, 1460. (g) Jarava-Barrera, C.; Parra, A.; Lopez, A.; Cruz-Acosta, F.; Collado-Sanz, D.; Carḍenas, D. J.; Tortosa, M. *ACS Catal.* **2016**, *6*, 442. (h) Zhao, K.; Zhi, Y.; Wang, A.; Dieter, Enders. *ACS Catal.* **2016**, *6*, 657. (i) Ma, C.; Huang, Y.; Zhao, Y. *ACS Catal.* **2016**, *6*, 6408. (j) Kang, T.-C.; Wu, L.-P.; Yu, Q.-W.; Wu, X.-Y. *Chem. - Eur. J.* **2017**, *23*, 6509. (k) Li, X.; Xu, X.; Wei, W.; Lin, A.; Yao, H. *Org. Lett.* **2016**, *18*, 428.

(15) For selected examples of synthesis of diarylmethine stereogenic centers: (a) Paquin, J.-F.; Defieber, C.; Stephenson, C. R. J.; Carreira, E. M. *J. Am. Chem. Soc.* **2005**, *127*, 10850. (b) Matsuzawa, H.; Miyake, Y.; Nishibayashi, Y. *Angew. Chem., Int. Ed.* **2007**, *46*, 6488. (c) Tolstoy, P.; Engman, M.; Paptchikhine, A.; Bergquist, J.; Church, T. L.; Leung, A. W.-M.; Andersson, P. G. *J. Am. Chem. Soc.* **2009**, *131*, 8855. (d) Wang, Z.-Q.; Feng, C.-G.; Zhang, S.-S.; Xu, M.-H.; Lin, G.-Q. *Angew. Chem., Int. Ed.* **2010**, *49*, 5780. (e) Shintani, R.; Takatsu, K.; Takeda, M.; Hayashi, T. *Angew. Chem., Int. Ed.* **2011**, *50*, 8656. (f) Do, H.-Q.; Chandrashekar, E. R. R.; Fu, G. C. *J. Am. Chem. Soc.* **2013**, *135*, 16288. (g) Song, S.; Zhu, S.-F.; Yu, Y.-B.; Zhou, Q.-L. *Angew. Chem., Int. Ed.* **2013**, *52*, 1556. (h) Xu, B.; Li, M.-L.; Zuo, X.-D.; Zhu, S.-F.; Zhou, Q.-L. *J. Am. Chem. Soc.* **2015**, *137*, 8700.

(16) Ameen, D.; Snape, T. J. *MedChemComm* **2013**, *4*, 893.

(17) (a) Brewitz, L.; Kumagai, N.; Shibasaki, M. *J. Fluorine Chem.* **2017**, *194*, 1. (b) Matsuzawa, A.; Noda, H.; Kumagai, N.; Shibasaki, M. *J. Org. Chem.* **2017**, *82*, 8304.

(18) (a) Sun, Z.; Weidner, K.; Kumagai, N.; Shibasaki, M. *Chem. Eur. J.* **2015**, *21*, 17574. (b) Noda, H.; Amemiya, F.; Weidner, K.; Kumagai, N.; Shibasaki, M. *Chem. Sci.* **2017**, *8*, 3260.

(19) (a) Arteaga, F. A.; Liu, Z.; Brewitz, L.; Chen, J.; Sun, B.; Kumagai, N.; Shibasaki, M. *Org. Lett.* **2016**, *18*, 2391. (b) Liu, Z.; Takeuchi, T.; Pluta, R.; Arteaga Arteaga, F.; Kumagai, N.; Shibasaki, M. *Org. Lett.* **2017**, *19*, 710.

(20) Sun, B.; Balaji, P. V.; Kumagai, N.; Shibasaki, M. *J. Am. Chem. Soc.* **2017**, *139*, 8295.

(21) Sun, B.; Pluta, R.; Kumagai, N.; Shibasaki, M. *Org. Lett.* **2018**, *20*, 526.

(22) For reviews, see: (a) Yoon, T. P.; Ischay, M. A.; Du, J. *Nat. Chem.* **2010,** *2*, 527; (b) Tellis, J. C.; Kelly, C. B.; Primer, D. N.; Jouffroy, M.; Patel, N. R.; Molander, G. A. *Acc. Chem. Res.* **2016,** *49*, 1429; (c) Shaw, M. H.; Twilton, J.; MacMillan, D. W. C. *J. Org. Chem.* **2016,** *81*, 6898; (d) Reckenthäler, M.; Griesbeck, A. G. *Adv. Synth. Cat.* **2013,** *355*, 2727; (e) Prier, C. K.; Rankic, D. A.; MacMillan, D. W. C. *Chem. Rev.* **2013,** *113*, 5322; (f) Narayanam, J. M.; Stephenson, C. R. *Chem. Soc. Rev.* **2011,** *40*, 102. (g) Twilton, J.; Le, C.; Zhang, P.; Shaw, M. H.; Evans, R. W.; MacMillan, D. W. C. *Nat. Rev. Chem.* **2017,** *1*, 0052;

(23) (a) Zuo, Z.; Ahneman, D. T.; Chu, L.; Terrett, J. A.; Doyle, A. G.; MacMillan, D. W. C. *Science* **2014,** *345*, 437; (b) Zuo, Z.; Gong, H.; Li, W.; Choi, J.; Fu, G. C.; MacMillan, D. W. C. *J. Am. Chem. Soc.* **2016,** *138*, 1832; (c) Noble, A.; McCarver, S. J.; MacMillan, D. W. C. *J. Am. Chem. Soc.* **2015,** *137*, 624; (d) Johnston, C. P.; Smith, R. T.; Allmendinger, S.; MacMillan, D. W. C. *Nature* **2016,** *536*, 322; (e) Chu, L.; Lipshultz, J. M.; MacMillan, D. W. C. *Angew. Chem., Int. Ed.* **2015,** *54*, 7929.

(24) (a) Tellis, J. C.; Primer, D. N.; Molander, G. A. *Science* **2014,** *345*, 433; (b) Karakaya, I.; Primer, D. N.; Molander, G. A. *Org. Lett.* **2015,** *17*, 3294; (c) Primer, D. N.; Karakaya, I.; Tellis, J. C.; Molander, G. A. *J. Am. Chem. Soc.* **2015,** *137*, 2195; (d) Amani, J.; Sodagar, E.; Molander, G. A. *Org. Lett.* **2016,** *18*, 732; (e) El Khatib, M.; Serafim, R. A.; Molander, G. A. *Angew. Chem., Int. Ed.* **2016,** *55*, 254; (f) Ryu, D.; Primer, D. N.; Tellis, J. C.; Molander, G. A. *Chem. -Eur. J.* **2016,** *22*, 120; (g) Tellis, J. C.; Amani, J.; Molander, G. A. *Org. Lett.* **2016,** *18*, 2994; (h) Amani, J.; Molander, G. A. *J. Org. Chem.* **2017,** *82*, 1856.

(25) (a) Patel, N. R.; Kelly, C. B.; Jouffroy, M.; Molander, G. A. *Org. Lett.* **2016,** *18*, 764; (b) Jouffroy, M.; Primer, D. N.; Molander, G. A. *J. Am. Chem. Soc.* **2016,** *138*, 475; (c) Corce, V.; Chamoreau, L. M.; Derat, E.; Goddard, J. P.; Ollivier, C.; Fensterbank, L. *Angew. Chem., Int. Ed.* **2015,** *54*, 11414.

(26) Terrett, J. A.; Cuthbertson, J. D.; Shurtleff, V. W.; MacMillan, D. W. C. *Nature* **2015**, *524*, 330.

(27) Corcoran, E. B.; Pirnot, M. T.; Lin, S.; Dreher, S. D.; DiRocco, D. A.; Davies, I. W.; Buchwald, S. L.; MacMillan, D. W. C. *Science* **2016**, *353*, 279.

(28) (a) Oderinde, M. S.; Jones, N. H.; Juneau, A.; Frenette, M.; Aquila, B.; Tentrarelli, S.; Robbins, D. W.; Johannes, J. W. *Angew. Chem., Int. Ed.* **2016**, *55*, 13219; (b) Oderinde, M. S.; Frenette, M.; Robbins, D. W.; Aquila, B.; Johannes, J. W. *J. Am. Chem. Soc.* **2016**, *138*, 1760.
(29) Shaw, M. H.; Shurtleff, V. W.; Terrett, J. A.; Cuthbertson, J. D.; MacMillan, D. W. C. *Science* **2016**, *352*, 6291.
(30) Welin, E. R.; Le, C.; Arias-Rotondo, D. M.; McCusker, J. K.; MacMillan, D. W. C. *Science* **2017**, *355*, 380.
(31) Heitz, D. R.; Molander, G. A. *J. Am. Chem. Soc.* **2016**, *138*, 12715.
(32) Shields, B. J.; Doyle, A. G. *J. Am. Chem. Soc.* **2016**, *138*, 12719.
(33) (a) Hager, D.; MacMillan, D. W. C. *J. Am. Chem. Soc.* **2014**, *136*, 16986; (b) Jin, J.; MacMillan, D. W. C. *Angew. Chem., Int. Ed.* **2015**, *54*, 1565.
(34) Le, C.; MacMillan, D. W. C. *J. Am. Chem. Soc.* **2015**, *137*, 11938.
(35) Joe, C. L.; Doyle, A. G. *Angew. Chem., Int. Ed.* **2016**, *55*, 4040.
(36) Luca, O. R.; Gustafson, J. L.; Maddox, S. M.; Fenwick, A. Q.; Smith, D. C. *Org. Chem. Front.* **2015,** *2*, 823.
(37) Lowry, M. S.; Goldsmith, J. I.; Slinker, J. D.; Rohl, R.; Pascal, R. A.; Malliaras, G. G.; Bernhard, S. *Chem. Mater.* **2005,** *17*, 5712.
(38) For early examples of reactions driven by energy transfer from excited photosensitizer to organic molecules, see: (a) Demas, J. N.; Addington, J. W. *J. Am. Chem. Soc.* **1976,** *98*, 5800; (b) Juris, A.; Gandolfi, M. T.; Manfrin, M. F.; Balzani, V. *J. Am. Chem. Soc.* **1976,** *98*, 1047; (c) Juris, A.; Manfrin, M. F.; Maestri, M.; Serpone, N. *Inorg. Chem.* **1978,** *17*, 2258; (d) Marciniak, B.; Buonocore, G. E. *Spectrosc. Lett* **1990,** *23*, 149.
(39) For a recent example of reaction driven by energy transfer: Teders, M.; Henkel, C.; Anhäuser, L.; Strieth-Kalthoff, F.; Gómez-Suárez, A.; Kleinmans, R.; Kahnt, A.; Rentmeister, A.; Guldi, D.; Glorius, F. *Nat. Chem.* **2018**, *10*, 981.
(40) For a recent review on energy transfer catalysis mediated by visible light: Strieth-Kalthoff, F.; James, M.; Teders, M.; Pitzer, L.; Glorius, F. *Chem. Soc. Rev.* **2018**, doi: 10.1039/c8cs00054a.
(41) Luo, Y.-R. Comprehensive Handbook of Chemical Bond Engergies; CRC Press: Boca Raton, FL, 2003.
(42) Ohkubo, K.; Mizushima, K.; Iwata, R.; Souma, K.; Suzuki, N.; Fukuzumi, S. *Chem. Commun* **2010,** *46*, 601.
(43) Arias-Rotondo, D. A.; McCusker, J. K. *Chem. Soc. Rev.* **2016**, *45*, 5803.
(44) Tsuda, T.; Yazawa, T.; Watanabe, K.; Fujii, T.; Saegusa, T. *J. Org. Chem.* **1981**, *46*, 192.